# Gene-Environment Interactions Between Manganese Toxicity and Early-Onset Parkinson's Disease Genes

By

Sudipta Chakraborty

Dissertation

Submitted to the Faculty of the

Graduate School of Vanderbilt University

in partial fulfillment of the requirements

for the degree of

DOCTOR OF PHILOSOPHY

in

Neuroscience

May, 2015

Nashville, Tennessee

Approved:

Aaron Bowman, Ph.D.

Keith Erikson, Ph.D.

Bill Valentine, Ph.D.

Michael Aschner, Ph.D.

*To my family, for their sacrifices and unconditional love,*

*and in loving memory of Dadu.*

*I hope I've made you all proud.*

## ACKNOWLEDGEMENTS

The work presented in this thesis would not have been possible without the support of many mentors and colleagues. I would first like to thank Miki Aschner, my mentor, for taking me under his wing and guiding me through this journey. I will be eternally grateful for Miki's role in fostering scientific freedom and critical thinking that have allowed me to develop into a strong, independent scientist. I am honored to consider Miki as a life-long mentor, colleague and friend. I would also like to thank the other members of my thesis committee, Aaron Bowman, Keith Erikson and my chair, Bill Valentine, for their thought-provoking discussions, constructive feedback, and relentless support that have always challenged me to improve both my approach to scientific problems and my presentation skills.

I am also indebted to the Neuroscience Graduate Program through the Vanderbilt Brain Institute (VBI) for the valuable knowledge I gained during my earlier years. The classroom instruction, delivered by many talented scientists and aimed to develop molecular knowledge and enhance presentation skills, has been fundamental in my growth as a neuroscientist. I would also like to thank my funding support from Vanderbilt's Center in Molecular Toxicology, as well as the National Institute of Environmental Health Sciences. The research presented in this thesis would not have been possible without their financial support. I also appreciate the administrative assistance from the VBI's Mary Michael-Woolman, Roz Johnson, Shirin Pulous and Beth Sims and Molecular Toxicology's Alycia Buford, Wil Comstock and Kakie Mashburn for both academic and extracurricular needs. Their hard work and dedication is well treasured.

My success has also been largely influenced by several colleagues in the Aschner lab. I am forever grateful to Daiana Avila, who first taught me the ways of the worms. I would also like to thank former graduate students Kirsten Helmcke, Jenny Madison, Anna Griffin, Priscila Gubert and former postdoc Ebany Martinez-Finely, for their support, friendship and guidance. A big thanks goes out to Julia Bornhorst – I will forever remember our extremely productive, powerful and fun collaboration with fond memories. The Aschner group faced the difficult obstacle of transitioning from Vanderbilt University to Albert Einstein College of Medicine in 2013. Several colleagues made this transition with me, and I will be forever grateful for our camaraderie and support of each other during this challenging time. Special thanks go to the postdocs Pan Chen, Sam Caito and Cari Lopez-Granero for their technical and professional guidance and valued friendship from Vanderbilt to Einstein. I also cannot be grateful enough for the beautiful friendships and support from my colleagues Thuy Nguyen, Marion Park and Megan

Culbreth. Thank you, girls, for keeping me (somewhat) sane during such a difficult phase in my life. Our memories in both Music City and the Big Apple, both professionally and personally, will be forever cherished. Thank you also to my new Einstein friends, Meagan & Ryan Vogt – your friendship and support means more to me than you know.

Graduate school is both an enlightening and trying process. I could not have survived it without the support of many wonderful friends in Nashville, including (in no particular order): Hayley & Hank Clay, Emily & AJ Baucum, Elizabeth Conrad, Christi & Will French, Sarah & Scott Collier, Andrew & Abby Hardaway, Elizabeth Meredith, Brad Kraemer, Alexia Melo Carrillo, Terry Jo Bichell, Teniel Ramikie, Gloria Laryea, Martin Schmidt, Erin Watt, Rachel Game, Juli Fister, Cait Gordon, Jamie & James Saxon and Bobby Madamanchi, among many others. A special thanks goes to Gunnar Kwakye, my "grad school life coach" and dear friend who helped shape my professional and personal approaches to the highs and lows of grad school. It has been such a comfort and joy to learn from, commiserate with, and celebrate with you all.

Thank you to my wonderful family. To my mother and father who have sacrificed so much for my brother and I, and have always encouraged me to exceed expectations and reach for the highest dreams – thank you for your unconditional support and love, Mommy and Daddy. I hope I have made you proud through this long process. To my brother, whose humor, distractions and interesting perspectives have helped me cope with the challenges along the way – thank you, Ricky. To my aunt and uncle, who have always been like second parents to me – thank you both for believing in me and loving me over the years. I would also like to thank my new Henriquez/Ziccolella family members. I feel so honored to have joined such a warm and incredible family, and sincerely appreciate your support of me during this time. Lastly, I would like to thank Dadu, who I wish could have seen me reach this milestone. Dadu was an inspiration to me in pursuing higher education, and was always supportive of my academic goals. I miss you, Dadu, and I hope I've made you proud.

Last, but certainly not least, I'd like to thank my amazing best friend/soul mate/husband. I am eternally grateful to have found you here in Nashville, Chrissy. Your unwavering support, kindness, encouragement and love have made this entire thesis possible. Thank you so much for inspiring me to be the very best I can be. I've truly learned from the best, and look forward to many, many more years of scientific and life discoveries with the one I love.

## LIST OF FIGURES

Figure

1. Schematic illustrating the basal ganglia circuitry involved in both direct and indirect pathways ..... 3

2. The mammalian Mn transport system ..... 20

3. *C. elegans* dopaminergic head neurons ..... 32

4. *pdr-1* mutants are hypersensitive to an acute Mn exposure ..... 53

5. Enhanced Mn accumulation in *pdr-1* and *djr-1.1* mutants is reversed by WT α-Syn expression ..... 55

6. Mn-induced oxidative stress is exacerbated in *pdr-1* and *djr-1.1* mutants, but rescued by α-Syn expression ..... 57

7. Increased *skn-1* mRNA expression in *djr-1.1* and *pink-1* mutants ..... 59

8. DAergic neurodegeneration in WT and *pdr-1* mutants is attenuated by α-Syn expression ..... 61

9. Increased α-Syn expression in *djr-1.1* deletion mutants ..... 63

10. *pdr-1* mutants show alterations in mRNA expression of Mn exporter, but not importer, genes ..... 83

11. Overexpression of *fpn-1.1* in *pdr-1* mutants rescues Mn-induced lethality ..... 85

12. Overexpression of *fpn-1.1* in *pdr-1* mutants decreases levels of highly

pro-oxidant metals ..... 87

13. Overexpression of *fpn-1.1* in *pdr-1* mutants improves mitochondrial integrity and antioxidant response ..... 89

14. Overexpression of *fpn-1.1* in *pdr-1* mutants improves the DA-dependent basal slowing response ..... 91

15. Basic model summarizing the findings of Chapter III ..... 92

## LIST OF SUPPLEMENTARY TABLES AND FIGURES

Supplementary Table

1. Conditions for ICP-MS/MS (Agilent 8800 ICP-QQQ). ..... 111

2. Conditions for ICP-MS (ICAP Qc, Thermo Fisher Scientific) ..... 111

3. Conditions for LA (LSX213G2+, CETAC Technologies) ..... 111

Supplementary Figure

1. Decreased basal respiration in *pdr-1* mutants that is not rescued by *fpn-1.1* overexpression ..... 112

## LIST OF ABBREVIATIONS

3-MT ..... 3-methoxytyramine
6-OHDA ..... 6-hydroxydopamine
α-Syn ..... alpha-synuclein
AADC ..... aromatic acid decarboxylase
AC ..... adenylate cyclase
ADE ..... anterior deirid
ANOVA ..... analysis of variance
ATP ..... adenosine triphosphate
BBB ..... blood brain barrier
BCA ..... bicinchoninic acid
BSR ..... basal slowing response
*C. elegans* ..... *Caenorhabditis elegans*
cAMP ..... cyclic adenosine monophosphate
CEP ..... cephalic
CGC ..... *Caenorhabditis* Genetics Center
Cl ..... chloride
Co ..... cobalt
COMT ..... catechol-*O*-methyltransferase
CTS ..... consensus transport sequence
Cu ..... copper
DA/DAergic ..... dopamine/dopaminergic
DAT ..... dopamine transporter
DCF-DA ..... 2',7'-dichlorodihydrofluorescein diacetate
DCT1 ..... divalent cation transporter 1
DMT1 ..... divalent metal transporter 1
EDTA ..... ethylenediaminetetraacetic acid
EPA ..... Environmental Protection Agency
EPR ..... electron paramagnetic resonance
ETC ..... electron transport chain
Fe ..... iron

FPN ..... ferroportin
GABA/GABAergic..... gamma-aminobutyric acid/-ergic
GFAAS ..... graphite furnace atomic absorption spectroscopy
GFP ..... green fluorescent protein
GKC..... Gene Knockout Consortium
GPe ..... globus pallidus, external segment
GPi..... globus pallidus, internal segment
GSH..... glutathione
GSSG ..... glutathione disulfide
$H_2O_2$ ..... hydrogen peroxide
HIF..... hypoxia inducible factor
ICP-MS..... inductively coupled plasma mass spectrometry
IPD..... idiopathic Parkinson's disease
IRE..... iron responsive element
KO ..... knockout
L-DOPA ..... L-3,4-dihdyroxyphenylalanine
L1..... 1st larval stage
LPS..... lipopolysaccharide
MAO ..... monoamine oxidase
MCT..... monocarboxylate transporter
MeHg..... methylmercury
Mfn2..... mitofusin 2
MMT ..... methylcyclopentadienyl manganese tricarbonyl
$Mn/MnCl_2$ ..... manganese/manganese chloride
MPTP..... 1-methyl-4-phenyl-1,2,3,6-tetrahydropyridine
MRI..... magnetic resonance imaging
mRNA..... messenger ribonucleic acid
MSN..... medium spiny neuron
mtDNA..... mitochondrial deoxyribonucleic acid
MTS..... mitochondrial targeting sequence
Na/NaCl..... sodium/sodium chloride
Ni ..... nickel
NLS..... nuclear localization signal/sequence

Nrf2 ..... Nuclear factor (erythroid-derived)-like 2
OVR ..... overexpressing
PAS ..... para-aminosalicylic acid
PC ..... pyruvate carboxylase
PD ..... Parkinson's disease
PDE ..... posterior deirid
pdr-1 ..... Parkinson's disease-related 1
PINK1 ..... PTEN-induced putative kinase 1
PPM ..... serine/threonine protein phosphatase
RNAi ..... ribonucleic acid interference
ROS ..... reactive oxygen species
SNpc ..... substantia nigra pars compacta
SNpr ..... substantia nigra pars reticulata
SO ..... superoxide
SPCA ..... secretory pathway $Ca^{2+}/Mn^{2+}$ ATPase
STN ..... subthalamic nucleus
Tf/TfR ..... transferrin/transferrin receptor
TH ..... tyrosine hydroxylase
TPN ..... total parenteral nutrition
UPS ..... ubiquitin proteasome system
UV ..... ultraviolet
VBM ..... voxel-based morphometry
VDAC ..... voltage-dependent anion channel
VMAT2 ..... vesicular monoamine transporter 2
WT ..... wildtype
Zn ..... zinc

## TABLE OF CONTENTS

DEDICATION ..... ii

ACKNOWLEDGEMENTS ..... iii

LIST OF FIGURES ..... v

LIST OF SUPPLEMENTARY TABLES AND FIGURES ..... vii

LIST OF ABBREVIATIONS ..... viii

Chapter

I. INTRODUCTION TO GENE-ENVINROMENT INTERACTIONS: PARKINSON'S DISEASE AND MANGANESE TOXICITY ..... 1

- Parkinson's Disease ..... 1
  - Introduction ..... 1
  - The Dopaminergic System ..... 1
  - PD Pathophysiology: Molecular Mechanisms ..... 5
  - PD Models ..... 8
    - Pharmacological Models ..... 8
      - MPTP ..... 8
      - 6-OHDA ..... 9
      - Pesticides ..... 10
      - LPS ..... 10
    - Genetic Animal Models ..... 11
      - Parkin ..... 11
      - PINK1 ..... 12
      - DJ-1 ..... 13
      - α-Syn ..... 14
- Manganese ..... 15
  - Routes of Exposure ..... 15
  - Intestinal Uptake and Release ..... 16
  - Transport Across the Cell Membrane ..... 18
  - Buffering and Other Regulatory Mechanisms ..... 21
  - Manganese Efflux ..... 24
  - Manganese Toxicity ..... 25
  - Manganism & PD ..... 26
    - Shared Molecular Mechanisms ..... 29
- *Caenorhabditis elegans* as a Neurotoxicity Model ..... 31
  - PD Genetics Homology in *C. elegans* ..... 35
    - parkin/pdr-1 ..... 35
    - pink1/pink-1 ..... 36
    - dj1/djr-1.1 & djr-1.2 ..... 36
  - Manganese Transporter Homology in *C. elegans* ..... 37
    - Uptake via DMT1/SMF1-3 ..... 37

Efflux via FPN/FPN-1.1-1.3 ..... 39
Intracellular Buffering via PMR1/CePMR-1 ..... 39
Overview of Specific Aims ..... 40

II. THE EFFECTS OF *PDR-1, PINK-1 AND DJR-1.1* LOSS IN MANGANESE -INDUCED TOXICITY AND THE ROLE OF α-SYN IN *C. ELEGANS* ..... 42
Introduction ..... 42
Materials & Methods ..... 46
Results ..... 52
Discussion ..... 62
Conclusions ..... 73

III. LOSS OF *PDR-1/PARKIN* INFLUENCES MANGANESE HOMEOSTASIS THROUGH ALTERED *FERROPORTIN* EXPRESSION IN *C. ELEGANS* ..... 74
Introduction ..... 74
Materials & Methods ..... 77
Results ..... 82
Discussion ..... 90
Conclusions ..... 98

IV. DISCUSSION AND FUTURE DIRECTIONS ..... 99

Supplementary Tables and Figures ..... 111

References ..... 113

# CHAPTER I

# INTRODUCTION TO GENE-ENVIRONMENT INTERACTIONS: PARKINSON'S DISEASE AND MANGANESE TOXICITY

## Parkinson's Disease

### *Introduction*

Parkinson's Disease (PD) is one of the most common neurodegenerative disorders in the U.S. population, with a median age of onset around 60 years[1]. This disease affects more than 1% of the population over the age of 60 by causing preferential damage to the nigrostriatal circuit of the brain. More specifically, distinct degeneration of dopaminergic (DAergic) neurons in the substantia nigra pars compacta (SNpc) is the prominent pathological hallmark of the disease, along with the presence of α-synuclein-rich Lewy body inclusions. These features ultimately lead to motor dysfunction, with cardinal symptoms including bradykinesia (slowness in movement), tremors, rigidity, and postural instability[2]. Cognitive deficits and emotional and behavioral problems are also seen in diseased individuals. Later stages of the disease are often marked by appearance of a masked face, along with a forward-flexed posture, gait freezing, shuffling steps, and gastrointestinal issues[1].

### *The Dopaminergic System*

While the selectivity in PD-associated cell death remains poorly understood, it is advantageous to understand how the DAergic system operates in cells. The neurotransmitter dopamine (3,4-dihydroxyphenethylamine, DA) is synthesized in a two-

step process, starting with hydroxylation of the amino acid tyrosine via the rate-limiting enzyme tyrosine hydroxylase (TH) to produce L-DOPA (L-dihydroxyphenylalanine)[3]. DA is then produced from L-DOPA via decarboxylation by AADC (aromatic acid decarboxylase)[4]. Upon synthesis, DA is packaged into synaptic vesicles by the vesicular monoamine transporter 2 (VMAT2) for release into the synaptic cleft[5]. DA itself can be metabolized by monoamine oxidase (MAO) into the metabolite DOPAC (3,4-dihydroxyphenylacetic acid), or by catechol-O-methyl transferase (COMT) into 3-MT (3-methoxytyramine)[6, 7]. In addition to metabolism, free dopamine is typically cleared from the synaptic cleft by the dopamine transporter (DAT), localized to axon terminals, that helps recycle the neurotransmitter for future storage and release. This 12-transmembrane domain transporter is a symporter, with dopamine reuptake coupled to the co-transport of two $Na^+$ ions and one $Cl^-$ ion[8, 9].

There are four major DAergic neural circuits in the brain: the tuberoinfundibular[10], mesocortical[11], mesolimbic[12] and nigrostriatal pathways[13], with the last circuit implicated in PD. The DAergic neurons of the nigrostriatal pathway send their projections from the SNpc to the striatum, which in primates, consists of the caudate nucleus and putamen[14]. This circuit is a vital component of the basal ganglia region implicated in PD, which is comprised of the SN, striatum, globus pallidus and subthalamic nucleus (STN), and interacts with the motor cortex and thalamus. The ultimate functional output of the striatum involves the coordination of movement[15]. This system uses two antagonistic circuits to maintain balance: the direct and indirect pathways[16] (**Fig 1**). The direct pathway starts with excitatory, glutamatergic input from the motor cortex to stimulate the striatum, which is mostly composed of inhibitory, GABAergic medium spiny neurons

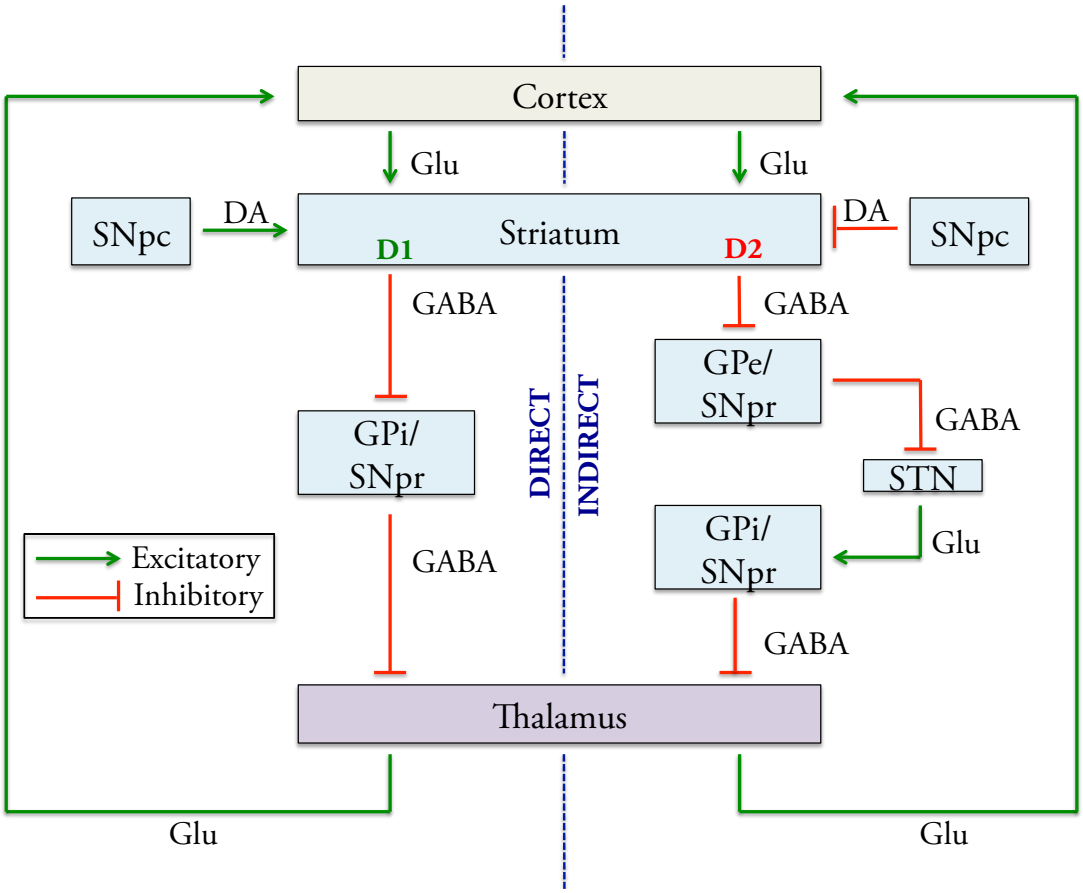


**Figure 1.** *Schematic illustrating the basal ganglia circuitry involved in both direct and indirect pathways.* DA: dopamine; Glu: glutamate; GPe: globus pallius external segment; GPi: globus pallidus internal segment; SNpc: substantia nigra pars compacta; SNpr: substantia nigra pars reticulate; STN: subthalamic nucleus.

(MSNs), resulting in inhibition of the inhibitory cells of the globus pallidus internal segment (GPi) and the substantia nigra pars reticulate (SNpr). This disinhibition results in increased stimulation of the excitatory neurons of the thalamus, resulting in increased excitation of the motor cortex to produce a hyperkinetic response[17]. Meanwhile, the indirect pathway starts with similar input from the motor cortex to stimulate the striatum, which then inhibits the inhibitory cells of the globus pallidus external segment (GPe) and SNpr from inhibiting the excitatory cells of the STN. This results in stimulation of the GPi/SNpr, resulting in inhibition of the thalamus to decrease stimulation of the motor cortex to produce a hypokinetic response. Additionally, the SNpc modulates this antagonistic circuitry through DAergic stimulation of the striatum[17].

The intricacies of this pathway revolve around DA's modulatory effects on its receptors. There are 5 different DA receptors subdivided into two families: D1-like (D1 and D5) and D2-like (D2, D3 and D4) receptors. These receptors are G-protein coupled receptors (GPCRs) that differ in their downstream targets and biochemical properties[18]. D1-like receptors are coupled to Gα-Syn proteins and activate the enzyme adenylate cyclase (AC) to stimulate cyclic AMP (cAMP) production for a net excitatory effect; D2-like receptors are coupled to $G\alpha_{i/o}$ proteins and inhibit AC to prevent cAMP production for a net inhibitory effect[19, 20] (**Fig 1**). Interestingly, D2 and D3 receptors offer a further level of DA regulation, as they can also be found as presynaptic autoreceptors that participate in a negative feedback loop to sense extracellular dopamine and help inhibit further synthesis or release[21]. In relationship to the basal ganglia circuitry, D1-like receptors are expressed by MSNs of the direct pathway, while D2-like receptors are expressed by MSNs of the indirect pathway[22]. Dopamine stimulates D1-like receptors at

the striatum to increase thalamic excitation of the cortex via the direct pathway, while it inhibits the striatum through D2-like receptors via the indirect pathway to decrease inhibition of thalamic excitation of the cortex (**Fig 1**). Thus, in the case of PD, the loss of DAergic input to the striatum affects both pathways to decrease thalamic excitation of the motor cortex, resulting in the characteristic hypokinetic responses of the disease.

***PD Pathophysiology: Molecular Mechanisms***

Upon understanding the role of the SNpc in the neural movement circuitry, it is apparent that the loss of DAergic innervation to the striatum would result in the opposite outcome of the direct pathway to produce the characteristic hypokinetic response seen in PD. However, the molecular mechanisms behind PD pathophysiology are still not fully understood. Currently known cellular processes that may be behind the neurodegeneration include aberrant protein folding and aggregation; mitochondrial dysfunction and increased oxidative stress; and proteasomal impairments[23]. In terms of PD-associated protein aggregation, the best example is the role of the protein alpha-synuclein (α-Syn). Aggregation of this protein into cellular inclusions known as Lewy bodies is considered to be a pathological hallmark of PD[24]. Yet, the physiological role of α-Syn is still not fully understood. Studies have linked α-Syn to presynaptic vesicle formation and recycling, as well as decreased vesicular DA release that may be related to its ability to bind phospholipids and vesicular fusion machinery[25-27]. α-Syn aggregation has also been shown to affect TH and AADC activity, implicating impaired dopamine biosynthesis as a potential mechanism behind its toxicity[28, 29]. Additionally, α-Syn has been shown to interact with and modulate DAT, though it remains unclear

whether this results in enhanced DA reuptake via increasing DAT clustering[30], or through an attenuation of its activity[31].

Mitochondrial dysfunction and oxidative stress also play a major role in PD pathophysiology. Several studies have implicated impaired Complex I activity in the electron transport chain (ETC) and impaired mitochondrial protease activity in PD patients[32, 33]. Moreover, downregulation of genes encoding vital mitochondrial proteins have been evident in DAergic neurons from patients suffering with PD[34]. Changes in mitochondrial organization have also been associated with PD. The importance of mitochondrial integrity has specifically come under investigation, as two PD-associated proteins, PINK1 and Parkin, have recently been identified as key modulators of mitophagy, and will also be discussed later in this section. This process involves the degradation of damaged mitochondria that require mitochondrial PINK1 to recruit cytoplasmic Parkin, an E3 ubiquitin ligase, to facilitate the turnover[35]. Moreover, these proteins also interact with mitochondrial fusion and fission factors, such as mitofusin 2 (Mfn2) and Drp1, to maintain a proper balance in mitochondrial network integrity[36, 37]. Thus, in the absence of either of these proteins in their functional form, aggregation of damaged mitochondria, and/or an imbalance between mitochondrial fusion and fission, can result in cell death.

Outside of direct mitochondrial deficits in PD, overall oxidative stress is also evident. Oxidative stress can be viewed as an imbalance between the production of reactive oxygen and nitrogen species (RONS) and the cellular antioxidant defense mechanisms against RONS. A key factor in tilting the balance towards enhanced RONS levels is dopamine itself, a strong auto-oxidant that can produce damaging quinones

and free radicals to promote cell death[38]. Toxins, metals and oxygen itself can further catalyze the formation of these reactive intermediates, as redox-active metals can enhance the natural redox cycling of quinones to further generate excess free radicals. DA quinones can promote cellular damage by conjugating with cysteine residues of proteins, resulting in alterations in protein function, such as that seen with tyrosine hydroxylase and α-Syn[39, 40]. Quinone formation has also been associated with decreased mitochondrial function[41]. Antioxidants like glutathione (GSH) can counteract these damaging effects by acting as a quinone quencher[42]. GSH is a tripeptide composed of glutamate, glycine and cysteine, with the reactive thiol group in the cysteine residue acting as the RONS scavenger[43]. A decreased ratio of reduced forms vs. oxidized forms (GSH/GSSG) is often used as a measure of increased oxidative stress, with decreased levels of reduced GSH found in the SN of PD brains[44]. As this system also depends on a physiological balance, both GSH depletion and GSH overproduction can result in DAergic cell death, with the latter most likely representing a compensatory mechanism to protect against further cell death.

Connecting these pathophysiological perturbations in PD are impairments in proteasomal or autophagic function, resulting in protein or organellar accumulation, respectively. The ubiquitin proteasome system (UPS) is a key system in mediating the process of protein degradation[45]. This process begins with poly-ubiquitination of substrate proteins by ubiquitin-conjugating enzymes, followed by degradation of the tagged proteins in the 26S proteasome[46]. Proteasomal enzymatic activity has been shown to be impaired in the SN of idiopathic PD patients[47]. Furthermore, as age is a significant risk factor for neurodegenerative diseases like PD, it has also been shown

that aging is associated with alterations in the proteasome system[48]. One of the enzymes involved in the UPS is Parkin, which also happens to be a major genetic risk factor for an early-onset, autosomal recessive form of PD. Interestingly, patients with *parkin* mutations do not show the characteristic Lewy body pathology[49], suggesting that Parkin may play a role in their formation. Parkin has been shown to ubiquitinate a glycosylated form of α-Syn[50] that may also involve targeting the protein synphillin-1, an α-Syn-interacting protein[51]. As aforementioned, in addition to protein degradation, Parkin also mediates organelle turnover by participating in mitophagy. Thus, the loss of *parkin* can be majorly detrimental to the cell, as both abnormal protein and mitochondrial buildup can result in cell death.

***PD Models***

Currently, several types of models exist to understand how the mechanisms behind PD may result in DAergic cell death. Both pharmacological and genetic tools have been used to explore the disease, with attempts to recapitulate the major features of the disease, including DAergic cell death and/or motor deficits.

*Pharmacological Models*

MPTP**:** 1-methyl-4-phenyl-1,2,3,6-tetrahydropyridine (MPTP) and its metabolite $MPP^+$ (1-methyl-4-phenylpyridinium ion) are well-known neurotoxins used to model PD. The discovery of MPTP as a PD model arose accidentally, as illicit Californian drug users in the 1980s were diagnosed with Parkinsonism after using a contaminated batch of MPPP, a synthetic drug that mimics effects of morphine and meperidine. Researchers later identified MPTP in the drug as the culprit behind the Parkinsonism[52]. MPTP was

later confirmed to produce Parkinsonism in monkeys exposed to MPTP in addition to SN-selective cell death[53]. MPTP is converted into $MPP^+$ by MAO-B and then taken up by DAT into DAergic neurons, where it inhibits mitochondrial Complex I activity. MPTP administration in primates results in Parkinsonism that responds to L-DOPA and shows all cardinal motor symptoms of PD. Similar results have been achieved in studies using mice. However, MPTP-induced lesions of the SNpc do not present with the formation of Lewy bodies.

6-OHDA: This model utilizes 6-hydroxydopamine (6-OHDA), or oxidopamine, to result in degeneration of the nigrostriatal pathway, and represents the first-ever pharmacological PD model[54]. Administration of this DA analog must be done locally through intracranial injections, as 6-OHDA does not pass the blood brain barrier (BBB) and can unselectively affect all catecholaminergic neurons[55]. Once in the brain, 6-OHDA acts as a hydroxylated DA analog and is taken up into DAergic neurons via DAT[56]. 6-OHDA is of particular interest in PD due to its endogenous nature as a toxic DA metabolite that is produced from a non-enzymatic reaction between DA, hydrogen peroxide and free iron at physiological concentrations[57]. Moreover, *in vivo* production of 6-OHDA is more likely to occur in the highly oxidizing environment of DA neurons, as 6-OHDA auto-oxidation increases production of hydrogen peroxide and free radicals, including the superoxide ion and hydroxyl radical[58]. These RONS are most likely generated through 6-OHDA metabolism or direct inhibition of complex I and IV of the mitochondrial ETC[59, 60], and result in PD-associated molecular signatures, including increased lipid peroxidation, protein denaturation and increased GSH[58].

Pesticides: Exposure to pesticides has long been associated as environmental risk factors for the development of PD. One such pesticide is rotenone, a plant flavonoid that is used as a broad-spectrum pesticide. Rotenone is able to easily cross the BBB and does not require DAT to enter DAergic neurons[61], where it inhibits complex I of the ETC[62], resulting in the production of RONS. Unlike the other toxin models, rotenone exposure does exhibit α-Syn Lewy body inclusions, as well as degeneration of DAergic cells in the nigrostriatal pathway that results in PD-like motor deficits[63]. However, some doubts have been cast on the selectivity of rotenone-induced cell death towards nigrostriatal DAergic neurons[64, 65]. Another pesticide used as a toxin model of PD is paraquat, a non-selective herbicide that shares structural similarities with MPTP[66]. While paraquat cannot cross the BBB, its precise uptake mechanism is unknown. Studies indicate that paraquat may enter the brain through a carrier-mediated mechanism like a neutral amino acid transporter similar to LAT-1[67], followed by a DAT-independent, $Na^+$-dependent uptake mechanism to facilitate entry into DAergic neurons[61, 68]. Once inside neurons, paraquat induces rampant oxidative stress by producing superoxide free radicals from undergoing redox cycling[69], as well as promoting a pro-apoptotic cascade involving Bak and Bax, cytochrome c release and caspase-9 activation[70]. Similar to rotenone, paraquat exposure in rodents does result in α-Syn aggregation in the SNpc, as well as loss of nigrostriatal DAergic neurons and motor impairments[66, 71].

LPS: Neuroinflammation has recently come to light as a component of PD pathogenesis. Accordingly, local administration of the bacterial endotoxin lipopolysaccharide (LPS) into the nigrostriatal tract results in DAergic neurodegeneration[72]. This model relies on LPS-

induced activation of glia that subsequently release soluble factors, such as cytokines, RONS, and lipid metabolites that induce nigral cell death and motor deficits in animals[73].

*Genetic Animal Models*

Although the majority of PD cases are sporadic in nature, about 10-20% of PD has documented genetic causes. Many PD-associated genes have been identified, including *dj-1*, *pink1*, *parkin*, *nurr1, lrrk2, uch-l1,* and *SNCA*[2]. In light of the work presented in this thesis, the current chapter will specifically focus on the three autosomal recessive genes responsible for early-onset PD, *parkin*, *pink1* and *dj1*, and the autosomal dominant gene for α-Syn, *SNCA*.

Parkin: *PARK2/parkin* encodes for a protein that consists of 465 amino acids, and contains a ubiquitin-like domain that is responsible for substrate recognition, along with RING finger domains that interact with other components of the UPS[74]. Parkin expression in the brain is distributed within basal ganglia structures, including the SN and caudate-putamen, but with some expression in the cerebellum as well[75]. Beside itself, Parkin has many substrates, including the synaptic vesicle-associated protein CDCrel-1[49], α-Syn[50], synphilin-1[51], and the membrane receptor Pael-R[76]. Parkin has also recently been shown to form an E3 ligase multi-protein complex with DJ-1 and PINK1, two other proteins implicated in PD[77]. Homozygous mutations found in *parkin* have been linked to an early-onset familial form of PD, with no presence of Lewy bodies[74]. *Parkin* mutants show altered intracellular localization, along with altered substrate binding and enzymatic activity. Consequently, a functional effect of mutations in this gene is an inability to degrade substrate proteins[78]. *Parkin* -/- mice show an

increase in extracellular striatal DA concentration[79], while wildtype *parkin* seems to increase cell surface expression of DAT for increased DA reuptake[80]. *Parkin* -/- mice also show impairments in synaptic plasticity[81], as parkin seems to negatively regulate the strength and number of excitatory synapses[82]. However, while *parkin* knockout mice do not show overt loss of DAergic neurons[79], mice expressing a truncated version of Parkin show both DAergic degeneration as well as hypokinetic deficits[83].

PINK1**:** Similar to *parkin*, homozygous mutations in *PARK6/pink1* also result in an early-onset form of PD[84]. Its protein product, PINK1 (PTEN-induced kinase 1) is a mitochondrial serine/threonine kinase with an N-terminal mitochondrial targeting sequence. PINK1 distribution appears to be uniform through the cortex, striatum, thalamus, brainstem and cerebellum[85]. Familial mutations result in defective kinase activity[86] that is normally necessary for mitochondrial integrity, as its phosphorylation targets include mitochondrial fission and fusion factors[87], as well as the mitochondrial serine protease HtrA2[88]. Early effects of PINK1 loss in rats include decreased Complex I levels and increased ETC proton leak prior to the development of PD symptomatology[89]. Moreover, wildtype PINK1 has been shown to protect against mitochondrial toxin-induced DAergic cell death, as well as reducing apoptotic caspase levels and cytochrome c release from mitochondria[90]. Despite not showing loss of DAergic neurons, *pink1* knockout mice show impaired DA release and age-dependent motor deficits that were accompanied by reduced striatal DA levels[91, 92]. As both *parkin* and *pink1* knockout models have not confidently shown selective DAergic neurodegeneration on their own, a fish model and mouse embryonic fibroblasts lacking both *parkin* and *pink1* shows both DAergic cell loss, locomotor dysfunction, and overt

mitochondrial deficits[93]. Such evidence brings to light the interconnected pathways between PINK1 and Parkin in PD, with Parkin able to rescue PINK1 loss[94]. Parkin is a PINK1 phosphorylation target, as PINK1's kinase activity necessary to recruit Parkin to mitochondria with a lowered membrane potential[35, 95, 96]. Various modulators of this interaction have recently been introduced, including the Mtfn2 and voltage-dependent anion channels (VDACs)[36, 97]. The teamwork between Parkin and PINK1 reveals the importance of maintaining proper mitochondrial trafficking and turnover, signifying an impaired clearance of defective mitochondria as a potential mechanism behind PD pathophysiology.

DJ-1: Moreover, mutations in *PARK7/dj-1* are also responsible for an autosomal recessive, early-onset form of PD[98]. Originally identified as an oncogene, this gene encodes for DJ-1, a redox-sensitive chaperone protein that translocates from the cytoplasm to mitochondria following oxidation of a cysteine residue[99]. DJ-1 shows both peroxiredoxin-like peroxidase and glyoxylase activity[100, 101]. Mutations in *dj-1* result in increased RONS levels and impaired mitochondrial energetics[102], while overexpression of WT DJ-1 protects against DA toxicity and cell loss[103]. However, similar to *parkin* and *pink1* knockout mice, DJ-1$^{-/-}$ mice do not show overt DAergic neurodegeneration in the SN, but do show alterations in DA reuptake and mitochondrial dysfunction[104, 105]. DJ-1 may also protect cells through stabilization of the antioxidant transcription factor Nrf2 by blocking its interaction with its inhibitor protein Keap1[106]. Interestingly, DJ-1 has also been shown to form a multi-protein complex with parkin and pink1[77], though this remains controversial. Moreover, DJ-1 up-regulation can rescue the loss of PINK1-mediated sensitization of DAergic neurons in the SNpc to a mitochondrial toxin[94]. The

rescue of *pink1* loss-mediated mitochondrial deficits by DJ-1 was also seen in *Drosophila*, but showed no rescue in *parkin* mutants[107]. These data reveal a role of DJ-1 acting in parallel with the parkin/pink1 pathway.

α-Syn: As previously mentioned, α-Syn plays a curious role in PD. *SNCA* encodes for this protein[108]. As the physiological role of α-Syn remains unclear, it is still under debate whether the protein is neuroprotective or neurotoxic. This disparity may be related to the overall expression level of the WT form. Low or wildtype expression of the protein may be protective against oxidative insults[109], while high intracellular levels can promote abnormal and pathogenic aggregation of the protein[110]. Toxicity could also arise from its genetic state, as PD-associated mutations (A53T, A30P and E46K) can result in increased aggregation of the protein[111, 112]. A53T transgenic mice show aggregation of α-Syn that led to progressive neurodegeneration and significant motor deficits in contrast to mice expressing WT α-Syn[113]. Recent evidence has also suggested that the distinctive pathogenic mutations may result in unique fibril conformations, with A53T and E46K mutations exhibiting differences in secondary structures[111]. A53T transgenic mice also exhibit mitochondrial DNA damage and degeneration in neocortical, brainstem and motor neurons[114]. However, the severity of PD-associated phenotypes in their regional selectivity in α-Syn-mice may also be dependent on specific promoter-driven expression. Mice overexpressing a pan-neuronal promoter-driven α-Syn for broad neuronal expression show preferential mitochondrial dysfunction in nigrostriatal DAergic neurons significantly earlier before loss of striatal dopamine[115]. Moreover, similar to the early-onset genetic models discussed above, transgenic α-Syn models have also struggled to recapitulate full DAergic neurodegeneration, despite showing

subtle changes in the nigrostriatal circuitry and/or damage to motor neurons and other neuronal circuits[116]. As with the potential interplay between the aforementioned autosomal recessive genes, interactions also exist with α-Syn itself. In addition to the aforementioned putative role of Parkin-mediated α-Syn regulation, DJ-1 has recently been found to protect against α-Syn (A30P)-mediated toxicity in DAergic neurons[117], with wildtype DJ-1 able to reduce α-Syn dimerization[118]. As can be expected, the loss of both *pink1* and overexpression of the A53T α-Syn mutation in mice results in increased neurotoxicity compared to either the loss of *pink1* or the expression of A53T alone[119]. Similarly, *pink1* overexpression has also shown rescue of α-Syn-induced locomotion and aging effects in *Drosophila*[120].

## Manganese

*Portions of this section have been published in the book chapter "Manganese" in Binding, Transport and Storage of Metal Ions in Biological Systems written by Chakraborty, Martinez-Finley, Caito, Chen and Aschner, as well as a review article in Toxicology Research written by Chen, Chakraborty, Peres, Bowman and Aschner.*

### *Routes of Exposure*

Manganese (Mn) is an essential heavy metal that comprises nearly 0.1% of the earth's crust. It is the 5$^{th}$ most abundant metal and 12$^{th}$ most abundant element overall, usually existing in its natural form in the environment as oxides, carbonates and silicates. As erosion produces a naturally ubiquitous presence of Mn in air, soil and waterways, the human population is readily exposed to Mn through a variety of environmental sources. However, the primary route of Mn exposure is through dietary

intake, as several Mn-containing foods are found in human diets. Legumes, rice, nuts and whole grains contain the highest Mn levels, while Mn is also found in leafy green vegetables, tea, chocolate, and fruits like blueberries and acai[121]. Mn-containing nutritional supplements and vitamins are commonly taken on a daily basis, in addition to infant formulas that contain a trace element-enriched solution. The abundant Mn-containing dietary sources allow humans to obtain the proper Mn levels (2.3 mg/day for men and 1.8 mg/day for women) necessary for several important physiological processes, including development, digestion, reproduction, immune function, energy metabolism and antioxidant defenses.

Outside of dietary sources, exposure to inorganic forms of Mn can occur in several industrial settings, as Mn is used in the manufacturing of steel, batteries, fireworks, as well as ceramics, cosmetics, leather, glass and textiles. On the other hand, organic Mn is also highly prevalent in the environment, as Mn is a major component of the antiknock gasoline additive methylcyclopentadienyl Mn tricarbonyl (MMT), as well as fungicides and pesticides (e.g. Maneb and Mancozeb), smoke inhibitors, and as a medical magnetic resonance imaging (MRI) contrast reagent[121].

***Intestinal Uptake and Release***

Ingestion is the most common route for Mn exposure. The typical adult ingests <5 mg Mn/kg, coming mostly from grains, rice, nuts, tea, and chocolate. Around 3-5% of ingested Mn is absorbed in adult humans, with radiolabeled $^{54}$Mn uptake studies showing that for a meal containing 1 mg Mn, adult males absorb 1.35 ± 0.51% while adult females absorb 3.55 ± 2.11%[122, 123]. Mammalian tissues typically contain 0.3-2.9

mg Mn/g wet tissue weight[124]. Turnover of ingested Mn is quick, with the mean retention of Mn 10 days after ingestion estimated at 5.0 ± 3.1% in women[125]. Mn levels are tightly controlled by absorption by the gastrointestinal (GI) tract and excretion by the liver. The majority of excreted Mn is in conjugation with bile in the liver and secreted into the intestines for elimination in the feces[122, 126]. There is a small amount of Mn that is reabsorbed in the intestines from the bile, forming an enterohepatic circulation[127]. Small amounts of Mn can also be excreted by the pancreas or via urine[122].

Molecular mechanisms of Mn uptake by intestinal cells are not well characterized. Early studies using rat brush border membrane vesicles found evidence of a lactoferrin receptor-mediated uptake of Mn[128]. Studies using the Caco-2 intestinal cell line derived from human colonic carcinoma revealed a biphasic uptake process, indicating that transport falls into its steady-state condition following a brief period of equilibration between intraceullar and extracellular components[129]. Moreover, *in vivo* studies using rat intestinal perfusions have found that intestinal Mn uptake involves a high affinity, low capacity active transport process that is rapidly saturable[130]. It is thought that Mn can enter cells either through passive diffusion or active transport via the divalent metal transporter 1 (DMT1)[131, 132]. DMT1 is a transporter that uses the cell membrane's proton gradient to move several divalent metals across the cell membrane, including Mn, Fe, and Cu[132], and will be discussed in more detail later in this chapter. Due to this shared transport mechanism, trace metals have been shown to influence the amount of Mn absorbed. Other dietary components that alter Mn absorption include phytates and ascorbic acid[133].

Absorption of Mn by the GI tract is modulated by a variety of factors. The concentration of Mn in the diet influences both the absorption of Mn and its elimination in bile. When instances of high Mn intake occur, either through the diet or environmental exposure, the GI tract absorbs less Mn, the liver increases metabolism, and there is increased biliary and pancreatic excretion[122, 134, 135]. Gender influences Mn uptake, with males absorbing significantly lower amounts of Mn than females[122, 123]. This may reflect men's higher iron status and higher serum ferritin concentrations, which may compete with Mn for transport by DMT1. Age is another determinant of Mn absorption. Younger individuals, particularly infants, absorb and retain higher levels of Mn than adults[136, 137], likely because their necessity for Mn is much higher than adults. Data concerning the intestinal absorption of Mn in infants compared to adults are limited, but studies have examined the detrimental effects of total parenteral nutrition (TPN) in severely ill or premature infants. These solutions are usually supplemented with a trace element solution that contains small amounts of Mn. However, unlike the minimal absorption of Mn from milk, the intravenous exposure to Mn-supplemented TPN solutions results in bypass of any intestinal control of absorption. Consequently, nearly 100% of Mn can be absorbed, resulting in conditions of toxicity in these vulnerable neonates. These infants also pass little stool, leading to even higher retention of Mn[138].

***Transport Across the Cell Membrane***

To date, Mn is a unique heavy metal in that it does not have its own group of cellular transport proteins. Rather, it "piggybacks" on transport systems known to regulate other heavy metals. $Mn^{3+}$ is mostly found complexed with the transferrin protein (Tf), which is then imported by the transferrin receptor (TfR). Following endocytosis of

this complex, Mn is released via endosomal acidification through a vacuolar ATPase (v-ATPase)[139], at which point $Mn^{3+}$ is converted to $Mn^{2+}$. However, divalent Mn is more prelavent than trivalent Mn and can be transported via the divalent metal transporter 1 (DMT1)[140]. DMT1-mediated Mn import, the primary mode of Mn uptake, is also dependent on the proton gradient generated by a v-ATPase[141]. DMT1 can be found on endosomal membranes to transport converted $Mn^{2+}$ into the cytoplasm, as well on the plasma membrane (**Fig 2**). DMT1 expression has been shown to co-localize with TfR[142], indicating overlap between the two systems.

DMT1, originally known as DCT1 (Divalent Cation Transporter 1) or NRAMP2 (Natural Resistance Associated Macrophage Protein 2), transports a variety of divalent metals, including $Mn^{2+}$, $Fe^{2+}$, $Cu^{2+}$, $Zn^{2+}$, $Co^{2+}$ and $Cd^{2+}$. It was originally associated with iron transport, as a missense mutation in anemic Belgrade rats or microcytic mice was found to impair Fe uptake[143, 144]; however, its affinity to Mn is similar to that of Fe[145]. It has 12 transmembrane domains, and metal transport is coupled to the co-transport of a proton. While having ubiquitous tissue expression, DMT1 shows highest localilzation in the intestine, kidneys and brain. Light and electron microscopy has also found DMT1 expression in glial cell bodies of the neocortex, subcortical white matter, and the hippocampus[146], while immunocytochemistry has found dense DMT1 staining in the caudate, putamen, and SNpr of the monkey basal ganglia[147]. Rat pups exposed to Mn have increased levels of Mn *in vivo*, as well as increased DMT1 protein expression throughout the brain[148]. Similarly, increased Mn uptake is seen upon impaired cellular iron status in astrocytic cultures, corresponding with enhanced DMT1 protein expression in these cultures[149].

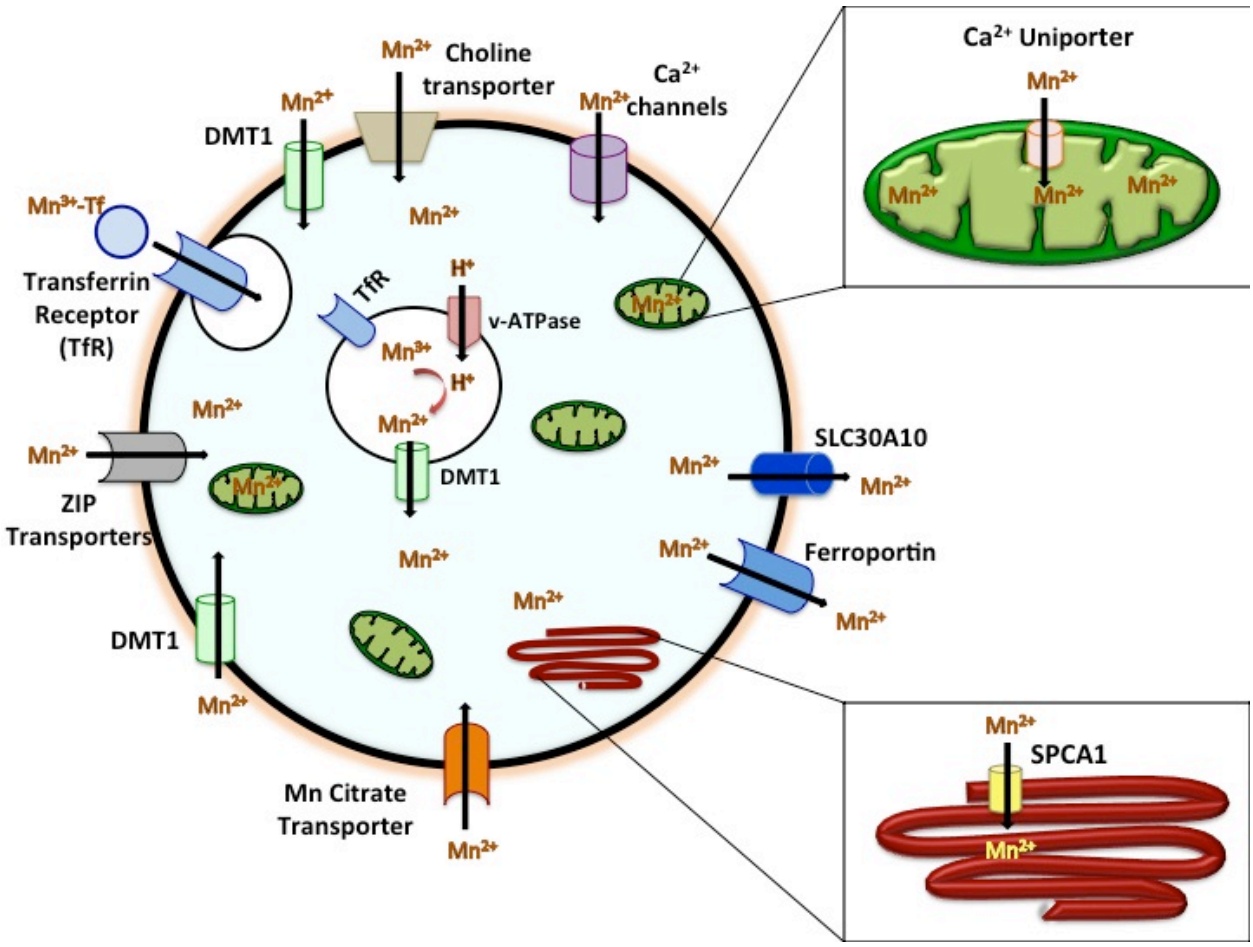


**Figure 2.** *The mammalian Mn transport system.* Various proteins involved in Mn transport into, within and out of the cell, including transport across the plasma membrane, as well as into the Golgi lumen and mitochondrial matrix.

While DMT1 is the primary mode of Mn uptake, other transporters also facilitate Mn uptake. For example, Mn can enter cells through the Zn transporters ZIP8 and ZIP14 that show high affinity for $Mn^{2+}$ among other metals[150, 151]. These proteins are $Mn^{2+}/HCO_3^-$ symporters that facilitate Mn uptake into the brain, liver and kidneys. Another example is the choline transporter; in situ rat brain perfusion techniques show inhibition of brain choline uptake by $Mn^{2+}$ and/or $Cd^{2+}$, but not $Cu^{2+}$ or $Al^{3+}$ ions[152]. Mn can also be taken up through voltage-gated and store-operated calcium channels, and ionotropic glutamate receptor $Ca^{2+}$ channels. These studies used electron paramagnetic resonance (EPR), calcium-selective dyes (Fura2) and calcium competition/inhibition studies to show the permeability of $Ca^{2+}$ channels by $Mn^{2+}$ ions[153-155]. Studies have also found a citrate transporter that can facilitate entry of Mn[156], and Mn-bound citrate may be a substrate for the organic anion transporter, the monocarboxylate transporter (MCT), or members of the organic anion transporter polypeptide or ATP-binding cassette families[157]. Despite the breadth of knowledge concerning non-DMT1 transport mechanisms, it is relatively unknown how much these secondary mechanisms contribute to overall Mn uptake (**Fig 2**).

***Buffering and Other Regulatory Mechanisms***

Upon entering the cytoplasm, further mechanisms exist to help buffer intracellular Mn concentrations. Mn shows preferential accumulation in the mitochondria and is taken up by the mitochondrial calcium uniporter[158, 159]. This uniporter contains an external activation site that can bind $Ca^{2+}$ to enhance uptake of both $Ca^{2+}$ and $Mn^{2+}$ through a specific transport site. Meanwhile, Mn efflux out of the mitochondria occurs through a very slow process that is $Na^{2+}$-independent[159]. Moreover, the Golgi complex

also helps to sequester intracellular Mn through the secretory pathway $Ca^{2+}$/ $Mn^{2+}$-ATPases (SPCAs). These pumps can bring in $Mn^{2+}$ into the Golgi lumen (**Fig 2**), and show high expression in the brain[160]. Mutations in the SPCA1 gene (*atp2c1*) result in Hailey-Hailey Disease, an adult-onset skin condition that is characterized by frequent blistering and erosions[161]. High $Mn^{2+}$ concentrations can inhibit ATPase activity of the pump, resulting in breakdown of Golgi organization in neurons that can be partially reversed by Mn chelation via EDTA (ethylenediaminetetraacetic acid)[162]. This indicates that SPCAs are effectively able to pump $Mn^{2+}$ into the Golgi complex at lower concentrations, whereas higher concentrations result in inhibition and breakdown.

Additional homeostatic processes can include binding to Mn-dependent metalloenzymes or proteins. As Mn is a vital cofactor for many enzymes, proper metalloregulation is key in promoting optimal intracellular Mn levels, with some of this regulation occurring in a cell type-specific manner. Within the brain, astroglia are thought to be a significant sink for Mn accumulation. This is primarily due to the localization of glutamine synthetase (GS) within astroglia, an enzyme necessary for the glutamate-glutamine shuffle. Nearly 80% of brain Mn is found associated with GS, as Mn is a necessary cofactor for GS activity[163]. Consequently, the abundance and selectivity of Mn accumulation in these cells can result in astroglia being the initial targets of toxicity. Similar to GS, there are several other enzymes that require Mn for proper enzymatic function. These include Mn-SOD or SOD2, the aforementioned antioxidant mitochondrial protein that converts superoxide into hydrogen peroxide and $O_2$. Another Mn-containing mitochondrial protein is pyruvate carboxylase (PC), which catalyzes the carboxylation of pyruvate to oxaloacetate and serves as a bridge between

carbohydrate and lipid metabolism[164]. PC can depend on a magnesium ion instead of one Mn ion as a cofactor for proper functioning[165]. Yet another Mn-containing metalloenzyme is arginase (ARG1 and ARG2). This enzyme plays a vital role in the urea cycle, and requires two Mn ions in order to convert arginine into urea and ornithine[166]. Finally, certain serine/threonine protein phosphatases (PPMs) are also metal-dependent (PP2C), requiring two $Mg^{2+}$ or $Mn^{2+}$ ions for their function in dephosphorylating proteins at their serine and threonine sites, a very important post-translational protein modification[167].

Genetic regulation of Mn transporter expression also plays a role in proper Mn homeostasis. Mammalian systems show evidence of the important role of transcriptional regulation of Mn transporters, such as that of DMT1[168]. DMT1 has four mRNA isoforms encoding four different proteins that differ either in their N- and C-terminals or 5' vs. 3' processing. Two of the alternatively spliced isoforms differ in their transcription start sites: Exon 1A contains an AUG codon that extends its N-terminal, while Exon 1B lacks this initiator codon and, consequently, has translation begin in exon 2. Meanwhile, two of the isoforms contain an iron responsive element (IRE) in the 3' UTR of the DMT1 mRNA. IREs serve as a very important sensing mechanism. If iron levels are low (which can indirectly affect intracellular Mn concentrations), iron regulatory proteins (IRPs) are thought to bind the IRE in the IRE-containing DMT1 isoforms to stabilize the IRE-containing message[169]. The presence of such isoforms and the influence of iron on their expression most likely has an effect on intracellular Mn concentrations as well, though further studies must be conducted to look at their direct relationship. Interestingly, Parkin has been shown to promote degradation of an isoform of DMT1 *in vitro* through

the proteasome[170].

***Manganese Efflux***

Until recently, the only known Mn efflux mechanism in vertebrates at the cell membrane was through the iron exporter ferroportin (FPN) (**Fig 2**). This protein consists of 12 transmembrane domains, with mutations resulting in the iron overload diseases "ferroportin disease" or type 4 haemochromatosis[171]. FPN is regulated by the hormone hepcidin, which promotes its internalization and degradation to help regulate optimal Fe levels; FPN mutations can also cause inefficient binding to hepcidin to impair this process[172]. In terms of Mn transport, Yin et *al.* have demonstrated that Fpn expression decreases Mn accumulation in cells to help ameliorate Mn-induced cytotoxicity by rescuing cell membrane leakage and Mn-induced reductions in glutamate uptake. Moreover, mice exposed to Mn exhibit increased FPN protein levels in the cortex[173]. These findings were further supported by export of Mn in *Xenopus laevis* oocytes expressing human FPN (SLC40A1)[174], where Mn accumulation was decreased in a concentration-dependent manner and could be inhibited by lower pH levels. Moreover, FPN-mediated Mn efflux can also be partially inhibited by addition of Fe, Co or Ni[174]. However, it is currently unclear whether FPN is able to export the same range of divalent metals that a transporter like DMT1 can import. Mitchell et *al.* showed evidence in oocytes of Co and Zn efflux through FPN, but also disagreed with previous studies in FPN's ability to efflux Mn[175]. Though additional studies must be conducted to further FPN's role in Mn toxicity, it is logical that Mn would share the same exporter as Fe in the same way they share uptake routes.

Interestingly, recent findings from Tuschl et *al*. have described the zinc transporter, SLC30A10*,* as another putative Mn exporter. This study utilized whole-genome homozygosity mapping and sequencing to find alterations in the *SLC30A10* gene sequence in families with hypermanganesemia and Parkinsonism. Human wildtype (WT) *SLC30A10,* and/or *SLC30A10* missense or nonsense mutations were inserted into the Mn-sensitive yeast strain *Δpmr1.* It was found that *Δpmr1*-expressing wildtype *SLC30A10* rescued growth, while *Δpmr1* expressing *SLC30A10* mutations retained Mn sensitivity, suggesting that WT *SLC30A10* is important for Mn efflux[176]. Moreover, a comprehensive study by Leyva-Illades et *al.* recently established SLC30A10 as a plasma membrane-localized Mn exporter (**Fig 2**) in both the invertebrate *Caenorhabditis elegans* model and primary midbrain neurons cultured from WT mice. Mutations in this gene associated with familial Parkinsonism resulted in impaired trafficking of the transporter to the cell surface, diminished Mn efflux and increased sensitivity to Mn exposure[177]. The role of impaired metal homeostasis in Parkinsonism is further supported by the ability of metal chelation in patients with mutated *SLC30A10* to improve clinical symptoms, decreased blood Mn levels and improved MRI hyperintensities in the basal ganglia[178, 179]. While chelation may take a longer duration to reverse Parkinsonism in patients carrying *SLC30A10* mutations, these studies still highlight the importance of treatable Parkinsonism that is associated with metal transporter mutations.

***Manganese Toxicity***

The wide variety of proteins involved in regulating Mn reflects the need to balance homeostasis between necessity and toxicity, as excess Mn can result in a

neurotoxic condition known as “manganism.” James Couper first identified this condition in 1837 in five industrial workers exposed to high levels of manganese from the use of manganese oxide in the production of chloride for bleaching power. Mn poisoning leads to irreversible damage to the basal ganglia brain region that is also affected in PD, resulting in similar cognitive, emotional and motor deficits[157, 180]. This condition mostly arises from occupational exposure to Mn, including miners, welders, smelters and other industrial workers who handle Mn-containing steel and other manufacturing, and subsequently inhale fumes containing high levels of Mn[181, 182].

In addition to industrial workers exposed to high Mn levels at their workplace, there are other populations at risk of Mn-induced toxicity. Patients suffering from hepatic encephalopathy or any stage of liver failure are at high risk of Mn toxicity, as a properly functioning biliary system is required for proper Mn excretion[183]. Similarly, unhealthy neonates partaking in Mn-supplemented TPN are also vulnerable to Mn toxicity[184]. Another significant population at risk for Mn poisoning are those suffering from Fe deficiency, one of the most common nutritional deficiencies in the world. This is due to the fact that Fe and Mn compete for the same transporters, resulting in higher Mn accumulation when Fe levels are low[185, 186]. Thus, in people suffering from chronic iron deficiency (e.g. iron deficiency anemia), low levels of Fe can result in high Mn accumulation over time.

***Manganism & PD***

Despite their overlap, manganism is still a differential diagnosis from PD, with distinctive areas of initial cell death that produce some contrasting symptomatology.

Though bradykinesia and rigidity are still noticeable, tremor is not as evident in Manganism patients[187]. Moreover, unlike PD, dystonia is more highly prevalent in manganism; patients also exhibit a tendency to fall backwards.[188] Similar to PD, however, manganism is progressive in nature, with only partial recovery of certain symptoms following elimination of the source of overexposure for an extended period of time[189].

While PD initially targets the DAergic cells of the SNpc, Mn preferentially accumulates in and damages the GABAergic cells of the globus pallidus and corpus striatum before spreading to other brain regions[187, 190, 191]. Consequently, the major difference lies in the fact that one condition destroys cells responsible for dopamine production, while the other targets the receptor cells that react to dopamine. Distinguishing between the two conditions relies heavily on a variety of biomarkers and tests specific for each condition. Diagnostics using magnetic resonance imaging (MRI) techniques can visualize the increased signal intensities in the globus pallidus in T1-weighted images, though they will disappear within six months to a year of removing the source of Mn exposure. Moreover, a positron emission tomography (PET) scan can also distinguish between manganism and PD: manganism patients show a normal scan, while PD patients show reduced striatal uptake of the radioactively labeled analog of the dopamine precursor DOPA (18-fluorodopa)[187, 192]. Another potential biomarker for manganism was recently identified using voxel-based morphometry (VBM). The study found that compared to healthy control subjects, welders chronically exposed to Mn possess decreased brain volumes in the globus pallidus and cerebellum that correlate with cognitive and motor deficits[193]. Another key difference between manganism and PD

is the lack of effectiveness of L-DOPA treatment for manganism, contrary to PD[194]. Instead, treatment with the metal chelators EDTA and sodium para-aminosalicylic acid (PAS) has shown to be beneficial in some cases[195, 196], though this option may be most beneficial before the condition has progressed too far.

The association between occupational exposure to Mn-containing fumes (e.g., those experienced by welders) and Parkinsonism remains controversial in the literature. A cross-sectional study conducted in 2006 found a higher prevalence of Parkinsonism in Alabama welders compared to age-matched control subjects[197]. The same group recently published another study showing that Mn-exposed welding workers had similar scores (>15) on a commonly used questionnaire for PD motor evaluation (UPDRS3, or Unified Parkinson's Disease Rating Scale motor subsection 3) compared to newly diagnosed, untreated idiopathic PD (IPD) patients[181]. Yet, other studies have not found an increased risk for PD in welders. A 2012 Danish study[198] and a 2005 study using data from movement disorder clinics[199] found no positive association between PD and welding. However, the former study relied on hospital contacts, and the latter study relied on specialty clinic surveys to define Parkinsonism, compared to clinical examinations and/or the UPDRS3. The discrepancies in these studies may be due to differences in defining PD in their cohorts, as well as varying welding exposures to Mn.

The association between non-occupational Mn exposure and Parkinsonism is also unclear. A 2009 study from a mining district in Mexico found attention impairments in a population where a majority of participants were exposed to Mn in ambient air at levels higher than the recommended Environmental Protection Agency's (EPA) guidelines for non-occupational environments (>0.05 $\mu g/m^3$)[200]. Similarly, a study on the

general population living near a ferromanganese refinery in Ohio found slight, subclinical impairments in postural balance upon chronic exposures to Mn in ambient air[201]. Moreover, a recent 2013 study on a population living close to a manganese processing plant found decreased olfactory function compared to a population living far from the plant[202]. Yet, other studies have found minimal effects of Mn on the general population. A study on the role of MMT from gasoline combustion compared garage mechanics vs. blue-collar workers and found no significant difference between the two groups in whole blood Mn concentrations, with no obvious health problems[203]. Likewise, a more recent study found limited evidence for any association between ambient metal exposure in adults and the risk of PD using a nurses' cohort and the EPA Air Toxics data[204]. More studies must be done to investigate the long-term effects of chronic, low-dose Mn exposure to the general human population, be it from gasoline combustion or other non-occupational sources found in ambient air.

*Shared Molecular Mechanisms*

Though the literature remains disputed in the connection between environmental Mn exposure and Parkinsonism, the molecular mechanisms behind both PD and manganism share several key processes. A major hallmark of both conditions is increased oxidative stress. Similar to dopamine oxidation in PD, high Mn levels can result in increased oxidative stress through a variety of mechanisms. Mn can directly inhibit complexes of the electron transport chain in the mitochondria that are responsible for ATP production. This inhibition results in both the leakage of damaging free radicals, as well as ATP depletion in the cell[205]. Recent *in vitro* evidence using the human neuroblastoma SH-SY5Y cell line has found Mn-induced changes at the DNA level, with

increased accumulation of DNA single strand breaks and oxidized thymine bases. However, pre-treatment with antioxidants could rescue these signs of oxidative damage, further supporting the role of Mn in increasing oxidative stress in human cells[206]. Mn can also result in apoptotic cell death through the activation of multiple caspases[207-209]. Moreover, Mn-exposed Gli3 cells (a human astrocyte line) show a loss in mitochondrial membrane potential and caspase-9 activation, with concomitant alterations in mitochondrial fission and fusion protein levels resulting in enhanced fragmentation[210]. Manganese has also been shown to affect glutamate transporter levels and overall glutamate neurotransmission, resulting in cell death from glutamate excitotoxicity, a phenomenon also seen in PD[211]. Another hallmark of both conditions is increased protein aggregation, with dopamine oxidation as a potential modifier of protein aggregation states in PD[212]. Similarly, Mn can induce aggregation of α-Syn[213]. The crosstalk is further evident by the fact that Mn itself can enhance DA oxidation[214] and cause internalization of DAT[215]; Mn accumulation following high doses requires functional DAT specifically in the striatum[216].

The interaction between Mn toxicity and PD-associated proteins has recently become a focus of studies in humans. Increased expression of a DMT1 isoform has been found in the SN of PD patient brains, while DMT1 expression is also significantly increased in MPTP-treated mice that also exhibit enhanced Fe accumulation and DAergic cell death[217]. Furthermore, a specific polymorphism in DMT1 (the CC haplotype) has recently been associated with PD in a Chinese cohort[218]. In the first study of its kind, Aboud and colleagues differentiated fibroblasts into human induced pluripotent stem cell (hiPSC)-derived early neural progenitor cells (NPCs) from a patient

carrying a mutation in *parkin* and a control subject. Though no difference in Mn cytotoxicity or mitochondrial fragmentation was found between the subjects, increased Mn-dependent RONS generation was found in the NPCs carrying the *parkin* deletion[219]. Furthermore, the increased RONS occurred in the face of decreased Mn accumulation in the *parkin* mutant cells. The role of dopamine in this interaction has been examined *in vitro*. Roth and colleagues found that human lymphocytes (immune cells that lack dopamine) from patients expressing mutated *parkin* show increased mitochondrial dysfunction from Mn exposure compared to control lymphocytes. However, they do not exhibit any difference in Mn-induced cell death or Mn accumulation[220]. Additionally, Parkin is able to selectively protect against Mn toxicity in a DAergic cell-specific manner[221]. Finally, rats exposed to Mn-containing welding fumes show increased protein levels of Parkin, in addition to the loss of TH and increased oxidative stress[222].

### *Caenorhabditis elegans as a Neurotoxicity Model*

*Portions of this section have been published in a review article in International Journal of Molecular Sciences written by Chakraborty, Bornhorst, Nguyen and Aschner[223], as well as a review article in Journal of Trace Elements in Medicine and Biology written by Chakraborty and Aschner[224].*

While the majority of animal studies in the PD literature utilize rodent models, the invertebrate *Caenorhabditis elegans* (*C. elegans*) model provides several appealing advantages to investigate the connection between Mn toxicity and PD genetics. While

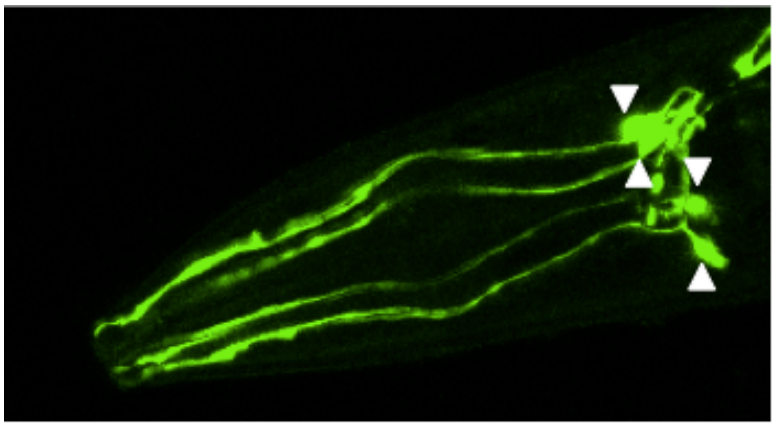

**Figure 3.** *C. elegans dopaminergic head neurons***.** Arrowheads denote the four DAergic neurons in the head of a nematode, with dendritic processes extending to the tip of the nose.

these nematodes do not possess a brain, they do contain all necessary components of the DAergic system[225]. This includes the homologs of the dopamine transporter (DAT-1)[226]; the vesicular monoamine transporter 2 (CAT-1)[227]; tyrosine hydroxylase (CAT-2)[228] and dopamine receptors (DOP-1 through DOP-4)[229]. Out of the total 302 neurons, hermaphroditic worms possess eight DAergic neurons: four CEP (cephalic) (**Fig 3**) and two ADE (anterior deirid) neurons in the head, as well as two PDE (posterior deirid) neurons in the tail[225]. Male worms contain six additional DAergic neurons in the tail. Neurons can be visualized through their transparent bodies using a fluorescent reporter, like green fluorescent protein (GFP), that can be driven under the dat-1 promoter (e.g., $p_{dat\text{-}1}$::GFP)[230]. Through the use of fluorescent and confocal microscopy, degeneration can be visualized by the presence of puncta and blebbing along dendritic processes; shrinking of soma; dendritic strand breaks; and loss of soma and dendrites.

Moreover, dopamine-dependent behaviors, such as basal slowing response (BSR) can also be assayed in *C. elegans*. BSR is a feeding behavior that is assayed via alterations in the number of body bends in response to food availability. Using animals lacking *cat-2,* the rate limiting enzyme of dopamine synthesis, Sawin et *al.* showed that dopamine is required for animals to sense a bacterial lawn. Exogenous dopamine administration can reverse this phenotype and rescue responses to WT levels. The authors also concluded that this response is due to the mechanical sensation, rather than chemosensory features, of bacterial stimuli[228]. Thus, this assay can be utilized to investigate the effects of a toxicant and/or genetic mutations on the integrity of the dopaminergic system, as a comparison between the WT and *cat-2* mutant response.

Additionally, the *C. elegans* genome has been fully characterized[231], allowing for ease in studying genetic models of PD. Especially with a short lifespan (two to three weeks) and a quick life cycle (three days), the ease in unbiased, forward genetic screens has made *C. elegans* an attractive model to study neurodegeneration in PD[232]. Nematodes are first mutagenized to induce DNA mutations, followed by the isolation of animals with distinctive phenotypes of interest. In terms of PD, these phenotypes typically involve altered DA neuronal morphology or a DA-specific behavior. Genetic mapping of progenies showing the modified trait is used to determine the location of the altered loci included[3]. Because *C. elegans* reproduce quickly to generate 200-300 worms in one brood, genetic screens involving large numbers of animals can be performed within a relatively short amount of time.

Alternatively, reverse genetics is also a simple approach to study the effects of a specific gene of interest that may be involved in neurodegeneration. Transgenesis in worms is typically accomplished through microinjection and bombardment techniques. The former involves microinjecting a plasmid containing the regulatory sequence of the gene of interest fused to a fluorescent reporter that can later be used as a readout for that gene. Similarly, subcellular targeting sequences (like the nuclear localization signal, NLS; or the mitochondrial targeting sequence, MTS), as well as cell or tissue-specific promoters (e.g., the aforementioned $p_{dat\text{-}1}$::GFP transgene) can also be included in the plasmid to drive targeted gene expression. Microinjection usually results in an unstable, extrachromosomal array, requiring the subsequent use of ultraviolet (UV) or gamma irradiation to fully integrate the transgene[233]. A second technique involves microparticle bombardment, otherwise known as biolistic transformation. Although this results in low-

copy expression, the desired transgene is fully integrated into the genome[234]. The commercial availability of genetic knockout animals through the *Caenorhabditis* Genetics Center (CGC) is possible due to distribution of isolated deletion mutants from both the National BioResource Project of Japan (NBRP) and the *C. elegans* Gene Knockout Consortium (GKC)[235].

***PD Genetics Homology in C. elegans***

In addition to showing conservation of the DAergic system, worms also contain homologs for several of the genes associated with autosomal recessive PD, including *parkin, pink1* and *dj1.* There is no known homolog for the *SNCA* gene in the *C. elegans* genome.

*parkin/pdr-1*

In *C. elegans*, *pdr-1* (PD related 1) is a homolog for *parkin* that shows conservation of its protein function as an E3 ubiquitin ligase. Similar to *parkin*, the *pdr-1* homolog is ubiquitously expressed in the worm, and shows high expression in both cell bodies and dendrites of neurons[236]. This gene in worms demonstrates how vulnerability to particular toxicants may be specified by a particular genetic mutation. For example, compared to wildtype worms, *pdr-1* knockout worms show increased lethality and shortened lifespan upon exposure to methylmercury (MeHg) that correspond to increased RONS induction. However, the *pdr-1* mutants do not show the same dopamine-dependent behavioral deficits that wildtype worms do upon MeHg exposure[237]. On the other hand, these same *pdr-1* knockout worms also exhibit increased lethality and shortened lifespan upon Mn exposure, yet they do show

enhanced Mn-induced DAergic neurodegeneration compared to wildtype worms. Interestingly, *pdr-1* deletion mutants do not exhibit sensitivity to paraquat, $FeCl_2$ or $CuCl_2$ treatment, but do show sensitivity to rotenone treatment[238].

*pink1/pink-1*

While the *pink1* homolog in worms, *pink-1*, has not been studied in depth, it shows conservation in cytoplasmic and mitochondrial localization, as well as its serine-threonine kinase domain. Moreover, in response to paraquat-induced RONS generation, *pink-1* deletion mutants exhibit shortened mitochondrial cristae and neuronal axon pathfinding defects[239]. More studies are necessary in examining whether its role in mitophagy, along with *pdr-1*'s contributions, is conserved in *C. elegans*.

*dj1/djr-1.1 and 1.2*

Nematodes contain two homologs for DJ-1 (DJR-1.1 and DJR-1.2) that exhibit differential tissue expression patterns. DJR-1.1 in *C. elegans* is detected in both the nucleus and cytoplasm, while DJR-1.2 shows cytosolic expression in head neurons[101]. DJR-1 knockout worms exhibit increased vulnerability to rotenone-induced toxicity that can be rescued by a combinatory treatment of the mitochondrial complex II activator D-ßhydroxybutyrate and the anti-apoptotic tauroursodeoxycholic acid[238]. DJ-1 also possesses glyoxalase activity that is vital in detoxifying reactive glyoxals to prevent the formation of advanced glycation end products that have been observed in PD. While DJR-1.1 is more efficient than DJR-1.2 in protecting worms against glyoxals, DJR-1.2's neuronal expression confers protection against gloxyal-induced DAergic cell death[101]. Furthermore, dauer-stage worms show markedly increased expression of DJR-1.2 that

is mediated by DAF-16, the *C. elegans* homolog for the mammalian FoxO protein that regulates entry into this stage. Moreover, *djr-1.2* expression is also likely to be regulated by insulin signaling[240].

### *Manganese Transporter Homology in C. elegans*

The *C. elegans* genome also contains homologs for key components of Mn transport. Similar to the PD-associated genes, worms homologs possess multiple isoforms for a particular gene that may contribute unique aspects of the total function.

#### *Uptake via DMT1/SMF1-3*

Au et *al.* characterized an intricate Mn transport mechanism in *C. elegans* by investigating the homologs for DMT1: SMF1, SMF2 and SMF3. Protein sequence analysis was conducted to find that all three homologs show high homology to human DMT1 and contain both the characteristic 12 transmembrane domains and a consensus transport sequence (CTS). Deletion mutants of the three homologs from the CGC were then used to assess whether loss-of-function or down-regulation of these transporters confers sensitivity to Mn exposure. Both *smf-1(eh5)* and *smf-3(ok1035)* deletion mutants exhibited heightened resistance to an acute (30 minutes) $MnCl_2$ exposure when compared to wild-type Bristol N2 worms. This was evident with a significantly higher $LD_{50}$ for these mutants 24 hours after treatment. *smf-1(eh5)* mutants were almost twice as resistant to Mn as wild-type worms, with an $LD_{50}$ of 94 mM $MnCl_2$ compared to the N2 $LD_{50}$ of 47 mM. *smf-3(ok1035)* deletion mutants showed an even higher level of resistance, with an $LD_{50}$ of 126 mM[241]. These data suggest that these two homologs somehow mediate Mn uptake, as the lack of functional SMF1 and SMF3 does not increase sensitivity to Mn compared to wildtype worms. On the other hand, *smf-*

*2(gk133)* deletion mutants exhibited hypersensitivity to Mn exposure compared to wild-type worms ($LD_{50}$ of 26 mM), suggesting that functional SMF2 is somehow protective against Mn toxicity in worms.

To further corroborate the role of the SMF proteins in regulating Mn homeostasis, metal content analysis was conducted using graphite furnace atomic absorption spectrometry (GFAAS). All strains showed increases in Mn accumulation in a dose-dependent manner. *smf-1(eh5)* deletion mutants accumulated less Mn than wildtype worms, though not significant at any of the concentrations assessed. However, *smf-3(ok1035)* mutants accumulated the least amount of Mn compared to all other strains, reaching significantly lower levels at 100 mM and 150 mM $MnCl_2$. Interestingly, the *smf-2* deletion mutants exhibited significantly higher Mn content than the other strains upon exposure to 35 mM, 100 mM and 150 mM $MnCl_2$[241]. These Mn content data paralleled the Mn toxicity evidence: without SMF1 and SMF3, the treated worms cannot accumulate Mn upon exposure, indicating a prominent role for uptake.

In order to investigate differential expression patterns, transgenic worms expressing GFP under the control of the *smf1*, *smf2,* or *smf3* promoters were created, in addition to strains expressing GFP-tagged SMF1, SMF2 and SMF3. Using both transcriptional and translational fusion strains, both SMF1 and SMF3 show localization to major epithelial tissues (intestine, rectal gland cells, uterus, vulva, epidermis and sensory organs), whereas SMF2 remains in minor epithelial (pharynx, pharyngeal-intestinal valve) 3. At the cellular level, SMF1 and SMF3 also both localize to the apical membrane, while SMF2 is mostly cytoplasmic. Upon Mn exposure, SMF1::GFP and SMF2::GFP reporter strains show no change in localization or expression. SMF3::GFP,

however, shows a remarkable change in both localization and GFP intensity upon acute exposure to Mn. One hour post-treatment, SMF3::GFP worms show a dramatic translocation of SMF3 into apical vesicular compartments in the intestine. However, five hours after treatment, this intestinal GFP signal significantly decreases and is no longer localized to apical vesicles. This process is completely reversible, as SMF3::GFP worms return their expression level and intracellular localization to normal by 30 hours post-treatment[241]. Thus, these studies indicate an interconnected network of Mn homeostatic control through three homologs: SMF1 and SMF3 are the DMT1 isoforms responsible for Mn uptake in *C. elegans*, with SMF3 being the most DMT1-like homolog.

*Efflux via FPN/FPN-1.1-1.3*

Similar to mammalian systems, Mn efflux is less understood than Mn uptake in worms. The *C. elegans* genome contains three homologs for this Mn/Fe exporter: FPN-1.1, FPN1.2 and FPN1.3. While not much is yet understood about their separate functions, *fpn-1.1* shows the highest homology to mammalian *fpn* and is expressed in the intestine and muscle. Its expression in mammalian cells results in iron export and plasma membrane localization, with iron deprivation resulting in internalization. However, while mammalian FPN has a hepcidin-binding domain, *C. elegans* lack hepcidin genes. Consequently, FPN-1.1 lacks the critical cysteine residue needed for this interaction and subsequent regulation[242].

*Intracellular buffering via PMR1/CePMR-1*

Intracellular Mn buffering in *C. elegans* has not yet been fully elucidated. However, the nematode genome does contain a homolog for the P-type ATPase pump

known to transport both $Ca^{2+}$ and $Mn^{2+}$into Golgi apparatus[243]. This homolog, CePMR-1, shows expression in hypodermal seam cells, intestine and spermatheca, with conservation of its subcellular localization in Golgi apparatus. *pmr-1* knockdown results in increased sensitivity to $MnCl_2$ exposure and enhanced resistance to paraquat. Further linking this pump to intracellular Mn regulation, *pmr-1* knockdown also ameliorates paraquat-induced toxicity of *smf-3* RNAi worms[244]. Interestingly, the loss of *pmr-1* also results in resistance against α-Syn-mediated DAergic cell death in *C. elegans*[245], providing additional support for the role of Mn toxicity in Parkinsonism.

Unlike mammalian evidence for Mn sequestration into mitochondria via the $Ca^{2+}$ uniporter[158], no studies have investigated a similar transport mechanism in *C. elegans*. However, our laboratory has found evidence of a putative MTS in the N-terminal of SMF-3[241]. While our published studies do not show mitochondrial localization in epithelial tissues, future studies should investigate the potential of SMF-3 mediated, mitochondrial Mn import in *C. elegans* neurons.

## Overview of Specific Aims

Though genetic causes have been linked to PD, there is evidence of heterogeneity in age-of-onset and symptomatology in these cases. Moreover, the majority of PD cases remain idiopathic in nature. Together, these findings suggest the possibility of contributions from environmental factors, like Mn, in PD pathogenesis. The convergence of Mn toxicity and Parkinsonism on the same brain region (basal ganglia) to produce similar phenotypic outcomes also warrants further investigation into the

"multiple-hit" hypothesis behind PD, which questions whether a particular genetic risk factor increases susceptibility of DAergic neurons to environmental risk factors. Using the invertebrate *C. elegans* model system, the work presented in this thesis aims to investigate putative gene-environment interactions between PD genetic risk factors and Mn toxicity. The overarching hypothesis of this thesis is that the presence of early-onset PD genetic risk factors will increase vulnerability to Mn toxicity in *C. elegans*, ultimately resulting in damage to the DAergic system.

**Chapter 2:** The effects of *pdr-1*, *pink-1*, and *djr-1* loss on Mn toxicity will be discussed. This chapter supports the protective nature of human wildtype α-Syn expression in *C. elegans* against Mn toxicity in the background of *pdr-1* and *djr-1* loss, and implicates a role of increased extracellular dopamine in preventing α-Syn–mediated rescue of DAergic neurodegeneration.

**Chapter 3:** The role of *pdr-1* in Mn homeostasis will be discussed. In particular, the loss of *pdr-1* results in altered mRNA expression of *fpn-1.1*, with *fpn-1.1* overexpression in *pdr-1* mutants improving Mn-induced lethality, oxidant metal accumulation, mitochondrial DNA integrity and DA-dependent behavioral output.

# CHAPTER II

## THE EFFECTS OF *PDR-1, PINK-1 AND DJR-1.1* LOSS IN MANGANESE -INDUCED TOXICITY AND THE ROLE OF α-SYN IN *C. ELEGANS*[246]

### Introduction

Parkinson's disease (PD) is the second most common neurodegenerative disorder in the U.S., affecting nearly 1% of the population [121]. With an age of onset typically around 60 years of age, this disease manifests a selective dopaminergic (DAergic) neuronal loss in the substantia nigra pars compacta (SNpc), resulting in overt motor and cognitive deficits [1]. The cardinal motor symptomatology of PD includes bradykinesia, rigidity, tremors and postural instability that may be preceded by emotional instability and cognitive problems [2]. As age remains the most significant risk factor for PD pathogenesis, the ever-increasing human lifespan has produced a financial and emotional burden worldwide. Untenable treatment options that do not target the etiology of PD are a major public health concern, and warrant further investigations into the specific mechanisms behind PD pathophysiology.

While the majority of PD cases are idiopathic, many genes have now been associated with the disease, including *DJ1*, *PINK1*, *parkin*, *NURR1, LRRK2, UCH-L1,* and *α-synuclein* [2]. The current study focuses on the major early-onset, familial PD genes: *parkin*, *pink1* and *dj1*. Homozygous mutations in the *PARK2/parkin* gene are responsible for nearly 50% of an autosomal recessive, early-onset, familial form of PD [74]. This gene encodes for an E3 ubiquitin ligase involved in the ubiquitin proteasome system (UPS) that targets substrates for degradation [49]. Mutations in this gene result in impaired ligase activity and substrate binding that can lead to increased protein

aggregation [78]. *Parkin* knockout (KO) models show a variety of PD-associated phenotypes, including hypokinetic deficits, DAergic cell loss [247] and increased extracellular dopamine (DA) levels in the striatum [79].

The PD-associated protein known as *PINK1*, or PTEN-induced kinase 1, is a mitochondrial-targeted protein that contains a highly conserved serine/threonine kinase domain [248, 249]. Homozygous mutations in *pink1* are also connected to autosomal recessive, early-onset PD [84]. These mutations typically result in impaired kinase activity [86] that is otherwise critical for maintaining mitochondrial integrity, as phosphorylation targets include mitochondrial fission and fusion factors [87], as well as the mitochondrially-located serine protease HtrA2 [88]. Wildtype *PINK1* has been shown to protect against mitochondrial toxin-induced DAergic cell death, as well as reducing apoptotic caspase levels and cytochrome c release from mitochondria [90]. *Pink1* mutants show increased DAergic cell death [250] and impaired DA release [91].

Recent studies have identified parkin as a PINK1 phosphorylation target. In fact, these two proteins work in parallel to promote mitophagy through a PINK1-mediated phosphorylation (and autophosphorylation) and recruitment of parkin to mitochondria with a lowered membrane potential [35, 95, 96]. Various modulators of this interaction have recently been introduced, including the mitochondrial fusion factor Mitofusin 2 (Mtfn2) and voltage-dependent anion channels (VDACs) [36, 97]. This novel role for both parkin and PINK1 reveals the importance of maintaining proper mitochondrial trafficking and turnover, signifying an impaired clearance of defective mitochondria as a potential mechanism in the pathophysiology of PD.

Additionally, mutations in the *PARK7/dj1* gene are also associated with autosomal recessive, early-onset PD [98]. This gene encodes for a protein that functions as an oxidative stress sensor, where oxidation of a cysteine residue results in translocation of the acidic isoform from the cytoplasm to mitochondria [99]. Mutations in *dj1* result in increased RONS levels, impaired mitochondrial energetics [102] and DAergic cell death, while overexpression protects against DA toxicity and cell loss [103]. Interestingly, DJ1 has also been shown to form a multi-protein complex with parkin and pink1 [77], though this remains controversial. Moreover, DJ1 up-regulation can rescue the loss of PINK1-mediated sensitization of DAergic neurons in the SNpc to a mitochondrial toxin [94]. The rescue of *pink1* loss-mediated mitochondrial deficits by DJ1 was also seen in *Drosophila*, but showed no rescue in *parkin* mutants [107]. These data reveal a role of DJ1 acting in parallel with the parkin/PINK1 pathway.

Another gene implicated in PD pathophysiology is *SNCA* [108] that encodes for α-synuclein (α-Syn), the major aggregated component of Lewy body depositions. Pathogenic mutations in the *SNCA* gene have been shown to promote increased aggregation of the protein [111, 112]. While the function of α-Syn remains unclear, high expression is found in neuronal presynaptic terminals. Recent evidence has implicated α-Syn in regulating synaptic vesicle release, mobility and recycling [25, 27], along with decreased DA release from vesicles in the background of α-Syn overexpression [26]. Wildtype α-Syn has been shown to inhibit tyrosine hydroxylase (TH) activity, suggesting a physiological role in controlling optimal DA biosynthesis [29]. However, aggregated forms are no longer able to inhibit TH activity, with higher TH phosphorylation present [251]. Studies have found that differential α-Syn levels may alter neuronal susceptibility to

toxins; wildtype or low levels of the protein may be protective against oxidative insults [109], while high intracellular levels can promote abnormal and pathogenic aggregation of the protein [110]. Elucidating the wildtype role of α-Syn and its expression levels in the background of other PD genes may provide deeper insight into the neuroprotective or neurotoxic nature of α-Syn in PD.

While genes such as *SNCA, parkin, pink1* and *dj1* may be associated with PD, the heterogeneity in age-of-onset, as well as 90% of cases being sporadic in nature, warrants investigation into the role of environmental factors in PD etiology. One such factor is manganese (Mn). This is an essential trace element that is necessary for proper immune function, bone growth, digestion, reproduction, as well as serving as an important cofactor for many enzymes [138]. However, overexposure can result in symptomatology that resembles PD [194, 252]. Outside of daily dietary Mn intake through various food sources, environmental sources of Mn exposure can include drinking water (groundwater), pesticides, manufacturing by-products, and airborne exposure upon combustion of the fuel additive methylcyclopentadienyl manganese tricarbonyl (MMT). However, excessive occupational Mn exposure may also arise from welding, steel mining, smelting, and other industrial occupations [253]. Several studies have already begun to examine gene-environment interactions between Mn exposure and PD-associated genes. For example, rats exposed to Mn-containing welding fumes show an increase in parkin protein levels [222]; Parkin was also shown to selectively protect against Mn-induced DAergic cell death *in vitro* [221]. Additionally, significant evidence exists for an association between Mn and α-Syn, with several studies finding Mn-induced changes in α-Syn expression levels, conformation and aggregation [213, 254].

In this work, the tractable, invertebrate *Caenorhabditis elegans* (*C. elegans*) model system expressing human wildtype α-Syn was used for the first time to examine the roles of several early-onset, PD-associated genes (*pdr-1*, *pink-1* and *djr-1.1)* and α-Syn in mediating Mn-induced neurotoxicity. We demonstrate a novel role for α-Syn in altering Mn accumulation in the background of mutated genes (*pdr-1* and *djr-1.1*) through the utilization of inductively coupled plasma-mass spectrometry (ICP-MS/MS), as well as visualizing intraworm Mn levels by laser ablation-inductively coupled plasma-mass spectrometry (LA-ICP-MS). Furthermore, we provide support for a neuroprotective role of wildtype α-Syn that may be dependent upon its expression level and only in the background of select genes, suggesting distinctive roles for each of the PD genes studied in Mn-induced DAergic neurotoxicity.

## Materials & Methods

*C. elegans Strains and Handling – C. elegans* strains were handled and maintained at 20°C as previously described [255]. The following control strains were used: N2, *wildtype* (*Caenorhabditis* Genetics Center, CGC); and BY200, $p_{dat-1}$::GFP(*vtIs1*) *V* (kindly provided by the Blakely laboratory, Vanderbilt University Medical Center). The following deletion mutants were used: VC1024, *pdr-1(gk448) III* (CGC); *pink-1(tm1779) II*; and *djr-1.1(tm918) II*. These deletion strains were also crossed with the BY200 strain for GFP control studies. The following α-synuclein-containing strains were kindly provided by the Caldwell laboratory (University of Alabama): UA44, $p_{dat-1}$::α-Syn, $p_{dat-1}$::GFP[*baIn11*]; UA88, *pdr-1(tm598),* $p_{dat-1}$::α-Syn, $p_{dat-1}$::GFP[*baIn11*]; UA84, *djr-*

*1.1(tm918),* $p_{dat\text{-}1}$::α-Syn, $p_{dat\text{-}1}$::GFP[*baIn11*]; and UA86, *pink-1(tm1779)*; $p_{dat\text{-}1}$::GFP; $p_{dat\text{-}1}$::α-Syn [*baIn11*].

*Preparation of $MnCl_2$* – $MnCl_2$ (>99.995 % purity) (Sigma-Aldrich) stock solutions were prepared in 85 mM NaCl. To prevent oxidation, fresh stock solutions were prepared shortly before each experiment.

*Acute Mn Treatments and Mn-Induced Lethality Assay* – 2,500 synchronized L1 worms per tube were acutely exposed to $MnCl_2$ in triplicates in siliconized tubes for 30 minutes. Worms were then pelleted by centrifugation at 7000 rpm for 3 minutes and washed four times in 85 mM NaCl. 30-50 worms were then pre-counted and transferred to OP50-seeded NGM plates and blinded. 48 hours post-treatment, the total number of surviving worms was scored.

*Mn Quantification in C. elegans* – Mn content was determined after ashing of L1 worms by ICP-MS/MS. Briefly, 50,000 synchronized L1 worms were acutely treated with $MnCl_2$. Worms were pelleted, washed five times in 85 mM NaCl and re-suspended in 1 mL 85 mM NaCl supplemented with 1% protease inhibitor. After sonication, an aliquot was taken for protein quantification using the bicinchoninic acid (BCA) assay-kit (Thermo Scientific). Subsequently, the suspension was mixed again, evaporated, and incubated with the ashing mixture (65%$HNO_3$/30%$H_2O_2$ (1/1) (both from Merck)) at 95°C for at least 12 h. After dilution of the ash with 2% $HNO_3$ including 10 µg/L Rh as internal standard to compensate drift effects, the Mn concentration was determined by ICP-

MS/MS (Agilent 8800 ICP-QQQ). The nebulizer gas flow and parameters of lenses, Q1, collision cell and Q2 were tuned daily on a daily basis for maximum sensitivity (an oxide ratio of <1.0% ($^{140}Ce1^{60}+/^{140}Ce+$) and a double charged ratio of <1.5% ($^{140}Ce++/^{140}Ce+$) with background counts <0.1 cps) (**Supplementary Figures, Table 1**). The limit of quantification (LOQ) for Mn was 0.10 µg/L calculated according to the 3σ-criterion [256]. Determinations of blank and certified reference material (CRM 414 (plankton) (Community Bureau of Reference of the Commission of the European Communities)) were performed periodically after 15 samples each.

Additionally, the Mn content was qualitatively confirmed by LA-ICP-MS analyses. Briefly, 50,000 synchronized L1 worms acutely exposed to $MnCl_2$ were pelleted and washed three times with 85 mM NaCl and two times with bidistilled water. Worms were prepared for analyses by drying single worms on microscopic slides (Thermo Scientific). The laser ablation system LSX213G2+ (CETAC Technologies) was coupled to an ICP-MS (ICAP Qc, Thermo Fisher Scientific). Slides were placed in the ablation chamber and ablated linewise using a quintupled Nd:YAG laser (wavelength 213 nm, repetition frequency 20 Hz spot, spot diameter 4 µm). The ablated material was transported into the ICP-MS by the carrier gas (He/Ar) and analytes were determined using the MS in KEDS mode (**Supplementary Figures, Tables 2 & 3**). In addition, a 10 µg/L Rh-solution including 2% $HNO_3$ was continuously delivered into ICP via a cyclonic spraychamber to compensate drift effects during analysis.

*RONS Measurement* – The formation of reactive oxygen and nitrogen species (RONS) in whole L1 worms was evaluated by a 5(&6)-Carboxy-2`,7`-dichlorodihydrofluorescein-

diacetate (carboxy-DCFH-DA)-based plate reader system. Briefly, a carboxy-DCFH-DA stock solution (50 mM in DMSO) (Invitrogen) was diluted 1:100 with M9 buffer, and synchronized L1 worms were exposed to 500 µM for 1 h in the dark. After 1 h, the worms were washed two times with M9 buffer and two times with 85 mM NaCl to remove all carboxy-DCFH-DA content outside the worm. 10,000 worms were transferred to each well of a 96 well plate and incubated with $H_2O_2$ (positive control) or $MnCl_2$ (respective $LD_{25}$ concentration). Immediately after incubation, the intracellular oxidation of carboxy-DCFH, which correlates with intracellular RONS, was monitored (excitation 485 nm/emission 535 nm) by a microplate reader (FLUOstar Optima microplate reader, BMG Labtechnologies), and kinetics were constructed up to 420 min. To exclude interfering fluorescence of the matrix, data were normalized to a control (dye-loaded cells without a RONS generator).

*Glutathione Quantification* – Total intracellular glutathione levels (reduced and oxidized GSH) have been determined using the "enzymatic recycling assay", as previously described [257, 258]. Briefly, whole worm extracts were prepared out of 50,000 L1 worms acutely exposed to $MnCl_2$. This was followed by washes with 85 mM NaCl and sonication of the pellet in 0.1 mL ice-cold extraction buffer (1% Triton X-100, 0.6% sulfosalicylic acid) and 1% protease inhibitor in KPE buffer (0.1 M potassium phosphate buffer, 5 mM EDTA). Intracellular GSH was quantified by measuring the change in absorbance per minute at 412 nm by a microplate reader after reduction of 5,5′-dithio-2-nitrobenzoic acid (DTNB, Sigma-Aldrich).

*TaqMan Gene Expression Assay* – Total RNA was isolated via the Trizol method. Briefly, following treatment, 1 mL of Trizol (Life Technologies) was added to each tube containing worms resuspended in 100 μl 85 mM NaCl, followed by three cycles of freezing in liquid nitrogen and thawing at 37°C. 200 μL of chloroform was then added to each tube, followed by precipitation using isopropanol and washing with 75% ethanol. Following isolation, 1 μg total RNA was used for cDNA synthesis using the High Capacity cDNA Reverse Transcription Kit (Life Technologies), per manufacturer's instructions. cDNA samples were stored at 4°C. Quantitative real-time PCR (BioRad) was conducted in duplicate wells using TaqMan Gene Expression Assay probes (Life Technologies) for each gene, using the *afd-1* (*actin* homolog) housekeeping gene for normalization after determining the fold difference using the comparative $2^{-\Delta\Delta Ct}$ method [259]. The following probes were used: human *SNCA* (Assay ID: Hs01103383_m1); *dat-1* (Assay ID: Ce02450891_g1); *skn-1* (Assay ID: Ce02407447_g1); and *afd-1* (Assay ID: Ce02414573_m1).

*Dopaminergic Degeneration Assay* – 2,500 synchronized L1 worms per tube were acutely exposed to $MnCl_2$. Upon washing, all worms were plated on OP50-seeded NGM plates. 48 hours post-treatment, 50 worms were transferred to fresh OP50-seeded NGM plates and blinded for subsequent imaging. At 72 hours post-treatment, 15 worms per condition were mounted onto 4% agar pads (in M9 buffer) and anesthetized with 0.2% tricaine/0.02% tetramisole in M9 buffer. Scoring of neuronal defects was performed using an epifluorescence microscope (Nikon Eclipse 80i) equipped with a Lambda LS Xenon lamp (Sutter Instrument Company) and Nikon Plan Fluor 20x dry and Nikon Plan

Apo 60x 1.3 oil objectives. Each worm was scored for the absence ("normal") or presence of any of the following morphological changes: puncta formation along dendritic processes; shrunken soma; and/or loss of soma and/or dendrites ("degenerated"). Representative confocal images (Carl Zeiss MicroImaging, Inc.) of each morphological phenotype were taken and processed as previously described [260].

*α-Syn Protein Levels* – The α-Syn protein level was quantified by SDS-PAGE/western blot analysis as described previously [261], with slight modifications. 150,000 synchronized L1 worms acutely treated with $MnCl_2$ were washed three times with 85 mM NaCl. Afterwards, the worm pellet was re-suspended on ice in lysis buffer (RIPA buffer (Sigma-Aldrich), 1% protease inhibitor), and the worm pellets were temporarily frozen in liquid nitrogen. The extracts were homogenized by sonication and centrifugation, followed by using an aliquot of the isolated supernatant for protein quantification by the BCA assay. 30 µg of the protein sample were separated by 12% denaturating SDS-PAGE and transferred to a nitrocellulose membrane (Whatman) by tank blotting. Membranes were blocked for 1 h in 5% bovine serum albumin (BSA) in Tris buffered saline (TBS) containing 0.1% Tween-20 (TBST). Subsequently, the blots were incubated with the primary mouse monoclonal anti-α-Syn antibody (1:500) (#sc-12767, Santa Cruz Biotechnology) or mouse monoclonal anti-β-actin antibody (1:10000) (Sigma-Aldrich) (as loading control) overnight at 4°C. Following incubation with an horseradish peroxidase (HRP)-conjugated secondary antibody for 1 h at room temperature, the visualization was obtained by Luminata™ forte western HRP substrate (Millipore) and detection by a chemiluminescence imaging system (ChemiDoc MP, Bio-

Rad). Protein levels were quantified by densitometric analysis with ImageJ software (National Institute of Health) and normalized to controls.

*Statistics* – Dose-response lethality curves and all histograms were generated using GraphPad Prism (GraphPad Software Inc.). A sigmoidal dose-response model with a top constraint at 100% was used to draw the lethality curves and determine the respective $LD_{50}$ values (values represent the respective Mn concentrations that induce 50% reduction in survival), followed by a one-way analysis of variance (ANOVA) with a Dunnett's *post-hoc* test to compare all strains to their respective control strains. In order to compare all α-Syn to non-α-Syn-containing strains, a one-way ANOVA using Bonferroni's multiple comparison post-hoc test was conducted. Two-way ANOVAs were performed on metal content, RONS, GSH, TaqMan gene expression and western blot densitometry data, followed by Bonferroni's multiple comparison post-hoc tests. Degeneration data was plotted as a stacked histogram and analyzed using an unpaired t-test between groups (vs. respective control strains).

## Results

*pdr-1 mutants are hypersensitive to acute Mn exposure* – Assessment of dose-response survival curves following acute Mn exposure revealed a leftward-shift in the curve for *pdr-1* mutant worms compared to N2 wildtype (WT) worms (**Fig 4A**). Thus, *pdr-1* mutants exhibited hypersensitivity to Mn-induced lethality ($LD_{50}$ = 5.59 mM) compared to WT worms ($LD_{50}$ = 10.43 mM). However, *djr-1.1* mutants were less

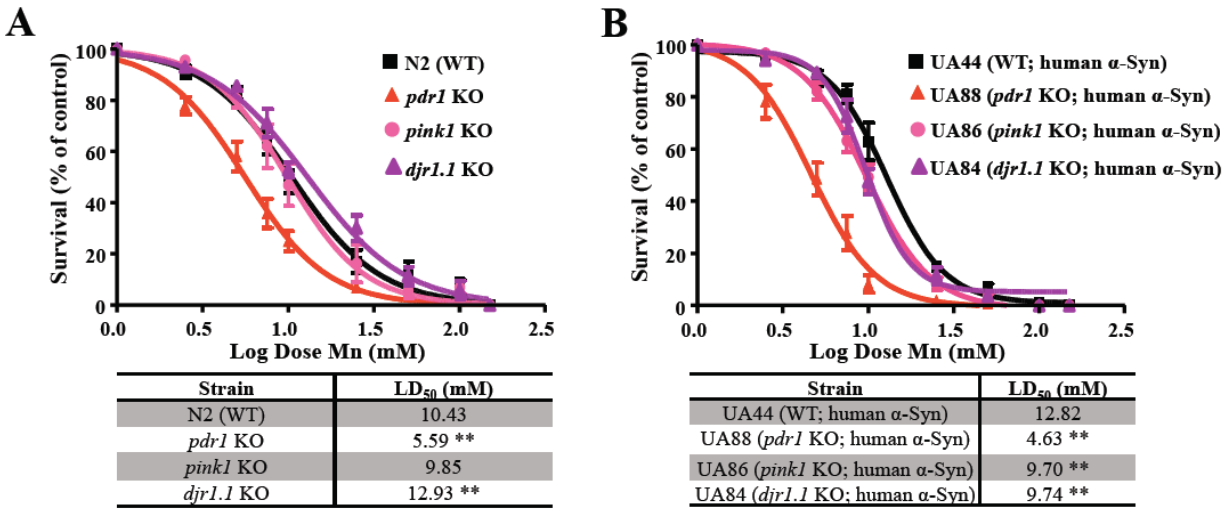


| Strain | $LD_{50}$ (mM) |
|---|---|
| N2 (WT) | 10.43 |
| *pdr1* KO | 5.59 ** |
| *pink1* KO | 9.85 |
| *djr1.1* KO | 12.93 ** |

| Strain | $LD_{50}$ (mM) |
|---|---|
| UA44 (WT; human α-Syn) | 12.82 |
| UA88 (*pdr1* KO; human α-Syn) | 4.63 ** |
| UA86 (*pink1* KO; human α-Syn) | 9.70 ** |
| UA84 (*djr1.1* KO; human α-Syn) | 9.74 ** |

**C**

| Strain | Statistical significance |
|---|---|
| N2 (WT) vs. UA44 (WT; human α-Syn) | ns |
| *pdr1* KO vs. UA88 (*pdr1* KO; human α-Syn) | ns |
| *pink1* KO vs. UA86 (*pink1* KO; human α-Syn) | ns |
| *djr1.1* KO vs. UA84 (*djr1.1* KO; human α-Syn) | * |

**Figure 4.** *pdr-1 mutants are hypersensitive to an acute Mn exposure.* (A,B) Dose-response survival curves following acute Mn exposure and the respective $LD_{50}$ doses. All values were compared to non-treated worms set to 100% survival and plotted against the logarithmic scale of the used Mn concentrations. (A) N2 (wildtype, WT) and *pdr-1*, *pink-1* and *djr-1.1* deletion mutants were treated for 30 min at L1 (larval) stage with increasing concentrations of $MnCl_2$. (B) UA44 (WT; human α-Syn), UA88 (*pdr-1* KO; human α-Syn), UA86 (*pink-1* KO; human α-Syn) and UA84 (*djr-1.1* KO; human α-Syn) were treated for 30 min at L1 stage with increasing concentrations of $MnCl_2$. (A,B) Data are expressed as means ± SEM from at least four independent experiments. Statistical analysis of the $LD_{50}$: **$p < 0.01$ versus respective wildtype worms. (C) Statistical comparison of respective non-α-Syn and α-Syn containing worms: *$p < 0.05$. KO = deletion mutants.

sensitive to acute Mn exposure vs. WT worms. Of the two djr-ortologues, the *djr-1.1* shows the highest homology to vertebrate *dj1* and broadest expression (similar to the other deletion mutants) [101, 262]. Therefore, all studies were carried out in the *djr-1.1* orthologue. Treating worms containing human WT α-Syn in addition to the respective genetic deletions (*pdr-1*, *pink-1* and *djr-1.1*) with Mn led to increased sensitivity compared to the WT α-Syn control strain (**Fig 4B**). One-way ANOVA analysis (comparing data from fig. 1A and B) showed a significantly increased sensitivity of the α-Syn-containing *djr-1.1* mutants compared to the *djr-1.1* mutants alone (**Fig 4C**).

*Enhanced Mn accumulation in pdr-1 and djr-1.1 mutants is attenuated by WT α-Syn expression* - To determine whether a genetic deletion and/or the presence of WT α-Syn alters Mn bioavailability in *C. elegans*, Mn content was measured by ICP-MS/MS. Overall, the analyzed strains (**Fig 5A, B**) showed a dose-dependent increase in Mn content (two-way ANOVA, concentration $p < 0.0001$). The *pdr-1* and *djr-1.1* deletion mutants exhibited an enhanced Mn accumulation compared to WT worms (fig. 5A). *pink-1* mutants showed Mn accumulation that was indistinguishable from WT worms (fig. 5A). Notably, the *pdr-1* and *djr-1.1* mutants containing α-Syn accumulated less Mn compared to the respective deletion mutants alone (**Fig 5C, D**). While the rescue effect was not significant for the *pdr-1* mutants (**Fig 5C**), the decrease in accumulation was significant at 7.5 and 10 mM Mn for the *djr-1.1* mutants (**Fig 5D**). Moreover, we qualitatively confirmed the intraworm Mn accumulation using LA-ICP-MS. WT and *djr-1.1* mutants, with and without α-Syn, were treated acutely with $LD_{50}$ dose (10 mM) (**Fig**

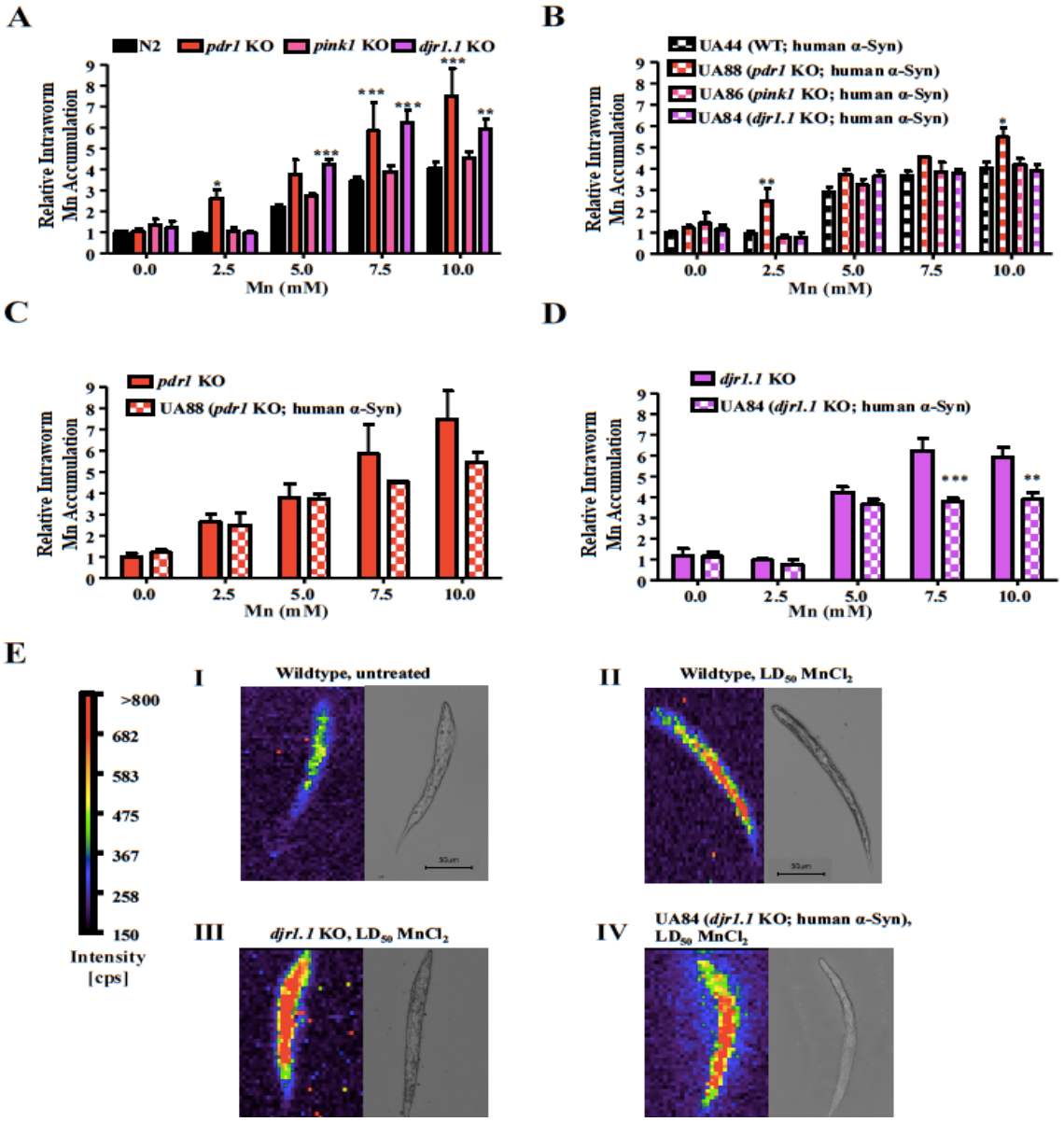


**Figure 5.** *Enhanced Mn accumulation in pdr-1 and djr-1.1 mutants is reversed by WT α-Syn expression.* (A-D) Intraworm Mn content after acute treatment with $MnCl_2$ was quantified by ICP-MS/MS. All values were normalized to non-treated wildtype (WT) worms. (A) N2 (WT) and *pdr-1*, *pink-1* and *djr-1.1* deletion mutants were treated at L1 stage for 30 min with increasing concentrations of $MnCl_2$. (B) UA44 (WT; human α-Syn), UA88 (*pdr-1* KO; human α-Syn), UA86 *(pink-1* KO; human α-Syn) and UA84 (*djr-1.1* KO; human α-Syn) were treated at L1 stage for 30 min with increasing concentrations of $MnCl_2$. (C) Comparing intraworm Mn content of *pdr-1* mutants and UA88 (*pdr-1* KO; human α-Syn) after 30 min treatment with $MnCl_2$ (data from A,B). (D) Comparing intraworm Mn content in *djr-1.1* mutants and UA84 (*djr-1.1* KO; human α-Syn) after 30 min treatment with $MnCl_2$ (data from A,B). (A-D) Data are expressed as means + SEM from at least six independent experiments. Statistical analysis by two-way ANOVA: (A) interaction $p < 0.001$, genotype $p < 0.001$, concentration $p < 0.001$; (B) interaction ns, genotype $p < 0.001$, concentration $p < 0.001$; (C) interaction ns, genotype ns, concentration $p < 0.001$; (D) interaction $p < 0.001$, genotype $p < 0.001$, concentration $p < 0.001$. ***$p < 0.001$, **$p < 0.01$, *$p < 0.05$. (E) 2D images and respective microscope images of WT worms (I, non-treated; II, 10 mM $MnCl_2$); *djr-1.1* deletion mutants (III) and UA84 (*djr-1.1* KO; human α-Syn) (IV) incubated with 10 mM $MnCl_2$ for 30 min. KO = deletion mutants; ns = not significant.

**4**). The images corroborate the ICP-MS/MS metal content analyses, showing increased Mn accumulation in the *djr-1.1* mutants compared to the α-Syn-containing *djr-1.1* mutants (**Fig 5E**).

*Mn-induced oxidative stress is exacerbated in pdr-1 and djr-1.1 mutants, but rescued by α-Syn expression* - Oxidative stress is implicated in Mn-induced neurotoxicity [263]. Additionally, *parkin*, *pink1* and *dj1* are all involved in regulating oxidative stress pathways[264]. Therefore, we investigated the relationship between Mn and their oxidative stress and defense responses by measuring the presence of RONS and total GSH levels. In order to determine the presence of RONS in whole worms, a carboxy-DCFH-DA based reader test system was established (data not shown). **Figure 6A** shows Mn-induced RONS levels in WT worms, *pdr-1* and *djr-1.1* mutants, along with their respective α-Syn-containing strains. In response to sub-lethal, acute Mn treatment (respective $LD_{25}$), WT worms showed a time-dependent increase in Mn-induced RONS that was exacerbated in *pdr-1*, *pink-1* and *djr-1.1* mutants (data are normalized to respective control (dye-loaded cells without a RONS generator) at each respective timepoint). As illustrated in **Fig 6A** (**c & d**), *pdr-1* and *djr-1.1* mutants containing α-Syn showed a lower Mn-induced RONS level compared to the non α-Syn containing deletion mutants.

Next, the redox status of the deletion mutants was examined by measuring total GSH levels. Notably, the deletion mutants contained significantly less total GSH than the WT worms (**Fig 6B**). Mn treatment resulted in a slight reduction of GSH levels, which did not attain statistical significance. The significant decrease at 10 mM Mn in the

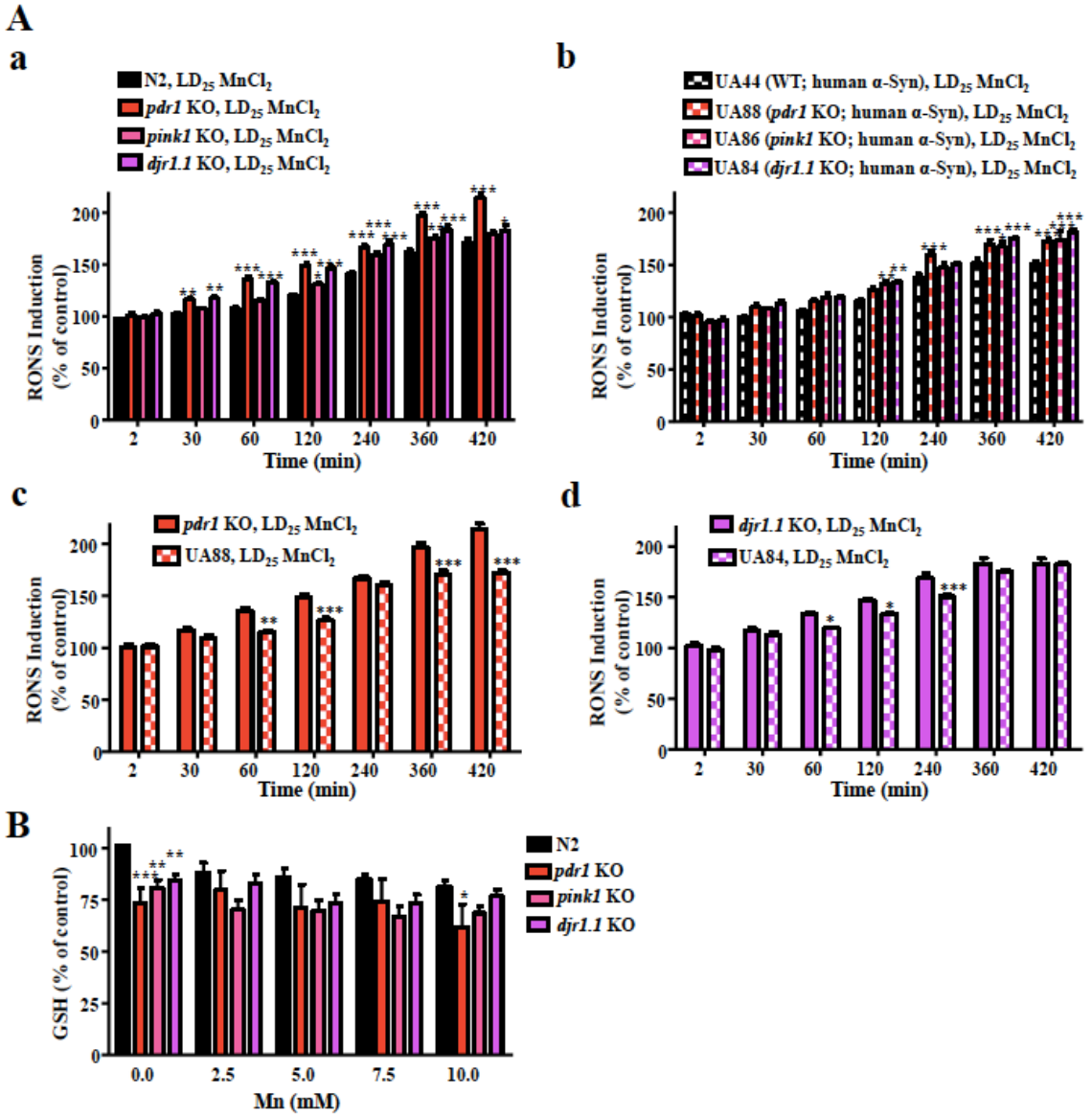


**Figure 6.** *Mn-induced oxidative stress is exacerbated in pdr-1 and djr-1.1 mutants, but rescued by α-Syn expression.* (A) (a) Effect of $MnCl_2$ on the RONS induction in N2 (WT) and *pdr-1*, *pink1* and *djr-1.1* deletion mutants after 1 h dye loading and subsequent $MnCl_2$ post-treatment with their respective $LD_{25}$ doses. (b) Effect of $MnCl_2$ on the RONS induction of UA44 (WT; human α-Syn), UA88 (*pdr-1* KO; human α-Syn), UA86 (*pink1* KO; human α-Syn) and UA84 (*djr-1.1* KO; human α-Syn) after 1 h dye loading and subsequent $MnCl_2$ post-treatment with their respective $LD_{25}$ doses. (c) Comparing Mn-induced RONS induction of *pdr-1* mutants and UA88 (*pdr-1* KO; human α-Syn) (see B,a and B,b). (d) Comparing Mn-induced RONS induction of *djr-1.1* mutants and UA84 (*djr-1.1* KO; human α-Syn) (see B,a and B,b). (A) Shown are mean values (+ SEM) of at least four measurements, which were normalized to the respective dye-loaded worms at the respective time-point. Statistical analysis by two-way ANOVA: (a,b,c) interaction $p < 0.001$, genotype $p < 0.001$, time $p < 0.001$; (d) interaction ns, genotype $p < 0.001$, time $p < 0.001$. (B) Total glutathione level of N2 (WT) and *pdr-1*, *pink1* and *djr-1.1* deletion mutants following 30 min exposure with increasing concentrations of $MnCl_2$. Data are expressed as means + SEM from at least five independent experiments. Statistical analysis by two-way ANOVA: interaction ns, genotype $p < 0.001$, concentration $p < 0.01$. (A-C) $p < 0.001$. ***$p < 0.001$, **$p < 0.01$, *$p < 0.05$. KO = deletion mutants; ns = not significant.

*pdr-1* mutants may be due to their Mn-induced lethality at this dose (**Fig 4A**). The α-Syn-containing deletion mutants showed similar effects as the deletion mutants alone (data not shown). Treatment with $H_2O_2$ as a positive control confirmed further that the inherently decreased levels of GSH in the mutants represent an innately defective oxidative stress response, as $H_2O_2$ treatment did not significantly alter the GSH levels from baseline levels as compared to WT worms (data not shown).

*Increased skn-1 mRNA expression in djr-1.1 and pink-1 mutants* – To determine whether the differences in oxidative stress levels are associated with differences in cellular defense responses against oxidative stress, expression of the antioxidant response gene *skn-1*, the orthologue of the vertebrate gene *nrf2*[265], was examined. Gene expression data reveal inherently upregulated *skn-1* mRNA levels in the deletion mutants compared to WT worms (**Fig 7A**), reaching statistical significance in the *pink1* and *djr-1.1* mutants. Acute Mn treatment resulted in an upregulation of *skn-1* mRNA at the $LD_{50}$ dose only in *djr-1.1* mutants. Interestingly, the *pdr-1* mutants containing α-Syn showed a slight, but not statistically significant, increase in *skn-1* mRNA expression vs. WT animals containing α-Syn, whereas the levels were decreased in the *pink-1* and *djr-1.1* mutants (**Fig 7B**).

*DAergic neurodegeneration in WT and pdr-1 mutants is attenuated by α-Syn expression* – Next, we determined whether α-Syn expression would ameliorate or exacerbate DA neurodegeneration in the deletion mutants upon acute Mn exposure. Visualization of the

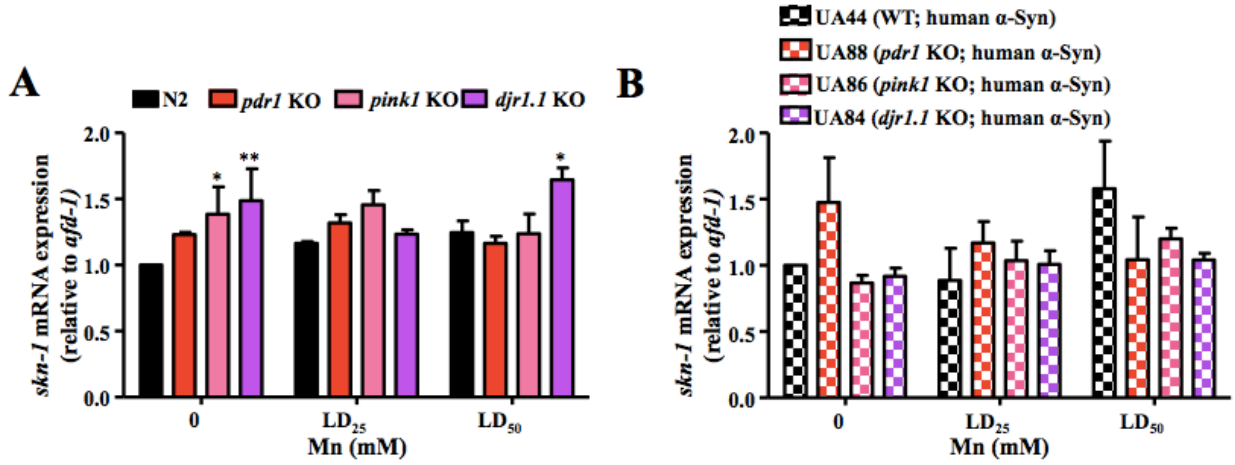


**Figure 7.** *Increased skn-1 mRNA expression in djr-1.1 and pink-1 mutants* - SKN-1 expression after acute treatment with $MnCl_2$. Relative gene expression was determined by qRT-PCR. (A) N2 (WT) and *pdr-1*, *pink-1* and *djr-1.1* deletion mutants were treated at L1 stage for 30 min with $MnCl_2$ at the respective $LD_{25}$ and $LD_{50}$ doses. (B) UA44 (WT; human α-Syn), UA88 (*pdr-1* KO; human α-Syn), UA86 (*pink-1* KO; human α-Syn) and UA84 (*djr-1.1* KO; human α-Syn) were treated at L1 stage for 30 min with $MnCl_2$ at the respective $LD_{25}$ and $LD_{50}$ doses. (A, B) Shown are mean values ± SEM of four independent experiments in duplicates normalized to the untreated wildtype and relative to *afd-1/β-actin* mRNA. Statistical analysis by two-way ANOVA: (A) interaction ns, genotype $p < 0.01$, concentration; (B) interaction ns, genotype ns, concentration ns. $^{**}p < 0.01$, $^{*}p < 0.05$ versus respective wildtype worms. KO = deletion mutants; ns = not significant.

architecture of the four cephalic (CEP) dopaminergic (DAergic) neurons in the head was performed using worms expressing green fluorescent protein (GFP) under the control of a promoter for the dopamine re-uptake transporter 1 (*C. elegans* orthologue for vertebrate DAT[226]), $p_{dat-1}$::GFP (*vtIs1*). Using an objective scoring system, the CEP neurons were scored as degenerated if they exhibited any of the following: discontinuous, punctated GFP signal in the dendrites (**Fig 8A, II**); shrinkage of the cell body (**Fig 8A, III**); and/or, ultimately, total loss of soma and/or dendritic GFP signal (**Fig 8A, IV**). Mn treatment did not significantly increase the inherent DAergic neurodegeneration in WT worms and deletion mutants (**Fig 8C, a-c**). Interestingly, the expression of α-Syn significantly attenuated the DAergic neurodegeneration in untreated WT worms and *pdr-1* mutants, and following acute Mn treatment at their respective $LD_{50}$. However, this effect was absent in the *djr-1.1* deletion mutants, as no significant change in DAergic neurodegeneration was noted in the α-Syn-containing *djr-1.1* mutants compared to the *djr-1.1* deletion mutants alone.

*Increased α-Syn and decreased dat-1 expression in djr-1.1 deletion mutants* - Prominent theories on PD-associated neurodegeneration implicate the role of α-Syn expression. Accordingly, *SNCA* mRNA and α-Syn protein levels were evaluated in the *pdr-1* and *djr-1.1* deletion mutants. To quantify the transcriptional level of *SNCA*, qRT-PCR was performed. Whereas *SNCA* mRNA expression in the untreated *pdr-1* mutants was slightly downregulated (not significant), it was inherently increased in the *djr-1.1* deletion mutants compared to WT worms. An acute Mn treatment at its respective $LD_{50}$ further enhanced the increased mRNA expression level in the *djr-1.1* mutants compared

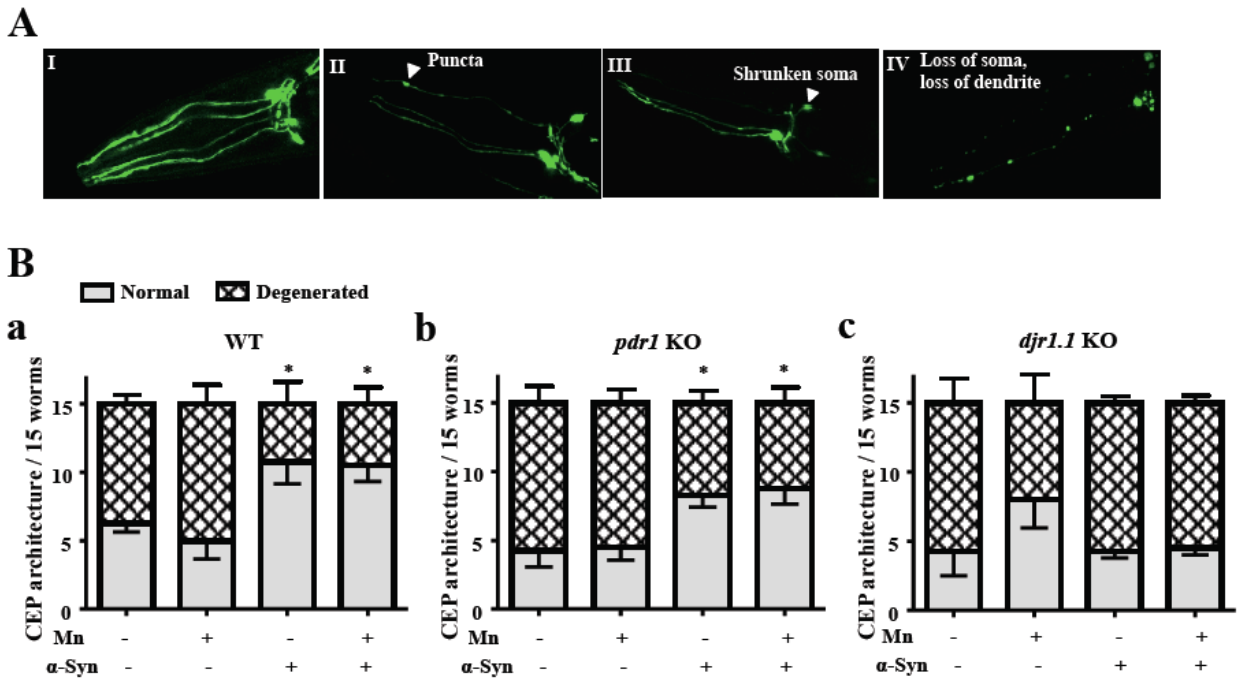


**Figure 8.** *DAergic neurodegeneration in WT and pdr-1 mutants is attenuated by α-Syn expression* – (A) Representative confocal images used in the scoring system: normal worms (I), worms showing puncta (II), shrunken soma (III) or loss of dendrites and soma (IV). (B) The CEP architecture of 15 worms per group of WT, *pdr-1* and *djr-1.1* mutants and the respective α-Syn-containing strains (UA44, UA86, UA88) were scored 72 hours after an acute, 30 min treatment with $MnCl_2$. Shown are mean values + SEM of at least four experiments each. *$p < 0.05$ versus respective non-treated worms without α-Syn. KO = deletion mutants; ns = not significant.

to WT worms (**Fig 9A**). Furthermore, western blot experiments corroborated these results, showing increased α-Syn protein levels (**Fig 9B**). The α-Syn protein level was slightly reduced in *pdr-1* mutants, though not reaching statistical significance. Mn treatment with the respective $LD_{50}$ resulted in a significant reduction of α-Syn protein levels in the *pdr-1.1* mutants compared to untreated WT worms. Notably, the *djr-1.1* mutants showed a Mn-induced increase in α-Syn protein levels corresponding to the gene expression data. *pink-1* mutants were indistinguishable from the WT in α-Syn gene expression and protein level (data not shown).

We further investigated possible interactions between α-Syn and the dopamine transporter (DAT), the protein responsible for synaptic DA clearance. Recent evidence points to α-Syn-mediated modulation of DAT as a potential mechanism behind the selectivity towards DAergic cell death in PD by decreasing DAT function to alter DAergic neurotransmission[266]. Using Real Time RT PCR, we show that *pdr-1* mutants have inherently higher *dat-1* mRNA levels, whereas the expression is reduced in both treated and untreated *djr-1.1* mutants compared to WT worms (**Fig 9C**). *pink-1* mutants were indistinguishable from the WT worm with respect to DA neurodegeneration and *dat-1* mRNA level (data not shown).

## Discussion

The specific interactions between environmental factors and various genetic deletions associated with PD pathophysiology remain poorly understood. In the present study, the invertebrate *C. elegans* model system was used to examine the effects of acute Mn exposure on DAergic neurotoxicity in the background of three PD-associated genes

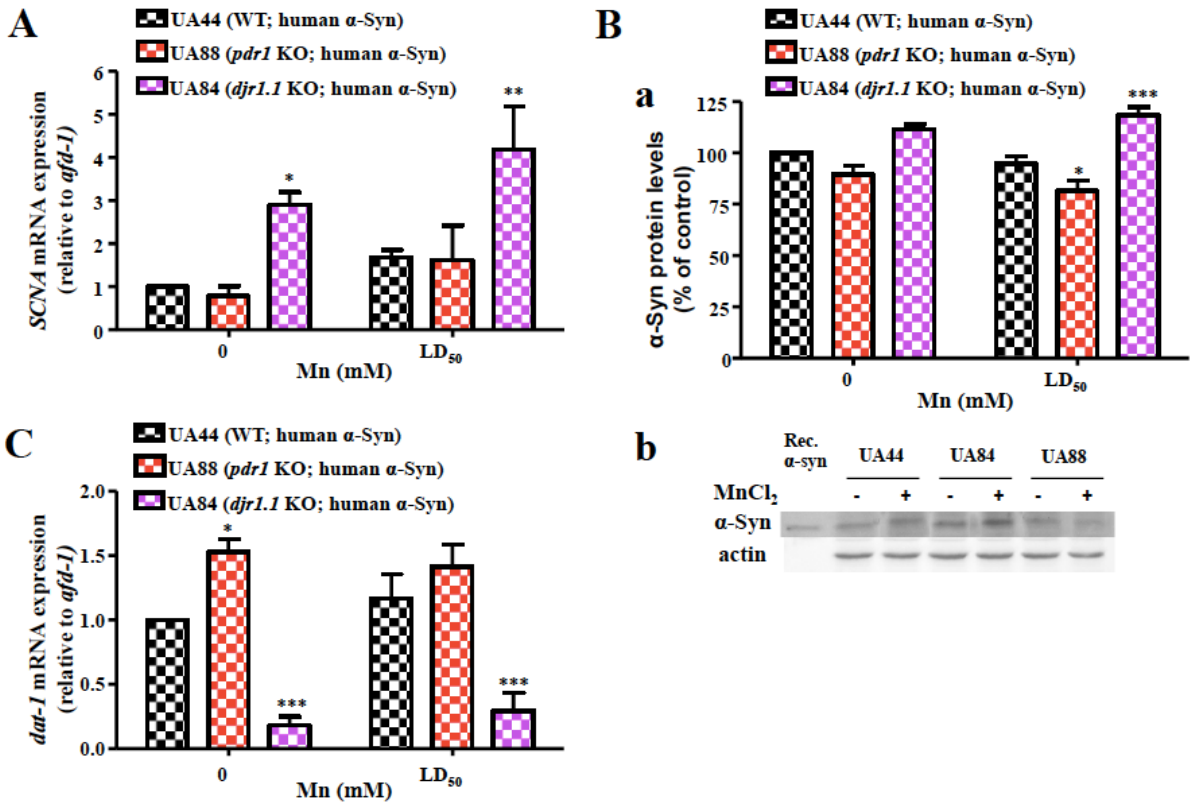


**Figure 9.** *Increased α-Syn expression in djr-1.1 deletion mutants* - (A*) SNCA* mRNA expression after acute treatment with $MnCl_2$. Relative gene expression was determined by qRT-PCR. UA44 (WT; human α-Syn), UA88 (*pdr-1* KO; human α-Syn)) and UA84 (*djr-1.1* KO; human α-Syn) were treated at L1 stage for 30 min with $MnCl_2$ at the respective $LD_{50}$. Data are expressed as means + SEM from at least four independent experiments in duplicates normalized to the untreated wildtype and relative to *afd-1/ β-actin* mRNA. Statistical analysis by two-way ANOVA: interaction ns, genotype $p < 0.001$, concentration $p < 0.05$. $^{**}p < 0.01$, $^{*}p < 0.05$ versus respective wildtype worms. (B) Effect of $MnCl_2$ on α-Syn protein level. UA44 (WT; human α-Syn), UA88 (*pdr-1* KO; human α-Syn)) and UA84 (*djr-1.1* KO; human α-Syn) were treated for 30 min at L1 stage with $MnCl_2$ at the respective $LD_{50}$. Subsequently, extracts were prepared and western blotting was performed. Shown is one representative western blot in (B,b). Shown are mean values + SEM of six independent experiments normalized to β-actin and to the untreated wildtype. Statistical analysis by two-way ANOVA: interaction ns, genotype $p < 0.001$, concentration ns. (C) *dat-1* mRNA expression after acute treatment with $MnCl_2$. Relative gene expression was determined by qRT-PCR. UA44 (WT; human α-Syn), UA88 (*pdr-1* KO; human α-Syn)) and UA84 (*djr-1.1* KO; human α-Syn) were treated at L1 stage for 30 min with $MnCl_2$ at the respective $LD_{50}$. Data are expressed as means + SEM from at least four independent experiments in duplicates normalized to the untreated wildtype and relative to *afd-1/β-actin* mRNA. Statistical analysis by two-way ANOVA: interaction ns, genotype $p < 0.001$, concentration ns. $^{***}p < 0.001$, $^{**}p < 0.01$, $^{*}p < 0.05$ versus respective wildtype worms. KO = deletion mutants; ns = not significant.

(*pdr-1/parkin*, *pink-1/pink1* and *djr-1.1/dj1*) in the absence or presence of wildtype human α-Syn, a pathological PD hallmark. The ease in genetic manipulation and breeding of nematodes allowed for the quick generation and assessment of crosses needed to evaluate DAergic neurodegeneration. Moreover, this model system allows for an alternative approach to otherwise time-consuming and costly vertebrate models that contain intricate nervous systems, hindering more rapid investigations into neurodegenerative mechanisms.

As the *pdr-1* mutants showed the highest sensitivity to acute Mn exposure, we examined whether they showed a differential Mn accumulation profile compared to WT worms. Interestingly, both *pdr-1* and *djr-1.1* mutants displayed significantly enhanced intraworm Mn accumulation, as shown by ICP-MS/MS. Mn accumulation inside the worms (and not just a measurement of metals bound to the outer worm cuticle) was also corroborated by the novel and optimized utilization of LA-ICP-MS[267]. Recently, our laboratory identified a network of Mn transporter genes responsible for controlling Mn homeostasis in worms. The *smf1-3* genes are orthologues for the mammalian divalent metal transporter 1 (DMT1), with SMF-3 serving as the primary Mn uptake transporter in *C. elegans* [241]. Interestingly, evidence has pointed to parkin-dependent, proteasomal degradation of DMT1 levels *in vitro* [170]. As the *pdr-1* gene shows conservation of its ubiquitin ligase activity in nematodes, one could hypothesize that the loss of *pdr-1* enhanced Mn uptake due to an increase in SMF-3 expression from the lack of *pdr-1*-mediated degradation. This interaction would be interesting to examine in this model system, as the *C. elegans* genome does not have nearly as many E3 ubiquitin ligases

as the human genome [268], reducing the amount of compensatory mechanisms that may be possible in vertebrate knockout models.

Furthermore, previous evidence in *Drosophila melanogaster* has shown increased lifespan in *parkin*-null flies upon exposure to metal chelators compared to controls, indicating a heightened sensitivity to endogenous copper ($Cu^{2+}$) and iron ($Fe^{2+}$) levels [269]. This interaction was further supported by evidence showing a rescue of the *parkin* null phenotype by overexpression of a metal transcription factor (MTF-1) [270]. However, previous *C. elegans* studies in *pdr-1* mutants found no increased sensitivity upon exposure to $Fe^{2+}$ and $Cu^{2+}$ [238]. Our current findings of enhanced intraworm Mn accumulation corroborate a distinctive connection between parkin and metal homeostasis that may be Mn-specific, as we have also previously found that the same *pdr-1* mutants do not show significantly increased methylmercury (MeHg) accumulation compared to WT worms[237].

Due to the close relationship between parkin and DJ1-associated pathways, it is possible that they may be directly regulating each other. New evidence suggests a novel role for DJ1 in reducing metal-induced cytotoxicity by directly binding metals *in vitro.* While this study found a weaker binding affinity for Mn compared to $Cu^{2+}$ and mercury ($Hg^{2+}$) [271], the alterations in Mn homeostasis in the worms may result in subsequent intracellular dyshomeostasis of other metals that DJ1 would typically sequester. Therefore, it is feasible that the enhancement in Mn accumulation in *djr-1.1* mutants could be due to the lack of metal binding in these animals. Notably, both *pdr-1* and *djr-1.1* mutants showed an analogous increase in Mn accumulation, yet they possessed differential neurodegeneration profiles. Parkin has recently been shown to

down-regulate DJ1 protein and mRNA levels [272], with *parkin* knockout mice showing increased DJ1 protein levels upon proteasomal inhibition [273]. The loss of parkin (*pdr-1* in our case) itself may be sufficient to cause proteasomal impairment from increased oxidative stress and abnormal accumulation of misfolded proteins. Thus, compared to the *djr-1.1* mutants, the amelioration of metal toxicity in *pdr-1* mutants may be due to increased expression of *djr-1.1* in these animals.

While manganism is distinctive from PD in terms of the initial site of metal accumulation and toxicity (globus pallidus), both medical conditions implicate enhanced oxidative damage. In the absence of genetic alterations, Mn itself can cause mitochondrial damage by inhibiting complex I of the electron transport chain (ETC) and oxidative phosphorylation [158]. Mn can also increase isoprostane (lipid peroxidation marker) generation and decrease ATP levels in a dose-dependent manner, resulting in increased neurodegeneration [263]. The increased intraworm Mn concentrations may also influence iron (Fe) concentrations, another heavy metal that competes with Mn for transport via DMT1 and the transferrin receptor (TfR) [274]. Furthermore, Fe has been implicated in PD by promoting oxidative damage via the Fenton reaction or altering oxidative response pathways [186, 217]. Mn has also been shown to exacerbate DA oxidation to produce damaging, reactive DA intermediates [214, 275]. The combination of Mn's own oxidative potential and enhancement of DA oxidation, represents a plausible mechanism for its selectivity towards DAergic neurodegeneration, and it has been previously corroborated in *C. elegans* [260].

The marked increase in baseline RONS induction in the *pdr-1* mutants was striking; however, this is not surprising, as parkin's significant role in mediating

mitophagy warrants impaired mitochondrial integrity in its absence [35, 276]. The similarly elevated basal RONS levels in the *djr-1.1* mutants do not quite reach the level of the *pdr-1* mutants. As noted earlier, several studies have affirmed DJ1's role as an oxidative stress sensor, indicating that loss of DJ1 would inherently result in an increased RONS production [99]. In the context of this particular assay in *C. elegans*, Mn treatment in WT animals does not seem to dramatically increase DCF fluorescence over time (data not shown). Thus, we hypothesize that the inherently enhanced RONS induction in *pdr-1* and *djr-1.1* mutants reflects a ceiling effect that limits further exacerbation upon acute Mn exposure. Given its role in recruiting parkin to damaged mitochondria, it was somewhat unexpected that *pink-1* mutants only showed a slightly enhanced RONS induction compared to WT worms. However, the presence of DJ1 in *Drosophila* is able to rescue mitochondrial deficits in the background of *pink1*, but not *parkin* loss [107]. This could account for the lack of an oxidative stress phenotype in the *pink-1* mutants, as well as the fact that these mutants did not take up as much Mn as the *pdr-1* and *djr-1.1* mutants.

While a trend was apparent towards a dose-dependent effect of Mn on GSH depletion in WT animals, the deletion mutants show no significant change with treatment. In particular, the baseline reduction in GSH levels in all deletion mutants suggests an inherently impaired ability to adapt to stressful stimuli, such as acute Mn exposure. This GSH reducation may also relate to the inherently high levels of RONS production in *pdr-1* mutants, as they show the lowest basal total GSH levels. Moreover, it has been shown that knocking down *pink1* in human neurons results in GSH reduction [264]. Similarly, DJ1 expression promotes upregulation of glutathione synthesis [277], which

corresponds with the finding in *djr-1.1* mutants, showing decreased GSH levels. Taken together, our data suggest a possible mechanism of neurotoxicity through compromised clearance of Mn-damaged mitochondria due to the loss of an intact Parkin/PINK1/DJ1 pathway, resulting in heightened RONS production that either cannot be inherently combated due to basal GSH deficiencies in the mutants, or is resulting in GSH consumption.

The observed increase in RONS induction and basal GSH depletion in mutants, showing enhanced Mn accumulation (*pdr-1* and *djr-1.1*) warranted further examination into whether these animals also have alterations in *skn-1* expression, the worm orthologue for *nrf2*. Nuclear factor erythroid 2-related factor 2, or Nrf2, is a transcription factor that promotes the upregulation of antioxidant genes upon oxidative-stress-induced translocation from the cytoplasm to the nucleus [278, 279]. Previous work has found *skn-1* mutants to be vulnerable to oxidative stress [280]. While not significant, *pdr-1* mutants showed a trend for increased *skn-1* mRNA expression, which was consistent with increased Nrf2 activity found in an induced pluripotent stem cell (iPSC) study in patients harboring *parkin* mutations [281]. Moreover, contrary to DJ1 acting as an Nrf2 stabilizer [106], we found significantly increased *skn-1* mRNA expression in the *djr-1.1* mutants. While we did not expect this increase, there may be a compensatory mechanism in these animals to counteract the basal GSH depletion that would otherwise protect against RONS production by upregulating *skn-1*-mediated antioxidant gene transcription.

Although α-Syn is known to be involved in the pathogenesis of PD, its role in both neuroprotection and neurodegeneration is controversial. Overexpression of α-Syn, as

well as its mutated forms (A30P, E46K, A53T), has been reported to be neurotoxic, while WT α-Syn has been implicated to be neuroprotective [109, 282, 283]. α-Syn is a neuronal protein in vertebrates that is ubiquitously expressed at high levels in all brain regions [284, 285], but it is not expressed in *C. elegans*. Therefore, worms expressing human WT α-Syn were utilized to address the role of α-Syn in the mutated background of *pdr-1*, *pink-1* and *djr-1.1* with respect to Mn homeostasis, oxidative stress and DAergic neurodegeneration.

There is increasing evidence that α-Syn interacts with metal ions, thereby affecting their homeostasis. Initial studies of the potential to bind metals came from the ability of certain metals to catalyze α-Syn aggregation [286]. Overall, two major types of interactions between metals and α-Syn have been reported. In addition to non-specific sites of electrostatic interactions, the C-terminus contains a $^{119}$DPDNEA motif binding site, suggesting that metal binding is driven by both electrostatic interactions and the residual structure of the α-Syn C-terminus. The C-terminal low-affinity sites have been reported to interact with different metal ions, with copper (Cu) and Fe most intensively studied [287, 288]. Although the majority of metal ions interact with α-Syn with low affinity, the protein possesses high affinity to $Cu^{2+}$ and $Fe^{3+}$ at the N-terminal region. Modifications by redox-active metal ions may be relevant for the aggregation properties of α-Syn [289, 290]. A co-incubation of α-Syn with $Mn^{2+}$ has been reported to induce partial folding of the protein and serve as an effective promoter of α-Syn aggregation [254].

In addition to its metal binding capacity, the role of α-Syn as a cellular ferrireductase has been recently identified, providing further evidence towards the multiple roles of α-Syn in metal homeostasis [291]. One very important outcome of the

present work is the novel role of α-Syn in altering Mn accumulation in the background of mutated *pdr-1* and *djr-1.1* worms, which may be partially due to an endogenous metal binding capacity. Even as α-Syn was only expressed in the DAergic neurons of the worms, the global alterations in Mn homeostasis were drastic; secretion of α-Syn into other regions cannot be excluded [292, 293]. In fact, an environmental toxin (i.e. rotenone) has been shown to promote the release of α-Syn from enteric neurons [294].

In terms of the role of α-Syn in modulating oxidative stress responses, the loss of *pdr-1* or *djr-1.1* in α-Syn-expressing worms resulted in reduced Mn-induced RONS production, compared to worms containing the genetic deletion alone. This effect was due to the reduced Mn accumulation in the presence of α-Syn in both *pdr-1* and *djr-1.1* deletion backgrounds. Additionally, attenuated oxidative stress, in accordance with the neuroprotective role of α-Syn, has been shown in cells expressing WT α-Syn, where protection against rotenone and maneb toxicity was conferred by preservation of mitochondrial function [109]. Additionally, WT α-Syn-expressing cells also showed the ability to attenuate decreased intracellular GSH levels upon serum deprivation [295]. An overexpression of α-Syn has been reported to increase the activity of superoxide dismutase (SOD), resulting in reduced oxidative stress [296, 297]. The results in the current study support the literature in finding a neuroprotective role of wildtype α-Syn against oxidative stress.

The second important outcome of the current study is the role of α-Syn as being either neuroprotective or neurotoxic in the background of certain genes. While the expression of α-Syn significantly attenuated the DAergic neurodegeneration in WT worms and *pdr-1* mutants, both basally and following acute Mn treatment, this effect

could not be observed in the *djr-1.1* deletion mutants. Analyzing the *SNCA* mRNA expression and α-Syn protein level revealed that this effect may be due to differential expression levels of α-Syn. The expression is slightly lower (not significant from WT) basally in the *pdr-1* mutants, consistent with clinical findings that patients with *parkin* mutations do not typically show α-Syn Lewy body deposition [298, 299]. However, α-Syn mRNA was upregulated by three-fold in the *djr-1.1* mutants.

These differential expression levels of α-Syn might affect neurotransmitter release, since one function of α-Syn is the modulation of the dopamine transporter (DAT). This transporter (DAT-1 in *C. elegans*) is involved in synaptic neurotransmitter clearance, and especially responsible for DA reuptake to remove excessive extracellular DA concentrations [300-302]. Inhibition of DAT leads to high extracellular DA levels [303, 304]. In *C. elegans*, we have already shown that upon Mn exposure, loss of *dat-1* is detrimental to worm survival, with extracellular DA exacerbating Mn-induced oxidative stress, lifespan reduction and DAergic neurodegeneration [260]. Moreover, previous observations in α-Syn-overexpressing cells show that increased α-Syn levels induce a dose-dependent reduction of DAT function, as hippocampal and DAergic neurons expressing two- to threefold WT α-Syn above normal levels (similar to the *djr-1.1* mutants in this study) show impaired neurotransmitter release [305, 306]. Remarkably, in the present study, *pdr-1* mutants showed lower basal α-Syn levels and inherently higher *dat-1* mRNA levels, corresponding to the reduced DAergic neurodegeneration, thus suggesting a neuroprotective role for α-Syn that implicates increased extrasynaptic DA clearance. While *pdr-1* mutants exposed to Mn showed reduced α-Syn protein levels and increased *dat-1* mRNA levels (not significant from WT), Mn treatment did not

attenuate the DAergic neurodegeneration seen in untreated α-Syn-containing *pdr-1* mutants. α-Syn in WT worms and *pink-1* mutants showed a similar neuroprotective effect. A study in *Drosophila* pointed out the synergistic effect of expression of α-Syn and *pink1*, allowing for enhanced protection and increased survival [307].

In contrast to the *pdr-1* mutants, the *djr-1.1* mutants containing α-Syn showed a three-fold upregulation of α-Syn mRNA and downregulation of *dat-1* mRNA, suggesting reduced synaptic DA clearance. However, these animals did not show an α-Syn-induced attenuating effect on DAergic neurodegeneration. Mn treatment resulted in increased α-Syn expression, consistent with observations that iron is modulating α-Syn at the transcriptional level [308]. While *dat-1* mRNA levels remained reduced, they were indistinguishable from the untreated *djr-1.1* worms. The DAergic neurodegeneration was also indistinguishable from the untreated *djr-1.1* animals containing α-Syn. Interestingly, the *djr-1.1* mutants containing α-Syn showed the same level of neurodegeneration as the *djr-1.1* deletion mutants alone, yet they showed less Mn accumulation; this implicates a more severe phenotype in the α-Syn-containing worms, as it took less Mn accumulation to produce the same level of DAergic neurodegeneration. The contrast in *SNCA* mRNA expression between *pdr-1* and *djr-1.1* mutants could be explained by post-transcriptional mechanisms that are regulated differentially by the two genes. Another possible explanation is promoter competition, as α-Syn is sharing the dat-1 promoter, but this has yet to be elucidated.

## Conclusions

The genetically amenable *C. elegans* model system was utilized to examine the neuroprotective or neurotoxic role of α-Syn in mediating Mn neurotoxicity in the background of loss in the PD-associated genes *pdr-1*, *pink-1* and *djr-1.1*. For the first time, the current study provides evidence for a neuroprotective role of α-Syn against Mn accumulation and Mn-induced oxidative stress in the background of *pdr-1* and *djr-1.1* loss. However, its neuroprotective role may be dependent upon its expression level, as increased levels in the *djr-1.1* mutants were associated with increased DAergic neurodegeneration. These findings also support the role of extracellular DA in exacerbating Mn neurotoxicity, with decreased *dat-1* levels promoting increased DAergic neurodegeneration in the *djr-1.1* mutants. Collectively, the findings presented in this chapter support the overarching hypothesis that the loss of genes associated with early-onset PD, namely *pdr-1* and *djr-1* in *C. elegans*, results in increased susceptibility to Mn toxicity.

# CHAPTER III

## LOSS OF *PDR-1/PARKIN* INFLUENCES MANGANESE HOMEOSTASIS THROUGH ALTERED *FERROPORTIN* EXPRESSION IN *C. ELEGANS*[309]

### Introduction

Parkinson's disease (PD) is the second most common neurodegenerative disorder, with a typical age of onset around 60 years of age[121]. This debilitating disease is characterized by selective dopaminergic (DAergic) cell loss in the substantia nigra pars compacta (SNpc) region of the brain. Hallmark symptoms of PD include bradykinesia, rigidity, tremors and postural instability that are often preceded by emotional instability and cognitive dysfunction. Unfortunately, PD is a progressive and irreversible condition[1]. Current treatments do not target the molecular origins of PD, warranting further examination into the mechanisms behind its pathophysiology.

Though PD is mostly idiopathic in its etiology, mutations in several genes have been connected to the disease[1]. For example, homozygous mutations in the *PARK2/parkin* gene are responsible for nearly 50% of an autosomal recessive, early-onset form of PD[74]. This gene encodes for an E3 ubiquitin ligase involved in the ubiquitin proteasome system (UPS) that targets substrates for degradation. Mutations in this gene result in impaired ligase activity and substrate binding that can lead to increased protein aggregation[78]. *Parkin* knockout animal models show a variety of PD-associated phenotypes, including hypokinetic deficits, DAergic cell loss and increased extracellular dopamine (DA) in the striatum[79, 247]. Parkin has also been more recently

identified as a key regulator of mitophagy, an intracellular autophagic process designed to eliminate damaged mitochondria from the cell[35].

Despite the known genetic associations, familial cases often present with heterogeneity in their age-of-onset and symptomatology, in addition to nearly 90% of all PD cases manifesting without genetic disturbances[310]. The idiopathic component of the disease suggests a contribution of environmental risk factors in the development of PD. One such factor is the heavy metal manganese (Mn), an essential trace element found in many food sources consumed daily by humans. Mn serves as a necessary cofactor for enzymes involved in several critical processes, including reproduction, metabolism, development, and antioxidant responses[138]. While deficiency is a rare concern, the essentiality of Mn is mirrored by its neurotoxicity upon overexposure. Mn poisoning, or manganism, typically occurs from occupational exposures in industrial settings, such as in welding, where Mn-containing fumes and/or products are abundant[196, 252]. Mn is also found as an antiknock agent methylcyclopentadienyl manganese tricarbonyl (MMT) in gasoline, but limited studies currently exist on the impact of Mn release from combustion on general human health[311, 312]. Mn is also found as a component in pesticides, making surface runoff from these agricultural uses an additional source of overexposure[121]. Moreover, Mn toxicity can also affect other susceptible populations, including ill neonates receiving TPN that is supplemented with a trace element solution containing Mn[138]. Another population at risk of Mn poisoning includes patients suffering from hepatic encephalopathy and/or liver failure, as Mn is excreted from the body through the biliary system[183, 313]. On the other hand, individuals with iron (Fe) deficiency (e.g., iron deficiency anemia), a highly prevalent nutritional condition, are at risk for

increased Mn body burdens. As Mn shares similar transport mechanisms with Fe, higher Mn levels are often seen in conditions of low Fe levels[314].

Tight regulation through an intricate system of transport mechanisms helps maintain proper Mn homeostasis in cells. The divalent metal transporter 1 (DMT1) represents the primary mode of divalent Mn import[132]. However, Mn efflux remains less understood than Mn import. We previously identified ferroportin (FPN), a well-known iron (Fe) exporter, as facilitating Mn export in cells and mice[173]. We have previously identified and characterized components of the Mn transport system in the *Caenorhabditis elegans* (*C. elegans*) model system. This nematode provides an attractive, alternative system that has a rapid life cycle, short lifespan, and large brood size. Additionally, the well-characterized genome allows for the utilization of various genetic mutants for studies. This nematode also conserves all necessary components of a fully functional DAergic system, allowing for the study of the effects of PD-associated genetic loss on the DAergic system. Our previous studies have identified SMF-1, SMF-2 and SMF-3 as the *C. elegans* homologs for DMT1, with SMF3 acting as the most DMT1-like homolog in its necessity to regulate Mn uptake[241]. Thus far, these proteins are the only known Mn importers in the worm. Furthermore, the worm contains 3 homologs for FPN: FPN-1.1, FPN-1.2 and FPN-1.3[315]. As of now, FPN-1.1 is the only known protein that conserves Fe efflux in *C. elegans*[242].

The overlap in sites of damage and similar symptomatology between manganism and Parkinsonism has warranted investigations into potential gene-environment interactions. For example, parkin has been shown to selectively protect against Mn-induced DAergic cell death *in vitro*[221], while rats exposed to Mn-containing welding

fumes show increased Parkin protein levels[222]. Our previous study using *C. elegans* found significantly enhanced Mn accumulation in *pdr-1* (*parkin* homolog) knockout worms compared to WT worms[246]. With the aforementioned relationships between PD-associated genes and Mn toxicity, we hypothesized that this enhancement is due to an alteration in Mn homeostasis, at the level of transport, in the background of *pdr-1* loss. In the present study, while no significant change in mRNA expression of importers was seen, we found a downregulation of *fpn-1.1* mRNA. Upon overexpression of this exporter in *pdr-1* mutants, we found decreased metal levels that were associated with improved survival and DA-dependent behavior. Together, our results provide further support for altered metal homeostasis as a component of the pathophysiology seen in Parkinsonism.

## Materials & Methods

*Plasmid constructs* – Full length wildtype (WT) *fpn-1.1* with C-terminal FLAG tag was PCR amplified using primers 5'-GGGGACAAGTTTGTACAAAAAAGCAGGCTACATGGCTTGGTTATCCGGAAAAG-3' and 5'-GGGGACCACTTTGTACAAGAAAGCTGGGTTTCACTTGTCATCGTCGTCCTTGTAGTCTTCA AAAGTTGGCGAATCCAAC-3' from cDNA library which was converted from total RNAs isolated from N2 worms (see below). The plasmid was created with Gateway recombinational cloning (Invitrogen). The above PCR product was initially recombined with the pDONR221 vector to create the pENTRY clone. Next, the *fpn-1.1* pENTRY construct was recombined into pDEST-*sur-5* vector[316], under the promoter of the acetoacetyl-coenzyme A synthetase (*sur-5*) gene. This plasmid was then used to create transgenic worms.

*C. elegans Strains and Strain Construction* – *C. elegans* strains were handled and maintained at 20°C as previously described[255]. Strains used were: N2, *wildtype* (*Caenorhabditis* Genetics Center, CGC) and VC1024, *pdr-1(gk448) III* (CGC). The MAB326 strain was created by microinjecting $P_{sur\text{-}5}$::*fpn-1.1* with pBCN27-R4R3 ($P_{rpl\text{-}28}$::PuroR, Addgene) and $P_{myo\text{-}3}$::mCherry (a gift from Dr. David Miller) into VC1024 strain. Over three stable lines were generated and analyzed. Representative lines were selectively integrated by using gamma irradiation with an energy setting of 3600 rad.

*Preparation of Manganese Chloride ($MnCl_2$)* – 2M $MnCl_2$ (> 99.995% purity) (Sigma-Aldrich) stock solutions were prepared in 85 mM NaCl. To prevent oxidation, fresh working solutions were prepared shortly before each experiment. The range of concentrations used in all experiments is based on Mn dose-response curves recently published by our laboratory[246].

*Mn-Induced Treatments and Lethality Assay* – 2500 synchronized L1 worms per group were acutely treated with $MnCl_2$ (0-100 mM) in siliconized tubes for 30 minutes. Worms were then pelleted by centrifugation at 7000 rpm for 3 minutes and washed four times with 85 mM NaCl. 30-50 worms were then pre-counted and transferred to OP50-seeded NGM plates in triplicate and blinded. 48 hours post-treatment, the total number of surviving worms was scored as a percentage of the original plated worm count.

*TaqMan Gene Expression Assay* – Total RNA was isolated via the Trizol method. Briefly, following Mn treatment, 1 mL of Trizol (Life Technologies) was added to each

tube containing 20,000 worms resuspended in 100 μl 85 mM NaCl, followed by three cycles of freezing in liquid nitrogen and thawing at 37°C. 200 μL of chloroform was then added to each tube, followed by precipitation using isopropanol and washing with 75% ethanol. Following isolation, 1 μg total RNA was used for cDNA synthesis using the High Capacity cDNA Reverse Transcription Kit (Life Technologies), per manufacturer's instructions. cDNA samples were stored at 4°C. Quantitative real-time PCR (BioRad CFX96) was conducted in duplicate wells using TaqMan Gene Expression Assay probes (Life Technologies) for each gene, using the *gpd-3* (*gapdh* homolog) housekeeping gene for normalization after determining the fold difference using the comparative $2^{-\Delta\Delta Ct}$ method[259]. The following probes were used: s*mf-1* (Assay ID: Ce02496635_g1); *smf-2* (Assay ID: Ce02496634_g1); *smf-3* (Assay ID: Ce02461545_g1); *fpn-1.1* (Assay ID: Ce02414545_m1); and *gpd-3* (Assay ID: Ce02616909_gH).

*Metal Quantification* – Total intraworm metal content was quantified using inductively coupled plasma mass spectrometry (ICP-MS), as previously described[246]. Briefly, 50,000 synchronized L1 worms were acutely treated with $MnCl_2$. Worms were then pelleted, washed five times with 85 mM NaCl and re-suspended in 1 mL 85 mM NaCl supplemented with 1% protease inhibitor. After sonication, an aliquot was taken for protein normalization using the bicinchoninic acid (BCA) assay kit (Thermo Scientific). Subsequently, the suspension was mixed again, evaporated, and incubated with the ashing mixture (65%$HNO_3$/30%$H_2O_2$ (1/1) (both Merck)) at 95 °C for at least 12 h. After dilution of the ash with bidistilled water, metal levels were determined by ICP-MS/MS.

*Relative Mitochondrial DNA Copy Number Quantification* – Relative mitochondrial DNA copy number was quantified using qPCR methods as previously described[317], with slight modifications. Briefly, 1,000 synchronized L1 worms were treated with $MnCl_2$ for 30 minutes, following by several washes. Total genomic DNA was then isolated using a 1X PCR buffer containing 0.1% Proteinase K, and subjected to the following lysis protocol in a thermal cycler (BioRad T100): 65°C for 90 minutes, 95°C for 15 minutes, and then hold at 4°C. Following lysis, DNA was diluted to 3 ng/µl, and real time PCR (BioRad CFX96) using SYBR Green (BioRad) was performed in triplicate with the following primers: *nd-1* for mtDNA (forward primer sequence: 5'-AGCGTCATTTATTGGGAAGAAGAC-3'; reverse primer sequence: 5'-AAGCTTGTGCTAATCCCATAAATGT-3') and *cox-4* for nuclear DNA (forward primer sequence: 5'-GCCGACTGGAAGAACTTGTC-3'; reverse primer sequence: 5'-GCGGAGATCACC TTCCAGTA-3'). The PCR reaction consisted of: 2µL of template DNA, 1µL each of mtDNA and nucDNA primer pairs (400nM final concentration each), 12.5µL SYBR Green PCR Master Mix and 8.5µL H2O. The following protocol was used: 50°C for 2 minutes, 95°C for 10 minutes, 40 cycles of 95°C for 15 seconds and 62°C for 60 seconds. The mitochondrial DNA content relative to nuclear DNA was calculated using the following equations: $\Delta C_T$ = (nucDNA $C_T$ – mtDNA $C_T$), where relative mitochondrial DNA content = $2 \times 2^{\Delta CT}$.

*Glutathione Quantification* – Total intracellular glutathione levels (reduced and oxidized GSH) have been determined using the "enzymatic recycling assay", as previously described[257]. Briefly, whole worm extracts were prepared out of 40,000 L1 worms

acutely exposed to $MnCl_2$. This was followed by washes with 85 mM NaCl and sonication of the pellet in 0.12 mL ice-cold extraction buffer (1% Triton X-100, 0.6% sulfosalicylic acid) and 1% protease inhibitor in KPE buffer (0.1 M potassium phosphate buffer, 5 mM EDTA). After centrifugation at 10,000 rpm for 10 minutes at 4°C, the supernatant was collected, with an aliquot reserved for protein normalization using the BCA assay. Total intracellular GSH was quantified by measuring the change in absorbance per minute at 412 nm by a microplate reader (FLUOstar Optima microplate reader, BMG Labtechnologies) after reduction of 5,5′-dithio-2-nitrobenzoic acid (DTNB, Sigma-Aldrich). Hydrogen peroxide was used as a positive control.

*Basal Slowing Response Assay* – This assay of dopaminergic integrity was performed as previously described[228], with slight modifications. Briefly, 2500 synchronized L1 worms were acutely treated in siliconized tubes with $MnCl_2$ for 30 minutes. Following washes with 85 mM NaCl, treated worms were transferred to seeded NGM plates. 48 hours after treatment, 60 mm NGM plates with seeded with bacteria spread in a ring (inner diameter of ~1 cm and an outer diameter of ~3.5 cm) in the center of the plate. Two seeded and two unseeded plates per group were kept at 37°C overnight, and allowed to cool to room temperature before use. Once Mn-treated animals reached the young adult stage, animals were washed at least two times with S basal buffer and then transferred to the central clear zone of the ring-shaped bacterial lawn (5-10 worms per plate) in a drop of S basal buffer that was delicately absorbed from the plate using a Kimwipe. After a five-minute acclimation period, the number of body bends in a 20-second interval was scored for each worm on the plate. Data are presented as the

change (Δ) in body bends per 20-second interval between worms transferred to unseeded plates and those with bacterial rings. Worms lacking *cat-2* (the homolog for tyrosine hydroxylase) were used as a positive control, as these worms are impaired in bacterial mechanosensation[228]. General locomotion was assessed using the number of body bends/20 seconds of the group transferred to unseeded plates.

*Statistics* – Dose-response lethality curves and all histograms were generated using GraphPad Prism (GraphPad Software Inc.). A sigmoidal dose-response model with a top constraint at 100% was used to draw the lethality curves and determine the respective $LD_{50}$ values, followed by a one-way ANOVA with a Dunnett post-hoc test to compare all strains to their respective control strains. Two-way ANOVAs were performed on TaqMan gene expression, metal content, total GSH, relative mtDNA copy number and basal slowing response data, followed by Bonferroni's multiple comparison post-hoc tests.

## Results

*pdr-1 mutants show alterations in mRNA expression of Mn exporter-, but not importer-related genes* – We previously reported a statistically significant increase in Mn accumulation in *pdr-1* mutants vs. WT worms[246]. To test whether this enhancement was due to a change in transcription of Mn importer and/or exporter genes, we performed quantitative reverse transcription PCR (qRT-PCR) to examine *smf-1,2,3* (**Fig 10A-C**) and *fpn-1.1* gene expression (**Fig 10D**), respectively, following acute Mn exposure.

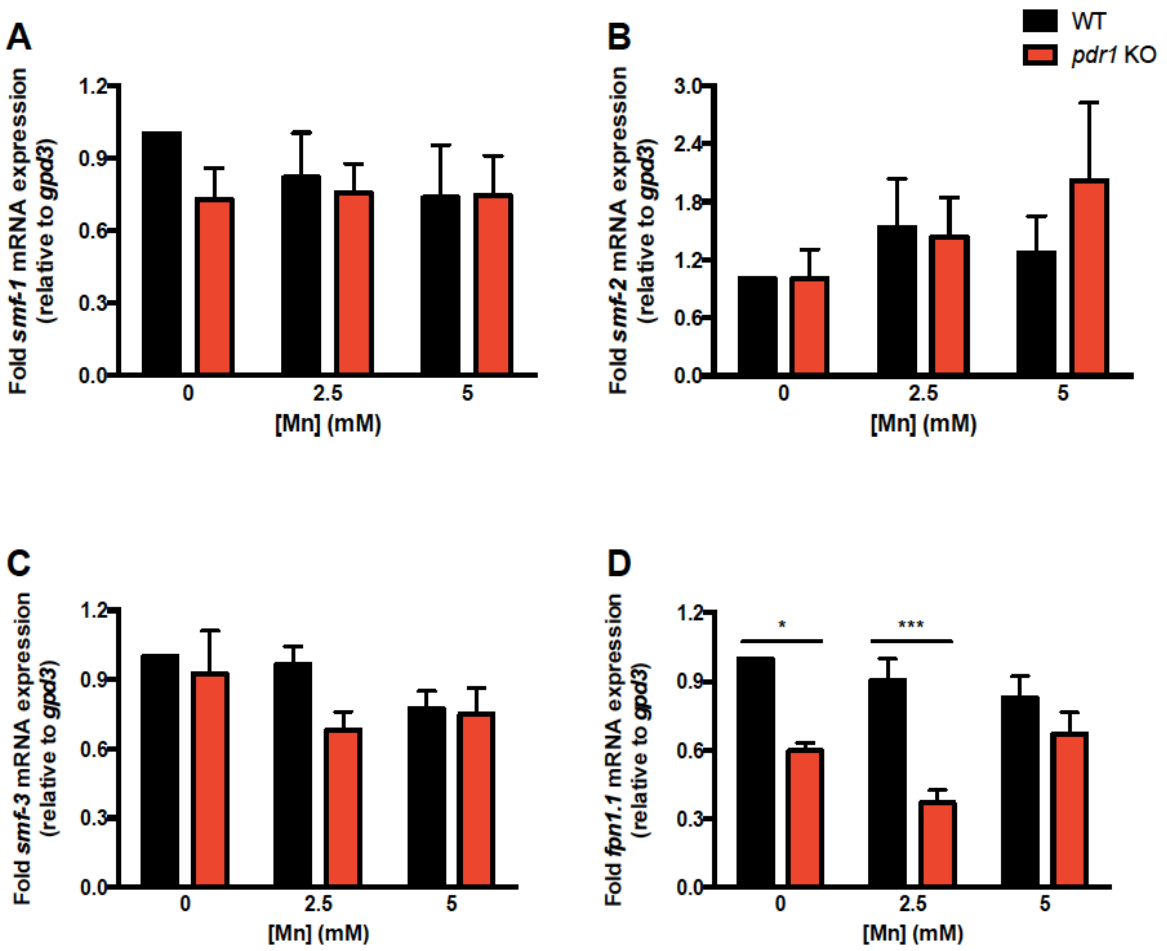


**Figure 10.** *pdr-1 mutants show alterations in mRNA expression of Mn exporter, but not importer, genes.* (A-D) *smf-1,2,3 and fpn-1.1* mRNA expression after an acute, 30 min treatment of L1 worms with 0, 2.5 and 5 mM $MnCl_2$. Relative gene expression was determined by qRT-PCR. (A) *smf-1* mRNA expression in N2 (WT) and *pdr-1* KO animals. (B) *smf-2* mRNA expression in N2 (WT) and *pdr-1* KO animals. (C) *smf-3* mRNA expression in N2 (WT) and *pdr-1* KO animals. (D) *fpn-1.1* mRNA expression in N2 (WT) and *pdr-1* KO animals. (A-D) Data are expressed as mean values + SEM of at least five independent experiments in duplicates normalized to the untreated wildtype and relative to *gpd3* mRNA. Statistical analysis by two-way ANOVA: (A) interaction, ns; genotype, ns; concentration, ns; (B) interaction, ns; genotype, ns; concentration, ns; (C) interaction, ns; genotype, ns; concentration, ns; (D) interaction, ns (trend level, $p=0.0639$); genotype, $p<0.0001$; concentration, ns. *$p < 0.05$, ***$p < 0.001$ vs. respective wildtype worms.

Two-way ANOVA analysis showed no overall effect of Mn treatment on transcription of any of the genes tested. However, while *pdr-1* mutants showed no significant changes in *smf-1,2,3* (the importers) mRNA expression (**Fig 10A-C**), a significant genotype difference ($p<0.0001$) was noted in *fpn-1.1* (the exporter) between *pdr-1* mutants and WT animals. *Post-hoc* analysis revealed a significant *fpn-1.1* downregulation at 0 and 2.5 mM $MnCl_2$ (**Fig 10D**).

*Overexpression of fpn-1.1 in pdr-1 mutants rescues Mn-induced lethality* – In addition to enhanced Mn accumulation, *pdr-1* mutants showed a leftward shift in the Mn dose-response survival curve, with WT worms exhibiting a $LD_{50}$ of 10.43 mM[246]. To determine whether downregulation of *fpn-1.1* may have played a role in exacerbating Mn-induced lethality of *pdr-1* mutants, we overexpressed *fpn-1.1* in the *pdr-1* mutant background. Upon Mn exposure, *pdr-1* mutants overexpressing *fpn-1.1* (*pdr-1* KO; *fpn-1.1* OVR) exhibited a rightward shift in the dose-response curve compared to *pdr-1* mutants alone (**Fig 11A**). The $LD_{50}$ of *pdr-1* KO; *fpn-1.1* OVR animals (10.84 mM) relatively normalized to previously published WT levels, while *pdr-1* mutants alone show a $LD_{50}$ of 7.416 mM (**Fig 11B**). Two-way ANOVA analysis showed a significant interaction effect ($p=0.0064$) between both genotype and treatment ($p<0.0001$).

*Overexpression of fpn-1.1 in pdr-1 mutants decreases levels of highly pro-oxidant metals* – Upon noting the improved survival in *pdr-1* KO; *fpn-1.1* OVR animals, we

A

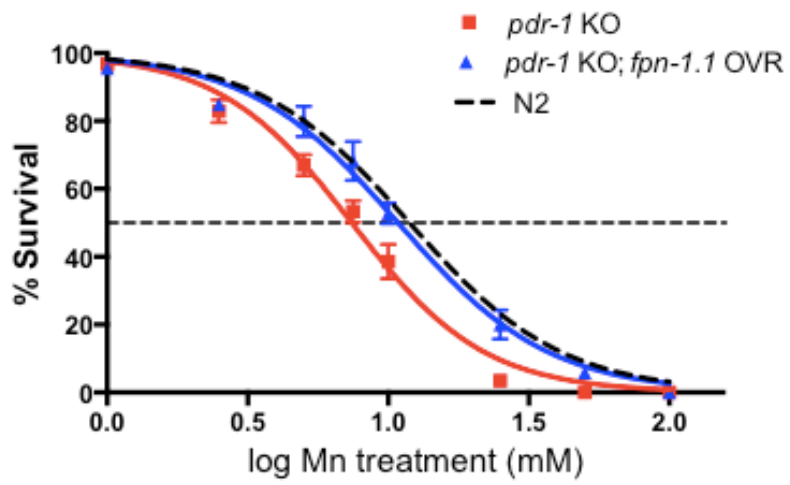


B

| Strain | Genotype | $LD_{50}$ (mM $MnCl_2$) |
|---|---|---|
| VC1024 | *pdr1(gk448) III* (KO) | 7.416 |
| MAB326 | *pdr1(gk448) III* (KO); *fpn1.1* OVR | 10.84 |

**Figure 11**. *Overexpression of fpn-1.1 in pdr-1 mutants rescues Mn-induced lethality.* (A,B) Dose-response survival curves following acute Mn exposure. All values were compared to untreated worms set to 100% survival and plotted against the logarithmic scale of the used Mn concentrations. (A) *pdr-1* KO animals and *pdr-1* mutants overexpressing *fpn-1.1* (*pdr-1* KO; *fpn-1.1* OVR) were treated at the L1 stage for 30 min with increasing $MnCl_2$ concentrations. Dashed curve represents the typical WT survival curve as previously published. (B) The respective $LD_{50}$ concentrations (mM $MnCl_2$) for both genotypes. Data are expressed as mean values + SEM from at least five independent experiments. Statistical analysis by two-way ANOVA: interaction, p=0.0064; genotype, p<0.0001; concentration, p<0.0001.

hypothesized that this attenuation in Mn-induced toxicity is associated with a decrease in redox active metal accumulation. Using inductively coupled plasma mass spectrometry (ICP-MS), we measured intraworm concentrations of various metals, including Mn, iron (Fe), zinc (Zn) and copper (Cu) following acute Mn exposure. To our surprise, Mn levels remained relatively similar between strains, though two-way ANOVA analysis revealed a significant treatment effect (**Fig 12A,** p=0.0165). However, endogenous Fe levels were significantly decreased in *pdr-1* KO; *fpn-1.1* OVR animals compared to *pdr-1* KOs alone (**Fig 12B**, p=0.0092), though further significance was not reached at the post-hoc level. No significant changes were seen in Zn levels (**Fig 12C**). However, similar to Fe, Cu levels were significantly decreased in *pdr-1* KO; *fpn-1.1* OVR animals compared to *pdr-1* KOs (**Fig 12D**, p=0.0256), with no post-hoc level differences. In summary, Mn levels stayed relatively the same, while Fe and Cu were both significantly decreased in *pdr-1* KO; *fpn-1.1* OVR animals. These results indicate that the improved survival is probably due to decreased levels of Fe and Cu, and suggests that *fpn-1.1* may prefer Fe and Cu as substrates over Mn.

*Overexpression of fpn-1.1 in pdr-1 mutants improves mitochondrial integrity and antioxidant response* – Increased Mn levels in *pdr-1* KOs (*vs.* WT animals) have been noted concurrently with significantly increased basal levels of RONS and depleted basal levels of total glutathione (GSH), suggesting an overall exacerbated environment of oxidative stress in *pdr-1* KO animals[246]. Therefore, we next sought to determine whether the significant decrease in Fe and Cu levels (**Fig 12**) and improvement in survival of *pdr-1* KO;*fpn-1.1* OVR animals (**Fig 11A**) were associated with improved defence

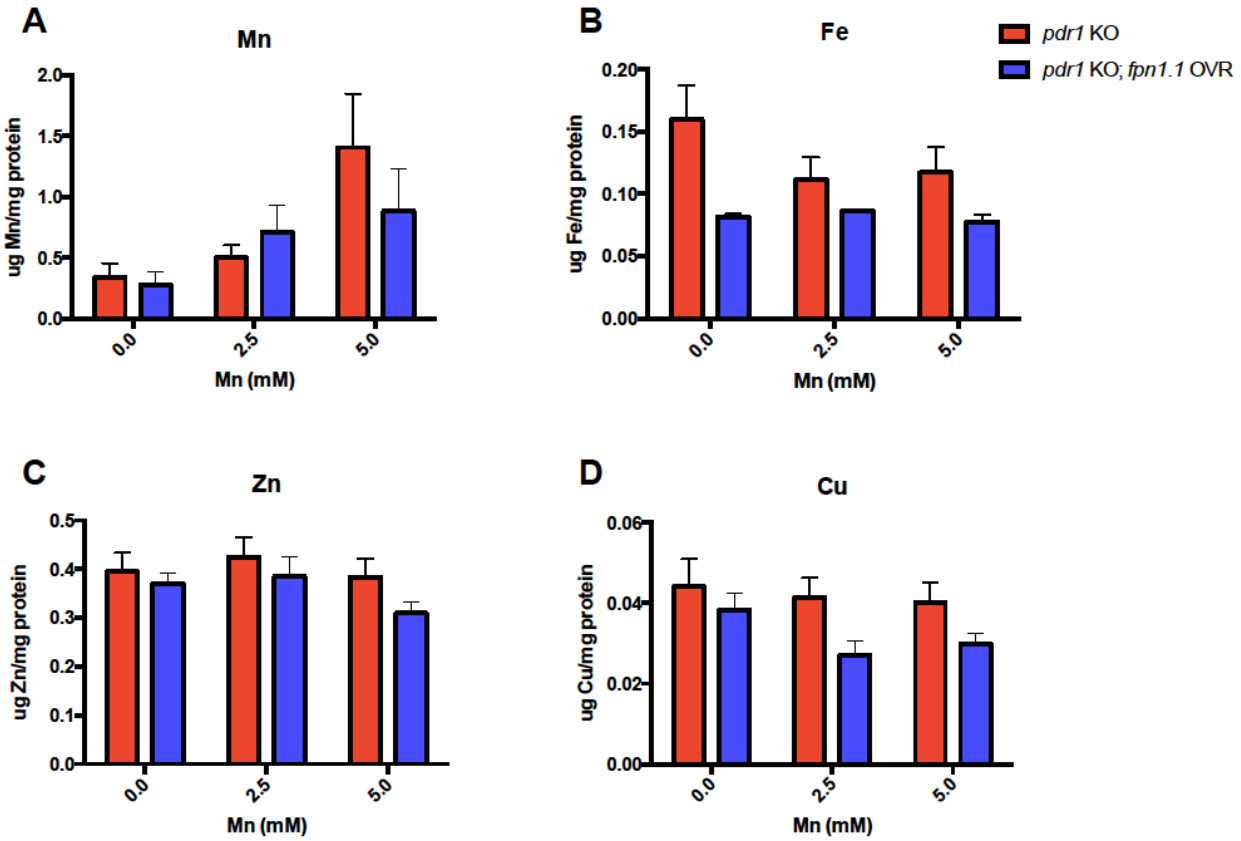


**Figure 12.** *Overexpression of fpn-1.1 in pdr-1 mutants decreases levels of highly pro-oxidant metals.* (A-D) Intraworm metal concentrations following acute, 30 min $MnCl_2$ treatment (0, 2.5 and 5 mM) at the L1 stage, as quantified by ICP-MS/MS. (A) Mn content (µg Mn/mg protein) in *pdr-1* KO and *pdr-1* KO; *fpn-1.1* OVR animals. (B) Iron (Fe) content (µg Fe/mg protein) in *pdr-1* KO and *pdr-1* KO; *fpn-1.1* OVR animals. (C) Zinc (Zn) content (µg Zn/mg protein) in *pdr-1* KO and *pdr-1* KO; *fpn-1.1* OVR animals. (D) Copper (Cu) content (µg Cu/mg protein) in *pdr-1* KO and *pdr-1* KO; *fpn-1.1* OVR animals. (A-D) Data are expressed as mean values + SEM from at least six independent experiments and normalized to total protein content. Statistical analysis by two-way ANOVA: (A) interaction, ns; genotype, ns; concentration, p=0.0165; (B) interaction, ns; genotype, p=0.0092; concentration, ns; (C) interaction, ns; genotype, ns; concentration, ns; (D) interaction, ns; genotype, p=0.0256; concentration, ns.

mechanisms against oxidative stress. This was investigated using two measures: relative mitochondrial DNA (mtDNA) copy number and total GSH levels. Alterations in mtDNA copy number have been associated with aging and degenerative processes[318]. Moreover, parkin has been shown to regulate mitochondrial turnover to maintain proper mitochondrial integrity[35]. Using a quantitative PCR (qPCR) technique, we found *pdr-1* KO animals had a significantly elevated mtDNA copy number relative to WT animals, whereas *pdr-1* KO;*fpn-1.1* OVR animals exhibited levels similar to WT animals (**Fig 13A**); two-way ANOVA analysis reveals a significant genotype effect (p=0.0116), though significance was not reached at the *post-hoc* level. Moreover, we previously published the basal depletion of total GSH in *pdr-1* KOs compared to WT controls. Given the reversal of increased mtDNA copy number in *pdr-1* KO;*fpn-1.1* OVR animals, we examined whether there was a similar rescue of GSH depletion. While statistical significance wasn't reached, there was a trend toward increased GSH levels in *pdr-1* KO;*fpn-1.1* OVR animals relative to *pdr-1* KOs (**Fig 13B**, p=0.09). In both measures, Mn treatment itself did not significantly affect the outcomes.

*Overexpression of fpn-1.1 in pdr-1 mutants improves the DA-dependent basal slowing response* –Loss of *parkin* is connected to PD-associated DAergic neurodegeneration, and we previously published similar results of *pdr-1* KOs showing increased DAergic neurodegeneration *vs.* WT worms with fluorescence microscopy[246]. Consequently, we investigated whether the visual effects of DAergic neurodegeneration persisted to alter a behavioral outcome of DAergic integrity. The basal slowing response is a DA-dependent behavior that affects the mechanosensation needed for proper food sensing

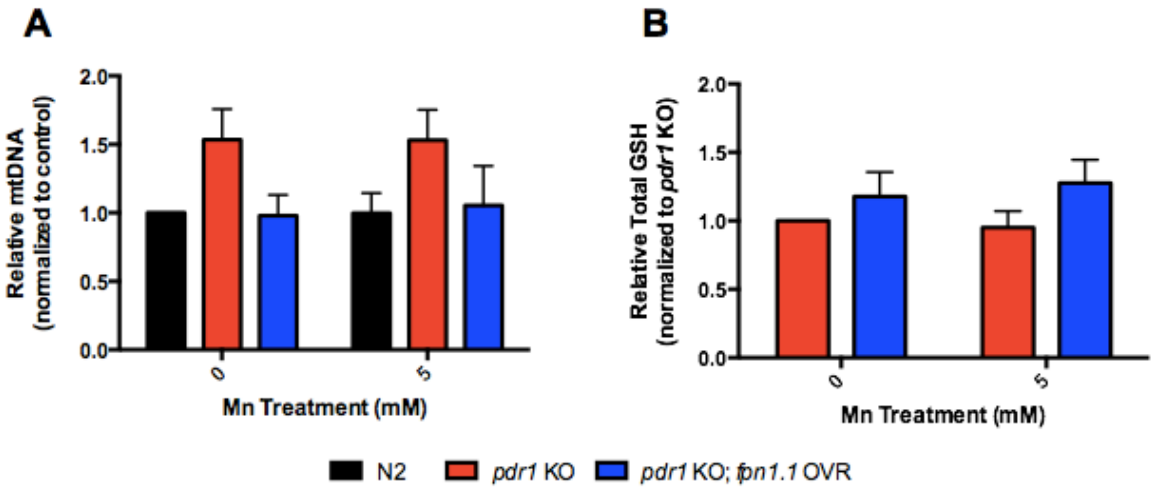


**Figure 13.** *Overexpression of fpn-1.1 in pdr-1 mutants improves mitochondrial integrity and antioxidant response.* (A) Relative mitochondrial DNA (mtDNA) copy number in *pdr-1* KO and *pdr-1* KO; *fpn-1.1* OVR animals following an acute, 30 min treatment with 0 and 5 mM $MnCl_2$. Relative gene expression was determined by qPCR. (B) Total glutathione (GSH) levels of *pdr-1* KO and *pdr-1* KO; *fpn-1.1* OVR animals following an acute, 30 min treatment with 0 and 5 mM $MnCl_2$. (A) Relative mtDNA copy number is expressed as a ratio of *nd-1* (mtDNA marker) to *cox-4* (nuclear DNA marker). Data are expressed as mean values + SEM of at least five independent experiments in duplicates normalized to the untreated N2 wildtype values. (B) Data are expressed as mean values + SEM of at least five independent experiments in duplicates, normalized to total protein content and relative to untreated *pdr-1* KO values. Statistical analysis by two-way ANOVA: (A) interaction, ns; genotype, p=0.0116; concentration, ns; (B) interaction, ns; genotype, ns (trend level, p=0.09); concentration, ns.

in *C. elegans*, as worms slow their movement when encountering a bacterial lawn. Worms lacking *cat-2*, the homolog for tyrosine hydroxylase, are defective in this response from the loss of dopamine synthesis and do not slow down[228]. Thus, the changes (Δ) in number of body bends between plates with and without bacteria reflect the integrity of DAergic neurons. Using this paradigm, *pdr-1* KO animals exhibited a significantly defective basal slowing response *vs.* WT animals ($p<0.001$) that was analogous to that of *cat-2* mutants (**Fig 14**). The *pdr-1* KO;*fpn-1.1* OVR animals showed a partial rescue of the response, without reaching statistical significance. However, in the presence of Mn treatment, *pdr-1* KO;*fpn-1.1* OVR fully restored the response to WT levels, with the changes (Δ) in number of body bends being significantly higher than *pdr-1* KOs alone ($p<0.01$). To ensure that these effects were not due to general locomotion differences, we compared the number of body bends per group on plates without bacterial lawns; there were no significant differences between all groups (Suppl. Fig. 1).

## Discussion

The relationship between genetic mutations and the contribution of environmental risk factors in the development of PD has yet to be clearly defined. In the present study, the *C. elegans* model system was utilized to investigate alterations in Mn homeostasis and toxicity in animals lacking *pdr-1/parkin*, a genetic risk factor for PD. We previously published evidence that animals lacking *pdr-1* show high sensitivity to an acute Mn exposure, with decreased survival and significantly elevated Mn accumulation compared to WT animals[246]. The present study aimed to determine whether the

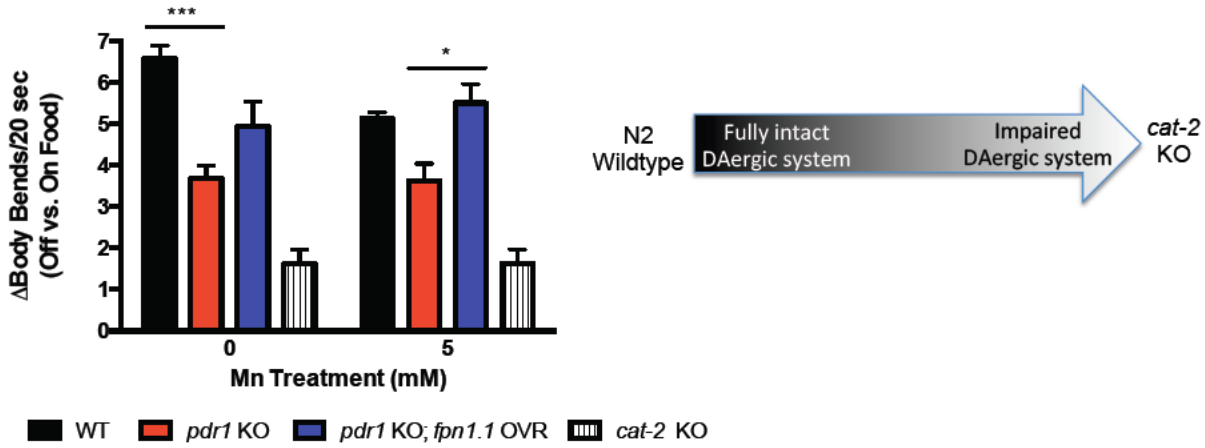


**Figure 14.** *Overexpression of fpn-1.1 in pdr-1 mutants improves the DA-dependent basal slowing response.* Behavioral data are expressed as the change (Δ) in body bends per 20 seconds between treated (5 mM $MnCl_2$) and untreated WT, *pdr-1* KO and *pdr-1* KO; *fpn-1.1* OVR animals placed on plates without food vs. plates with food. Schematic shows the spectrum of change, with N2 wildtype animals possessing a higher change in body bends (i.e., a fully intact DAergic system) to *cat-2* mutants possessing a smaller, almost negligible change in body bends (i.e., an impaired DAergic system). *cat-2* KO animals were used as a positive control. Statistical analysis by two-way ANOVA: interaction, ns (trend level, p=0.0872); genotype, p<0.0001; concentration, ns. ***p<0.001 vs. untreated WT, *p<0.05 vs. *pdr-1* KO.

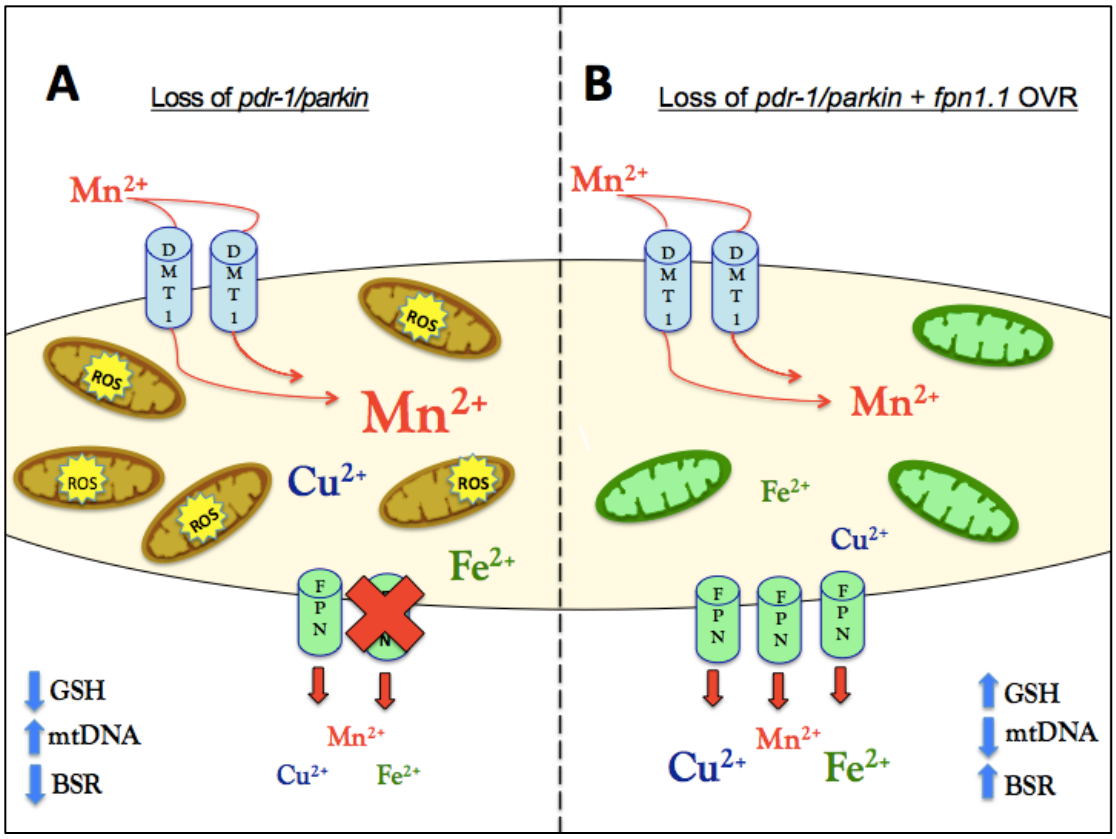


**Figure 15.** *Basic model summarizing the findings of Chapter 3.* (A) Loss of *pdr-1* results in increased Mn accumulation that is associated with downregulation of *fpn-1.1* mRNA, increased ROS production, basally depleted GSH, elevated mtDNA copy number and deficits in the DA-dependent basal slowing response (BSR) vs. WT animals. (B) Upregulation of *fpn-1.1* in *pdr-1* KO animals ameliorates Mn-induced toxicity of *pdr-1* KO's, including slight elevation of GSH, mtDNA copy number and BSR normalization to WT levels, and decreased accumulation of Fe, Cu and Mn.

enhanced Mn concentrations were due to altered expression of Mn transporters in *C. elegans* to affect Mn homeostasis. Parkin's role in regulating metal homeostasis has only recently begun to be investigated. Previous *in vitro* evidence has shown that parkin can modulate levels of the 1B isoform of DMT1 through ubiquitination[170]. Moreover, *Drosophila* studies show that both pharmacological (BCS/BPD) or genetic (increased expression of the metal responsive transcription factor 1, MTF-1) chelation of redox-active metals decreases oxidative stress, improves reduced lifespan and normalizes metal concentrations in *parkin* mutant flies[269, 270]. Therefore, parkin's regulation of metal homeostasis and its role as an E3 ligase raise the possibility of parkin-mediated regulation of Mn-responsive proteins. The *C. elegans* system represents an ideal model to study this possibility, as PDR-1 conserves its ligase activity[236], and their genome contains less E3 ligases[319] to minimize the possible compensatory mechanisms seen in vertebrate knockout models.

Contrary to *in vitro* evidence of parkin-mediated control of a DMT isoform, we observed no significant changes in expression of the *smf* genes, especially with *smf-3* being the most DMT1-like homolog[241]. Instead, significant downregulation of *fpn-1.1* was observed in *pdr-1* KOs compared to WT animals. These findings suggest that the loss of *pdr-1* in *C. elegans* results in increased Mn accumulation that may be from defective export, rather than from impaired uptake. Notably, we recently identified a novel role for SLC30A10 in Mn export that is associated with heightened risk for PD. However, no homologs for this protein are expressed in *C. elegans*[177]. Thus, for the present study, given the downregulation of *fpn-1.1* mRNA in *pdr-1* mutants, we investigated the effects of overexpressing the only known Mn exporter in *C. elegans*.

Mn uptake is modulated by a variety of proteins, including: DMT1, the transferrin receptor (TfR), the choline transporter, the citrate transporter, the magnesium transporter HIP14, the P-type transmembrane ATPase (ATP13A2), the solute carrier 39 family of zinc transporters, and calcium channels[252]. Among these, DMT1 has been given the most attention, as it is not only the primary mode of uptake, but is also associated with parkinsonism. Increased DMT1 expression has been found in the SNpc of PD patients, as well as in SNpc of MPTP mouse models[217]. Elevated DMT1 mRNA expression and DAergic neurotoxicity was also seen in rats exposed to Mn-containing welding fumes[320]. Moreover, specific polymorphisms in DMT1 have been found in a Chinese population suffering from PD[218]. These studies highlight altered metal homeostasis in the etiology of Parkinsonism. Interestingly, the overexpression of FPN in our *pdr-1* mutants altered not only Mn, but Fe and Cu levels to a greater extent. We were not surprised to observe a treatment effect for Mn, as this was the only exogenous treatment administered to the nematodes. However, we did expect to see a greater decrease in Mn concentrations. It may be possible that currently unidentified Mn importers or exporters in *C. elegans* may be compensating to prevent the expected rescue of Mn accumulation. For example, there may be additional exporters that share similarities with the newly established cell surface Mn exporter SLC30A10, which does not have any *C. elegans* homologs. It is also possible that FPN's affinity for Fe is greater than that of Mn, as the differential binding affinities have yet to be determined. Moreover, as FPN has not been shown to export Cu, the decrease in Cu levels may be a secondary effect of lowered intracellular Fe due to increased Fe efflux. Fe-deficiency

anemia has been associated with copper deficiencies, though the mechanism remains unknown[321, 322].

In addition to the well-characterized toxicity of Mn resulting in parkinsonian symptoms, enhanced iron accumulation in the SN is often seen in PD brains[217, 323], with pharmacological Fe chelation showing potential therapeutic value[324, 325]. Moreover, Mn treatment has been recently shown to disrupt general metal homeostasis in WT *C. elegans*, with excess Mn resulting in altered Fe and Cu levels[326]. Though the authors of this study used slightly higher Mn concentrations (10-30 mM) than the present study, this was most likely due to the use of older worms treated for 24 hours, rather than larval stage worms acutely treated for 30 minutes. However, as their lowest dose (10 mM) is within the range of the doses used in the present study, similar findings were seen with higher Mn concentrations (30 mM) corresponding with comparatively lower Fe and Cu levels overall[326]. The results in the present study provide further support of the interplay between metals, as exogenous Mn treatment results in the alteration of endogenous metal concentrations that may alter vital downstream processes. It is possible that the combined effects of decreased Fe and Cu levels, rather than the moderate to slight decrease in Mn levels, results in the amelioration of the *pdr-1* KO phenotypes (**Fig 15**).

Moreover, the recently discovered role of parkin as a mediator of mitophagy has introduced the potential significance of mitochondrial integrity in Parkinsonism[327]; loss of *parkin* could result in the accumulation of defective mitochondria to increase cellular oxidative stress. This could explain the significant increase in relative mtDNA copy number in *pdr-1* KO animals as a measure that could equate with increased

mitochondrial mass in *pdr-1* KOs. These data corresponds with our previously published findings that *pdr-1* KOs exhibit significantly increased RONS levels. Notably, it seems controversial in the literature whether increased mtDNA copy number is protective or damaging in degenerative processes[328, 329]. However, increased mtDNA copy number has been associated with aging, as well as a response to increased oxidative stress[318]. Therefore, the increased copy number may also be in response to increased oxidative stress from enhanced Mn accumulation to compensate for damaged mitochondria. This may be especially true due to the preferential accumulation of Mn in mitochondria[159]. Consequently, the beneficial alterations in Mn, Fe and Cu in *pdr-1* KO;*fpn-1.1* OVR animals would then help to reverse this effect by decreasing metal-induced oxidative stress. Additionally, while the increase in the antioxidant GSH in *pdr-1* KO;*fpn-1.1* OVR animals vs. *pdr-1* KO animals is moderate, it reaches trend-level significance. This may represent an improvement in the overall handling oxidative stress. It has been previously shown that neurons treated with increasing Fe concentrations show depletion in GSH content[330]. This is similar to the elevation in GSH content of *pdr-1* KO;*fpn-1.1* OVR animals that also exhibit decreased Fe accumulation. However, we are limited in the present study, as we have been unsuccessful in using the microplate assay format to measure both GSSG and GSH. While *pdr-1* KO;*fpn-1.1* OVR and *pdr-1* KO animals show no difference in *gcs-1* (homolog for the glutamate-cysteine ligase responsible for catalysing GSH synthesis) mRNA expression (data not shown), future studies should be done to determine whether this change in GSH is due to more reduced vs. oxidized forms of GSH.

Finally, we previously reported that *pdr-1* KO animals show an exacerbation of DAergic neurodegeneration compared to WT animals[246]. Currently, conflicting findings exist on the effects of Mn on DAergic neurodegeneration in *C. elegans*[260, 326]. However, this may be due to differences in treatment paradigms and doses. Additionally, fluorescence microscopy is a common technique to assess degeneration; however, microscopy for GFP visualization remains a mostly qualitative readout of cell death. Accordingly, we focused on an output parameter of an intact DAergic system by assaying a DA-dependent behavioural measure. The basal slowing response (BSR) is a well-known feeding response that requires DA and affects mechanosensation to properly recognize food sources (bacteria) in *C. elegans*[228]. Similar to our previous results, Mn treatment itself in WT animals did not result in a statistically significant decrease in BSR, though a slight decline was apparent. However, while *pdr-1* KOs show impairment in this response, the rescue of BSR deficits by *pdr-1* KO;*fpn-1.1* OVR animals normalizes to the WT response. These data suggest that the overexpression of FPN normalizes DAergic integrity in the background of *pdr-1* loss. The effect of Mn on BSR in *pdr-1* KO and *pdr-1* KO;*fpn-1.1* OVR animals is negligible. This may be due to the complete loss of *pdr-1* resulting in a "ceiling effect," such that the addition of Mn exposure does not further exacerbate the basal differences. However, the BSR in *pdr-1* KO;*fpn-1.1* OVR animals fully normalizes to WT levels upon treatment.

Notably, we cannot relate the improvement in BSR to the improved survival of *pdr-1* KO;*fpn-1.1* OVR animals, as it has been previously reported that ablation of DAergic neurons in nematodes does not affect overall survival[230]. However, the relationship between metals and dopamine toxicity is well known. Dopamine itself is a

strong oxidant that can undergo an auto-oxidation process to produce highly damaging intermediates, which makes a strong argument for the vulnerability of DA-specific brain areas to toxins and other oxidants[331]. Mn has been shown to catalyse dopamine oxidation[332], while Fe has been shown to specifically bind neuromelanin found in DAergic neurons[333]. Thus, the *pdr-1* KO; *fpn-1.1* OVR animals may show improvement in the DA-dependent BSR due to the lower bioavailability of Mn, Fe and Cu (**Fig 15**) that would otherwise participate in directly enhancing DA oxidation and/or indirectly producing damaging free radicals in an already susceptible cell type.

## Conclusions

In conclusion, the present study provides further support for altered metal homeostasis as a critical component of PD pathophysiology. Using the genetically tractable *C. elegans* system, we show a novel role of *pdr-1/parkin* in modulating metal homeostasis following an acute Mn exposure by influencing metal efflux. Though human mutations in FPN have not yet been associated with PD, our findings demonstrate the importance and specificity of PD genetics (e.g. loss of *pdr-1/parkin*) in interacting with environmental factors to exacerbate physiological processes that may lead to cell death. Future studies should focus on potential therapeutic routes that help understand the interplay between *pdr-1/parkin*-mediated mitochondrial dynamics and enhanced efflux of redox-active metals like Mn, Fe and Cu as a strategy against Mn-induced Parkinsonism.

# CHAPTER IV

# DISCUSSION AND FUTURE DIRECTIONS

In summary, the data presented in this thesis support the hypothesis that loss of function of early-onset PD disease genes, namely *pdr-1/parkin* and *djr-1.1/dj1*, results in increased vulnerability to Mn toxicity in *C. elegans*, as evidenced by enhanced Mn accumulation and oxidative stress in these backgrounds. Our findings further support the hypothesis that WT αS may have protective qualities, as its expression in the background of *pdr-1* and *djr-1.1* loss ameliorates Mn toxicity by reducing Mn levels and RONS production. Though WT αS rescues DAergic neurodegeneration in *pdr-1* KO animals that also exhibit increased *dat-1* mRNA, it does not in *djr-1.1* KO animals that show decreased *dat-1* mRNA. These findings indirectly support the role of extracellular dopamine in exacerbating Mn toxicity. Furthermore, our results show that *pdr-1* loss confers the highest vulnerability to Mn-induced lethality, concurrent with the highest Mn accumulation. We show evidence of decreased *fpn-1.1* mRNA expression in animals lacking *pdr-1*, with no change in expression of Mn importer genes, suggesting that Mn export, rather than import, is altered in these animals. Moreover, the overexpression of *fpn-1.1* in the background of *pdr-1* loss rescues toxic metal accumulation that concurrently improves mitochondrial and DAergic integrity.

An interesting phenomenon in Chapter 2 revolves around DAergic-specific expression of human αS driving global changes in Mn accumulation, considering we do not yet have the technical skills in quantifying metal content within neurons specifically.

One possibility for this finding is following the theory that the progressive nature of PD may be due to αS propagation from one brain region to another. The spread of αS was first identified in previous clinical studies, where patients suffering from PD received transplants of nigral embryonic DAergic neurons into their striatum. More than a decade after surgery, αS- and ubiquitin-containing Lewy bodies, as well as reduced immunostaining for DAT, were present in the grafted neurons[334, 335]. Researchers also believe that this phenomenon may help explain the selectivity of DAergic neurons in PD. as dopamine itself has been shown to enhance the formation of non-fibrillar αS oligomers in intracellular vesicles. Increased cystolic DA levels using L-DOPA treatment subsequently results in secretion of αS oligomers into the media[336]. Moreover, inhibition of the autophagy/lysosome pathway results in increased intercellular transfer of αS from donor neurons expressing αS to recipient cells, which then exhibit enhanced apoptotic cell death[337]. This is of particular interest in terms of Parkin's involvement in mitophagic processes that utilize this pathway, as well as its general role in protein clearance. In fact, a recent study provides evidence that mice lacking *parkin* show increased transfer of αS from the brain to the blood, with increased Parkin ubiquitination/activity aiding in αS clearance and turnover. Thus, the authors conclude that PD patients suffering from *parkin* mutations may not characteristically exhibit Lewy bodies due to the loss of αS sequestration through autophagic elimination[338].

The connection between environmental toxicants and αS aggregation has been well established. Uversky et *al*. first showed that $Mn^{2+}$ could accelerate the rate of αS fibril formation[254], with a later study finding that αS selectively exacerbates $Mn^{2+}$ (and

not $Fe^{2+}$)-induced cell death in DAergic cells expressing DAT[339]. More recent evidence in primates has confirmed that Mn exposure can induce αS aggregation in neurons of the frontal cortex[213]. However, the link between toxicants and transneuronal αS transport has only recently been examined. For example, exposure to rotenone in mice results in increased release of αS from enteric neurons into the surrounding media, with a higher amount of αS found in exosomes. These studies also utilized co-cultures to find that the rotenone-induced, released αS could be taken up into TH+ neurons and retrogradely transported into the soma[294]. Collectively, such evidence indicates the ability of αS to propagate from one cell to the other, though the mode of transport may not be well understood yet.

Our findings of global Mn-induced changes that are modulated by DA-specific αS expression may support this theory of αS propagation in *C. elegans*. In particular, the protective effects of WT αS in reducing whole-worm Mn toxicity and accumulation could be due to the spread of αS from DAergic neurons to neighboring cells to propagate its metal- quenching qualities. While this has yet to be determined, studies have found copper-and iron-binding sites, as well as its ability to alter Fe oxidation states[291, 340]. As these metal ions have been shown to share transport mechanisms and roles as cofactors, it may be possible for αS to also bind Mn. Future studies should examine its potential secretion in the context of a *pdr-1* mutant background, as our studies do not examine whether intracellular αS aggregation upon WT expression in this background is altered. It is also important to note that our studies did not investigate the effects of the aforementioned mutant forms of αS, and whether the opposite outcomes would be seen

(i.e., lack of a rescue of Mn accumulation and toxicity). Since αS is not endogenously expressed in *C. elegans* and has not been shown to be secreted in this system, however, a more likely possibility behind the global alterations may revolve around the direct control and influence of αS-expressing DAergic neurons on other cells. In fact, dopamine has been shown to act extrasynaptically in *C. elegans*; the DA receptors DOP-1 and DOP-3 are expressed on ventral motor cord neurons that are not postsynaptic to DAergic neurons[341]. Thus, I hypothesize that humoral DA secretions[342] could result in the control of any cell expressing a DA receptor, potentially including neurons in the gut where Mn absorption is greatly influenced.

A major question left unanswered in Chapter 3 is how the loss of *pdr-1* in *C. elegans* results in altered *fpn-1.1* expression. As worms conserve PDR-1 ligase activity, one would expect that the loss of *pdr-1* would result in the lack of FPN degradation, if FPN were a direct target of PDR-1. While it would have been beneficial to test this idea using Western blot techniques to assess FPN protein expression, the lack of commercially available *C. elegans*-specific antibodies made this difficult. Regardless, qRT-PCR methods revealed the opposite effect of decreased *fpn-1.1* mRNA levels in *pdr-1* KO animals. Although it is possible that the difference in mRNA levels may not correspond with protein expression, one could hypothesize that the *fpn-1.1* downregulation may be an indirect effect of *pdr-1* loss. As most E3 ubiquitin ligases have several target substrates, it may be possible that one of Parkin's targets is able to regulate FPN expression. The FPN system in *C. elegans* has not been extensively studied enough to fully understand how the exporters may be regulated in nematodes. In mammalian systems, however, some regulatory mechanisms have been investigated,

with the most prominent one being hepcidin, a peptide hormone. Hepcidin binds and inhibits FPN to control dietary iron absorption in mammals. However, the *C. elegans* genome does not contain any hepcidin-like genes.

There are other hepcidin-independent regulatory mechanisms to control FPN expression. These include the hypoxia-inducible factor 1 (HIF-1), a member of a transcription factor protein family that is stabilized under hypoxic conditions to promote upregulation of genes that foster survival in low-oxygen states. The *C. elegans* genome encodes a single homolog for HIF-1 (*hif-1*) that can modulate longevity in worms[343]. While evidence in *C. elegans* has found *hif-1* to act as a negative regulator of ferritin (*ftn-1* and *ftn-2*) transcription[344], no studies have yet examined whether the HIF-1-mediated control of FPN is conserved in nematodes. Some studies have also connected the Alzheimer's disease-associated amyloid precursor protein (APP) as another modifier of FPN function. Controversial findings suggest that APP may have ferroxidase activity[345, 346], with recent evidence indicating that endogenous APP may help stabilize cell-surface expression of FPN[346] to modulate iron export. The precise mechanism of the APP-FPN interaction, however, remains unclear. In *C. elegans*, it would be interesting to evaluate the expression of APL-1, the worm homolog of APP[347], in the background of *pdr-1* loss to determine whether altered APL-1 levels may be associated with FPN-1.1 downregulation; likewise, assessing *pdr-1* expression in the background of *apl-1* loss may also aid in further understanding this putative interaction.

Another potential intermediary of *pdr-1*-mediated *fpn1* regulation is Nrf2, the master regulator of neuroprotective antioxidant transcriptional responses. Activation of this transcription factor has been show to upregulate *fpn-1* mRNA in human and mice

macrophages, with microarray analysis confirming FPN1 to be an Nrf2 target gene. *skn-1* is the *C. elegans* homolog for the *nrf2* gene. While we show a slight increase in *skn-1* mRNA expression in *pdr-1* KOs (**Fig 7A**) vs. WT animals, it remained statistically insignificant. Our studies do not address whether SKN-1 activation and/or activity itself is altered in the background of *pdr-1* loss, which would provide a more mechanistic view at whether Nrf2-mediated regulation of FPN expression is conserved in *C. elegans*. Future studies should consider crossing worms containing a SKN-1 translational fusion reporter (SKN-1::GFP) with the *pdr-1* KO and *pdr-1* KO;*fpn-1.1* OVR animals to assess nuclear translocation of SKN-1 as an indication of its activation. It may also be worthwhile to assess the transcription of SKN-1's downstream targets, such as *gst-4,* in the background of *pdr-1* KO and *pdr-1* KO;*fpn-1.1* OVR animals.

DJ-1 has been shown to stabilize Nrf2 by preventing association with its inhibitor protein Keap1[106]. If the loss of *parkin* results in decreased DJ-1, as seen in neurons[272], loss of Nrf2 stabilization could then result in the decreased *fpn-1.1* expression seen in *pdr-1* KOs (**Fig 10D**). However, other evidence in neurons has found that activation of the Nrf2 pathway occurs in a DJ-1-independent manner[348]. Nonetheless, future studies should examine the potential role of Nrf2 in the Parkin-FPN relationship, as oxidative stress plays such a significant role in both Parkinsonism and metal dyshomeostasis. While the studies presented in this thesis do not identify what this intermediary may be, ongoing efforts include microarray analysis that may reveal new targets of *pdr-1,* which could subsequently regulate *fpn-1.1* expression in *C. elegans*.

A recurring issue throughout the studies presented in this thesis is the lack of a direct effect of Mn on any of the outcomes tested. While Mn treatment shows a dose-

dependent effect on lethality and Mn accumulation in WT worms, most of the outcomes do not show significant differences between untreated and treated WT animals. This may be due to the treatment paradigm used, with the possibility that an acute, 30-minute treatment in L1 larval worms is not sufficient to cause significant changes. This may also be compounded by the fact that the extracts for most of the biochemical techniques presented were isolated directly after treatment. It would be interesting to determine whether a longer exposure time and/or longer time post-exposure for extract preparation would produce different phenotypic outcomes than what is presented.

Moreover, the thick cuticle barrier has also posed several technical problems, most notably, the necessity of administering high Mn concentrations (in the millimolar range) to produce any effects. While ICP-MS methodology has been extremely valuable in revealing variable intraworm metal accumulation, the lack of clear, quantitative methods to assess metal uptake itself has hindered full understanding of Mn homeostasis in *pdr-1* KO animals. The LA-ICP-MS method at least provided confirmation that the metal levels revealed by ICP-MS did have any contributions from unwashed metals stuck to the outside cuticle (**Fig 5E**). However, this method still remains qualitative in nature, with ongoing efforts to determine how to quantitatively analyze these results. We have also attempted to optimize the cellular Fura-2 manganese extraction assay (CFMEA) established by our colleagues[349] for *C.* elegans, but were unsuccessful. Future studies should consider radiolabeled substrate (or fluorescence) uptake assays to determine whether Mn transport dynamics are altered. Another interesting finding in Chapter III points to a much higher overall concentration of Mn in worms compared to Fe. Typically, the reverse is the case in other systems.

Though previously published findings from our laboratory using GFAAS show Fe to be at a higher level than Mn in WT worms, this may be due to differences in the methods used (ICP-MS/MS vs. GFAAS) and the resulting sensitivities. The GFAAS findings were also expressed as metal content per 1000 worms, which is both a significantly smaller sample size compared to the 50,000-worm samples we used for ICP-MS/MS, and lacks the accuracy of protein normalization. However, a potential explanation is the lack of a circulatory system in worms, as most of Fe in mammalian systems is primarily required for hemoglobin in red blood cells[350].

Additionally, assessment of mitochondrial dynamics and oxidative stress proved to be difficult in *C. elegans* during the course of this project. The use of the DCF dye in Chapter 2 to measure RONS production was optimized from previous techniques used in the laboratory[237] to "pre-treat" worms with the dye before $MnCl_2$ exposure, in order to better catch the immediate effects of Mn treatment. While we were able to obtain robust readings of RONS production through this method, the use of this dye was based on its frequent use in the literature. However, this assay is not thorough in its detection abilities, as it cannot measure $H_2O_2$, along with the caveat of potential dye leakage that we may not have been aware of[351]. Future investigations using this dye in *C. elegans* should consider fluorescence microscopy to visualize dye loading within worms. Additionally, the contribution of RONS specifically from the mitochondria vs. total cellular RONS is not distinguished using DCF. Future experiments in Mn-treated worms should consider the use of a tool like the MitoSOX dye, which is rapidly oxidized by superoxide in mitochondria, and not by other forms of RONS, and can be assessed by its fluorescence. Moreover, another technical issue we encountered in assessing

oxidative stress was through the optimization of the cellular GSH recycling assay. Unfortunately, we were unable to measure oxidized GSH (GSSG) from the worms, leaving the assay to only dictate total GSH levels. While this can still be considered a readout of antioxidant response, it would be beneficial to utilize a method like HPLC to measure both GSH and GSSG for a fuller understanding of increased oxidative stress.

We also attempted to assess mitochondrial bioenergetics using the Seahorse Biosciences Extracellular Flux Analyzer, which provides oxygen consumption rates following administration of various mitochondrial toxins. While the use of this machine to assess a variety of endpoints (e.g., basal respiration, ATP production, proton leakage) at once is attractive, the high costs associated with supplies and use of the equipment limited the amount of trials necessary to optimize this system for *C. elegans*. We attempted to vary the conditions of the Seahorse experimental paradigm from the original protocol for cells, but the injection times and concentrations of the mitochondrial toxins used (oligomycin, FCCP and rotenone), may not have been sufficient for the toxins to properly enter and accordingly affect the worms. Therefore, we could only rely on the basal respiration endpoint measured by the machine prior to the injection of mitochondrial toxins. Basal respiration was slightly decreased in *pdr-1* KO's compared to WT worms, with the *pdr-1* KO;*fpn-1.1* OVR animals showing even more of a decrease (trend level, p=0.0738, **Supplementary Figure 1**). However, these changes were slight and not significant. Though the trend for a lack of rescue by *pdr-1* KO;*fpn-1.1* OVR animals is unexpected, we are not confident in these results truly reflecting the basal state of the worms, as this assay has not been used extensively in worms by other groups. However, if this were to be true, perhaps the rescue seen in *pdr-1* KO;*fpn-*

*1.1* OVR animals is independent of changes in mitochondrial respiration. Future experiments must fully optimize the drug concentrations and injection times of the Seahorse mitochondrial stress test in order to correctly assess the other parameters of mitochondrial bioenergetics.

Furthermore, the roles of Parkin and PINK1 as mediators of mitochondrial dynamics have not yet been extensively examined in *C. elegans*. This may be partially due to technical challenges with this model system. While we considered mtDNA copy number as a correlate of mitochondrial mass, we understand that this is not the most direct or comprehensive strategy in examining mitochondrial integrity. In terms of Parkin's role in mitochondrial turnover, future experiments should consider adding a combination of techniques that assess both total mitochondrial mass, and the amount of that mass undergoing stress, thereby capturing the direct effects of *pdr-1* loss and Mn exposure on mitochondrial dynamics. For example, mutilabeling using the mitochondrial dye MitoTracker Green, which labels all mitochondria independent of the membrane potential, in combination with the dye MitoTracker Red CMXRos, which is dependent on the membrane potential, can provide a ratio of red to green representing changes in mitochondrial membrane potential that is normalized to any changes in mitochondrial abundance. This could be combined with the use of the TMRE (tetramethylrhodamine, ethyl ester) dye in worms, which only accumulates in active mitochondria, with damaged, depolarized mitochondria unable to take up the dye. Using a combination of these methods (via fluorescence microscopy and/or flow cytometry), in addition to the qPCR-based method of mtDNA detection, would paint a more accurate picture of direct changes in mitochondrial dynamics.

Lastly, an accurate model of PD should reflect the signature DAergic neurodegeneration associated with the disease. Consequently, previous members of the laboratory have published findings that Mn selectively induces DAergic neurodegeneration in WT *C. elegans*[260]. However, I, along with other past and current members of the laboratory have not been able to reproduce these findings since that point, despite using the same treatment paradigm and imaging techniques. Interestingly, other groups have also struggled to reproduce the drastic degeneration seen in the published confocal fluorescent images. We attempted to formulate a new scoring method that considers all aspects of degeneration (shrunken soma, blebbing, etc) that may not have been considered previously, but still did not notice a drastic effect of Mn on DAergic neurons in WT animals (**Figure 8**). However, this may be even more indicative of Mn's role as an environmental risk factor, with Mn accumulation, overall metal dyshomeostasis and oxidative stress preceding any overt degeneration. Though we cannot reproduce the GFP signal changes published by Benedetto and colleagues[260], it is important to note that loss of the GFP signal in worms containing the $p_{dat\text{-}1}$GFP trasngene is not necessarily a true reflection of degeneration. Fluorescence microscopy remains a qualitative assessment, as GFP signal may be lost, while cell death may not have truly occurred. According to personal communications with various members of the *C. elegans* community, there is a consensus that accurate analysis of neurodegeneration outside of fluorescent visualization is lacking in this system. For this reason, the behavioral approach was viewed as an output parameter of DAergic system integrity. Another way to tackle this obstacle is to biochemically measure differences in dopamine levels. Ongoing efforts include the establishment of a liquid chromatography

mass spectrometry (LC-MS) method with our collaborators in Germany to measure worm DA levels for a more quantitative assessment of damage to the DAergic system.

In conclusion, these studies collectively support the role of impaired metal homeostasis as a consequence of genetic mutations associated with early-onset PD, as well as the "multiple-hit" model signifying the distinctive roles of genetic risk factors in increasing vulnerability to toxin-mediated cell death. Furthermore, these findings provide a foundation for future studies on the interplay between WT αS neuroprotection, *pdr-1*-mediated mitochondrial dynamics and enhanced metal efflux as therapeutic strategies against Mn-induced Parkinsonism.

## SUPPLEMENTARY TABLES AND FIGURES

**Table 1.** Conditions for ICP-MS/MS (Agilent 8800 ICP-QQQ)

| | |
|---|---|
| Power | 1550 W |
| Plasma gas | 15 L/min |
| Carrier gas | 1.0 L/min |
| Auxiliary gas | 0.9 L/min |
| Scan mode | single quad |
| Q1 | ion guide |
| Collision cell gas flow | He: 4.5 mL/min (purity: > 99.999 %)<br>$H_2$: 0.5 mL/min (purity: > 99.999 %) |
| Q2 | $^{55}Mn$, $^{103}Rh$ (ISTD) |
| Integration Time | 1.0 s |
| Replicates | 5 |

**Table 2.** Conditions for ICP-MS (ICAP Qc, Thermo Fisher Scientific)

| | |
|---|---|
| Power | 1550 W |
| Nebulizer Flow | 780 mL/min |
| Cool Flow | 14.0 L/min |
| Auxilliary Flow | 500 mL/min |
| Measurement mode | KEDS |
| Cell gas flow | 4.6 mL/min |

**Table 3.** Conditions for LA (LSX213G2+, CETAC Technologies)

| | |
|---|---|
| Repetition frequency | 20 Hz |
| Spot diameter | 4 µm |
| Scan rate | 4 µm/s |
| He-flow 1 | 500 mL/min |
| He-flow 2 | 300 mL/min |
| Additional Ar-flow | 400 mL/min |

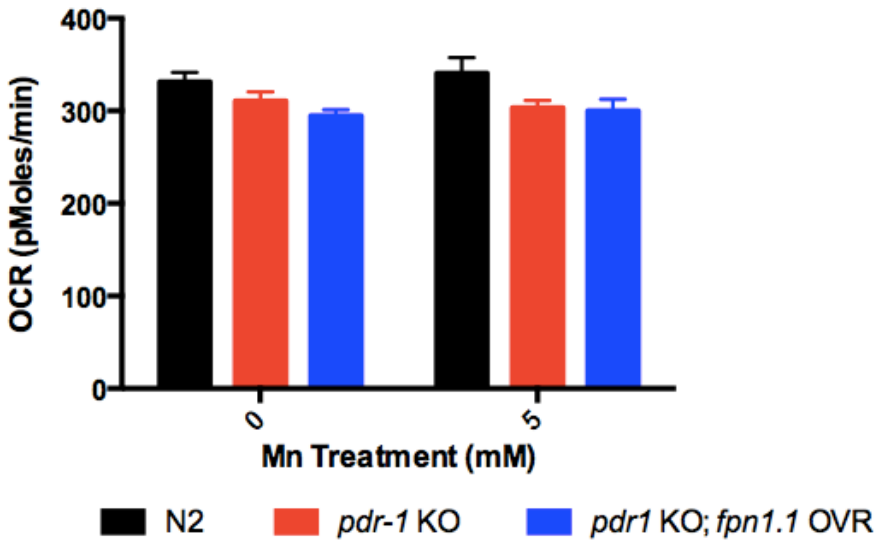


**Supplementary Figure 1.** Decreased basal respiration in *pdr-1* mutants that is not rescued by *fpn-1.1* overexpression. Statistical analysis by two-way ANOVA: interaction, ns; genotype, p=0.0738 (trend level); concentration, ns.

## REFERENCES


1. Lees, A.J., Hardy, J. & Revesz, T. Parkinson's disease. *Lancet* **373**, 2055-66 (2009).
2. Dawson, T.M., Ko, H.S. & Dawson, V.L. Genetic animal models of Parkinson's disease. *Neuron* **66**, 646-61 (2010).
3. Nagatsu, T., Levitt, M. & Udenfriend, S. Tyrosine Hydroxylase. The Initial Step in Norepinephrine Biosynthesis. *J Biol Chem* **239**, 2910-7 (1964).
4. Blaschko, H. The activity of l(-)-dopa decarboxylase. *J Physiol* **101**, 337-49 (1942).
5. Njus, D., Kelley, P.M. & Harnadek, G.J. Bioenergetics of secretory vesicles. *Biochim Biophys Acta* **853**, 237-65 (1986).
6. Rutledge, C.O. & Jonason, J. The rate of metabolism of dopamine, dihydroxyphenylacetic acid and methoxytyramine in rabbit brain in vitro. *Eur J Pharmacol* **4**, 264-9 (1968).
7. Yavich, L., Forsberg, M.M., Karayiorgou, M., Gogos, J.A. & Mannisto, P.T. Site-specific role of catechol-O-methyltransferase in dopamine overflow within prefrontal cortex and dorsal striatum. *J Neurosci* **27**, 10196-209 (2007).
8. Iversen, L.L. Role of transmitter uptake mechanisms in synaptic neurotransmission. *Br J Pharmacol* **41**, 571-91 (1971).
9. Hitri, A., Hurd, Y.L., Wyatt, R.J. & Deutsch, S.I. Molecular, functional and biochemical characteristics of the dopamine transporter: regional differences and clinical relevance. *Clin Neuropharmacol* **17**, 1-22 (1994).
10. Gudelsky, G.A. Tuberoinfundibular dopamine neurons and the regulation of prolactin secretion. *Psychoneuroendocrinology* **6**, 3-16 (1981).
11. Floresco, S.B. & Magyar, O. Mesocortical dopamine modulation of executive functions: beyond working memory. *Psychopharmacology (Berl)* **188**, 567-85 (2006).
12. Salamone, J.D. & Correa, M. The mysterious motivational functions of mesolimbic dopamine. *Neuron* **76**, 470-85 (2012).
13. Foley, J.M. & Baxter, D. On the nature of pigment granules in the cells of the locus coeruleus and substantia nigra. *J Neuropathol Exp Neurol* **17**, 586-98 (1958).
14. Bedard, P., Larochelle, L., Parent, A. & Poirier, L.J. The nigrostriatal pathway: a correlative study based on neuroanatomical and neurochemical criteria in the cat and the monkey. *Exp Neurol* **25**, 365-77 (1969).
15. Percheron, G., Fenelon, G., Leroux-Hugon, V. & Feve, A. [History of the basal ganglia system. Slow development of a major cerebral system]. *Rev Neurol (Paris)* **150**, 543-54 (1994).
16. Calabresi, P., Picconi, B., Tozzi, A., Ghiglieri, V. & Di Filippo, M. Direct and indirect pathways of basal ganglia: a critical reappraisal. *Nat Neurosci* **17**, 1022-30 (2014).
17. Albin, R.L., Young, A.B. & Penney, J.B. The functional anatomy of basal ganglia disorders. *Trends Neurosci* **12**, 366-75 (1989).

18. Missale, C., Nash, S.R., Robinson, S.W., Jaber, M. & Caron, M.G. Dopamine receptors: from structure to function. *Physiol Rev* **78**, 189-225 (1998).
19. Memo, M., Missale, C., Carruba, M.O. & Spano, P.F. Pharmacology and biochemistry of dopamine receptors in the central nervous system and peripheral tissue. *J Neural Transm Suppl* **22**, 19-32 (1986).
20. Memo, M., Missale, C., Carruba, M.O. & Spano, P.F. D2 dopamine receptors associated with inhibition of dopamine release from rat neostriatum are independent of cyclic AMP. *Neurosci Lett* **71**, 192-6 (1986).
21. Tang, L., Todd, R.D. & O'Malley, K.L. Dopamine D2 and D3 receptors inhibit dopamine release. *J Pharmacol Exp Ther* **270**, 475-9 (1994).
22. Gerfen, C.R. et al. D1 and D2 dopamine receptor-regulated gene expression of striatonigral and striatopallidal neurons. *Science* **250**, 1429-32 (1990).
23. Malkus, K.A., Tsika, E. & Ischiropoulos, H. Oxidative modifications, mitochondrial dysfunction, and impaired protein degradation in Parkinson's disease: how neurons are lost in the Bermuda triangle. *Mol Neurodegener* **4**, 24 (2009).
24. Trojanowski, J.Q. & Lee, V.M. Aggregation of neurofilament and alpha-synuclein proteins in Lewy bodies: implications for the pathogenesis of Parkinson disease and Lewy body dementia. *Arch Neurol* **55**, 151-2 (1998).
25. Diao, J. et al. Native alpha-synuclein induces clustering of synaptic-vesicle mimics via binding to phospholipids and synaptobrevin-2/VAMP2. *Elife* **2**, e00592 (2013).
26. Gaugler, M.N. et al. Nigrostriatal overabundance of alpha-synuclein leads to decreased vesicle density and deficits in dopamine release that correlate with reduced motor activity. *Acta Neuropathol* **123**, 653-69 (2012).
27. Murphy, D.D., Rueter, S.M., Trojanowski, J.Q. & Lee, V.M. Synucleins are developmentally expressed, and alpha-synuclein regulates the size of the presynaptic vesicular pool in primary hippocampal neurons. *J Neurosci* **20**, 3214-20 (2000).
28. Tehranian, R., Montoya, S.E., Van Laar, A.D., Hastings, T.G. & Perez, R.G. Alpha-synuclein inhibits aromatic amino acid decarboxylase activity in dopaminergic cells. *J Neurochem* **99**, 1188-96 (2006).
29. Perez, R.G. et al. A role for alpha-synuclein in the regulation of dopamine biosynthesis. *J Neurosci* **22**, 3090-9 (2002).
30. Lee, F.J., Liu, F., Pristupa, Z.B. & Niznik, H.B. Direct binding and functional coupling of alpha-synuclein to the dopamine transporters accelerate dopamine-induced apoptosis. *FASEB J* **15**, 916-26 (2001).
31. Wersinger, C. & Sidhu, A. Attenuation of dopamine transporter activity by alpha-synuclein. *Neurosci Lett* **340**, 189-92 (2003).
32. Unal Gulsuner, H. et al. Mitochondrial serine protease HTRA2 p.G399S in a kindred with essential tremor and Parkinson disease. *Proc Natl Acad Sci U S A* (2014).
33. Schapira, A.H. et al. Mitochondrial complex I deficiency in Parkinson's disease. *Lancet* **1**, 1269 (1989).
34. Elstner, M. et al. Expression analysis of dopaminergic neurons in Parkinson's disease and aging links transcriptional dysregulation of energy metabolism to cell death. *Acta Neuropathol* **122**, 75-86 (2011).

35. Vives-Bauza, C. et al. PINK1-dependent recruitment of Parkin to mitochondria in mitophagy. *Proc Natl Acad Sci U S A* **107**, 378-83 (2010).
36. Chen, Y. & Dorn, G.W., 2nd. PINK1-phosphorylated mitofusin 2 is a Parkin receptor for culling damaged mitochondria. *Science* **340**, 471-5 (2013).
37. Deng, H., Dodson, M.W., Huang, H. & Guo, M. The Parkinson's disease genes pink1 and parkin promote mitochondrial fission and/or inhibit fusion in Drosophila. *Proc Natl Acad Sci U S A* **105**, 14503-8 (2008).
38. Graham, D.G., Tiffany, S.M., Bell, W.R., Jr. & Gutknecht, W.F. Autoxidation versus covalent binding of quinones as the mechanism of toxicity of dopamine, 6-hydroxydopamine, and related compounds toward C1300 neuroblastoma cells in vitro. *Mol Pharmacol* **14**, 644-53 (1978).
39. Bisaglia, M. et al. Dopamine quinones interact with alpha-synuclein to form unstructured adducts. *Biochem Biophys Res Commun* **394**, 424-8 (2010).
40. Kuhn, D.M., Arthur, R.E., Jr., Thomas, D.M. & Elferink, L.A. Tyrosine hydroxylase is inactivated by catechol-quinones and converted to a redox-cycling quinoprotein: possible relevance to Parkinson's disease. *J Neurochem* **73**, 1309-17 (1999).
41. Jana, S. et al. Mitochondrial dysfunction mediated by quinone oxidation products of dopamine: Implications in dopamine cytotoxicity and pathogenesis of Parkinson's disease. *Biochim Biophys Acta* **1812**, 663-73 (2011).
42. Takahashi, N., Schreiber, J., Fischer, V. & Mason, R.P. Formation of glutathione-conjugated semiquinones by the reaction of quinones with glutathione: an ESR study. *Arch Biochem Biophys* **252**, 41-8 (1987).
43. Sies, H. Glutathione and its role in cellular functions. *Free Radic Biol Med* **27**, 916-21 (1999).
44. Sofic, E., Lange, K.W., Jellinger, K. & Riederer, P. Reduced and oxidized glutathione in the substantia nigra of patients with Parkinson's disease. *Neurosci Lett* **142**, 128-30 (1992).
45. Glickman, M.H. & Ciechanover, A. The ubiquitin-proteasome proteolytic pathway: destruction for the sake of construction. *Physiol Rev* **82**, 373-428 (2002).
46. Baumeister, W., Walz, J., Zuhl, F. & Seemuller, E. The proteasome: paradigm of a self-compartmentalizing protease. *Cell* **92**, 367-80 (1998).
47. McNaught, K.S., Belizaire, R., Isacson, O., Jenner, P. & Olanow, C.W. Altered proteasomal function in sporadic Parkinson's disease. *Exp Neurol* **179**, 38-46 (2003).
48. Zabel, C. et al. Proteasome and oxidative phoshorylation changes may explain why aging is a risk factor for neurodegenerative disorders. *J Proteomics* **73**, 2230-8 (2010).
49. Zhang, Y. et al. Parkin functions as an E2-dependent ubiquitin- protein ligase and promotes the degradation of the synaptic vesicle-associated protein, CDCrel-1. *Proc Natl Acad Sci U S A* **97**, 13354-9 (2000).
50. Shimura, H. et al. Ubiquitination of a new form of alpha-synuclein by parkin from human brain: implications for Parkinson's disease. *Science* **293**, 263-9 (2001).
51. Chung, K.K. et al. Parkin ubiquitinates the alpha-synuclein-interacting protein, synphilin-1: implications for Lewy-body formation in Parkinson disease. *Nat Med* **7**, 1144-50 (2001).

52. Langston, J.W., Ballard, P., Tetrud, J.W. & Irwin, I. Chronic Parkinsonism in humans due to a product of meperidine-analog synthesis. *Science* **219**, 979-80 (1983).
53. Langston, J.W., Forno, L.S., Rebert, C.S. & Irwin, I. Selective nigral toxicity after systemic administration of 1-methyl-4-phenyl-1,2,5,6-tetrahydropyrine (MPTP) in the squirrel monkey. *Brain Res* **292**, 390-4 (1984).
54. Ungerstedt, U., Ljungberg, T. & Steg, G. Behavioral, physiological, and neurochemical changes after 6-hydroxydopamine-induced degeneration of the nigro-striatal dopamine neurons. *Adv Neurol* **5**, 421-6 (1974).
55. Michel, P.P. & Hefti, F. Toxicity of 6-hydroxydopamine and dopamine for dopaminergic neurons in culture. *J Neurosci Res* **26**, 428-35 (1990).
56. Ljungdahl, A., Hokfelt, T., Jonsson, G. & Sachs, C. Autoradiographic demonstration of uptake and accumulation of 3H-6-hydroxydopamine in adrenergic nerves. *Experientia* **27**, 297-9 (1971).
57. Sachs, C. & Jonsson, G. Mechanisms of action of 6-hydroxydopamine. *Biochem Pharmacol* **24**, 1-8 (1975).
58. Blum, D. et al. Molecular pathways involved in the neurotoxicity of 6-OHDA, dopamine and MPTP: contribution to the apoptotic theory in Parkinson's disease. *Prog Neurobiol* **65**, 135-72 (2001).
59. Glinka, Y.Y. & Youdim, M.B. Inhibition of mitochondrial complexes I and IV by 6-hydroxydopamine. *Eur J Pharmacol* **292**, 329-32 (1995).
60. Tobon-Velasco, J.C. et al. 6-OHDA-induced apoptosis and mitochondrial dysfunction are mediated by early modulation of intracellular signals and interaction of Nrf2 and NF-kappaB factors. *Toxicology* **304**, 109-19 (2013).
61. Richardson, J.R., Quan, Y., Sherer, T.B., Greenamyre, J.T. & Miller, G.W. Paraquat neurotoxicity is distinct from that of MPTP and rotenone. *Toxicol Sci* **88**, 193-201 (2005).
62. Greenamyre, J.T., Higgins, D.S. & Eller, R.V. Quantitative autoradiography of dihydrorotenone binding to complex I of the electron transport chain. *J Neurochem* **59**, 746-9 (1992).
63. Betarbet, R. et al. Chronic systemic pesticide exposure reproduces features of Parkinson's disease. *Nat Neurosci* **3**, 1301-6 (2000).
64. Ferrante, R.J., Schulz, J.B., Kowall, N.W. & Beal, M.F. Systemic administration of rotenone produces selective damage in the striatum and globus pallidus, but not in the substantia nigra. *Brain Res* **753**, 157-62 (1997).
65. Ren, Y. & Feng, J. Rotenone selectively kills serotonergic neurons through a microtubule-dependent mechanism. *J Neurochem* **103**, 303-11 (2007).
66. Brooks, A.I., Chadwick, C.A., Gelbard, H.A., Cory-Slechta, D.A. & Federoff, H.J. Paraquat elicited neurobehavioral syndrome caused by dopaminergic neuron loss. *Brain Res* **823**, 1-10 (1999).
67. Fujita, M. & Shinozaki, K. Identification of polyamine transporters in plants: paraquat transport provides crucial clues. *Plant Cell Physiol* **55**, 855-61 (2014).
68. Shimizu, K. et al. Carrier-mediated processes in blood--brain barrier penetration and neural uptake of paraquat. *Brain Res* **906**, 135-42 (2001).
69. Bus, J.S. & Gibson, J.E. Paraquat: model for oxidant-initiated toxicity. *Environ Health Perspect* **55**, 37-46 (1984).

70. Fei, Q., McCormack, A.L., Di Monte, D.A. & Ethell, D.W. Paraquat neurotoxicity is mediated by a Bak-dependent mechanism. *J Biol Chem* **283**, 3357-64 (2008).
71. Manning-Bog, A.B. et al. The herbicide paraquat causes up-regulation and aggregation of alpha-synuclein in mice: paraquat and alpha-synuclein. *J Biol Chem* **277**, 1641-4 (2002).
72. Dutta, G., Zhang, P. & Liu, B. The lipopolysaccharide Parkinson's disease animal model: mechanistic studies and drug discovery. *Fundam Clin Pharmacol* **22**, 453-64 (2008).
73. Hoban, D.B. et al. Further characterisation of the LPS model of Parkinson's disease: a comparison of intra-nigral and intra-striatal lipopolysaccharide administration on motor function, microgliosis and nigrostriatal neurodegeneration in the rat. *Brain Behav Immun* **27**, 91-100 (2013).
74. Kitada, T. et al. Mutations in the parkin gene cause autosomal recessive juvenile parkinsonism. *Nature* **392**, 605-8 (1998).
75. Horowitz, J.M., Myers, J., Stachowiak, M.K. & Torres, G. Identification and distribution of Parkin in rat brain. *Neuroreport* **10**, 3393-7 (1999).
76. Imai, Y. et al. An unfolded putative transmembrane polypeptide, which can lead to endoplasmic reticulum stress, is a substrate of Parkin. *Cell* **105**, 891-902 (2001).
77. Xiong, H. et al. Parkin, PINK1, and DJ-1 form a ubiquitin E3 ligase complex promoting unfolded protein degradation. *J Clin Invest* **119**, 650-60 (2009).
78. Sriram, S.R. et al. Familial-associated mutations differentially disrupt the solubility, localization, binding and ubiquitination properties of parkin. *Hum Mol Genet* **14**, 2571-86 (2005).
79. Goldberg, M.S. et al. Parkin-deficient mice exhibit nigrostriatal deficits but not loss of dopaminergic neurons. *J Biol Chem* **278**, 43628-35 (2003).
80. Jiang, H., Jiang, Q. & Feng, J. Parkin increases dopamine uptake by enhancing the cell surface expression of dopamine transporter. *J Biol Chem* **279**, 54380-6 (2004).
81. Kitada, T. et al. Impaired dopamine release and synaptic plasticity in the striatum of parkin-/- mice. *J Neurochem* **110**, 613-21 (2009).
82. Helton, T.D., Otsuka, T., Lee, M.C., Mu, Y. & Ehlers, M.D. Pruning and loss of excitatory synapses by the parkin ubiquitin ligase. *Proc Natl Acad Sci U S A* **105**, 19492-7 (2008).
83. Lu, X.H. et al. Bacterial artificial chromosome transgenic mice expressing a truncated mutant parkin exhibit age-dependent hypokinetic motor deficits, dopaminergic neuron degeneration, and accumulation of proteinase K-resistant alpha-synuclein. *J Neurosci* **29**, 1962-76 (2009).
84. Valente, E.M. et al. Hereditary early-onset Parkinson's disease caused by mutations in PINK1. *Science* **304**, 1158-60 (2004).
85. Taymans, J.M., Van den Haute, C. & Baekelandt, V. Distribution of PINK1 and LRRK2 in rat and mouse brain. *J Neurochem* **98**, 951-61 (2006).
86. Sim, C.H. et al. C-terminal truncation and Parkinson's disease-associated mutations down-regulate the protein serine/threonine kinase activity of PTEN-induced kinase-1. *Hum Mol Genet* **15**, 3251-62 (2006).

87. Yang, Y. et al. Pink1 regulates mitochondrial dynamics through interaction with the fission/fusion machinery. *Proc Natl Acad Sci U S A* **105**, 7070-5 (2008).
88. Plun-Favreau, H. et al. The mitochondrial protease HtrA2 is regulated by Parkinson's disease-associated kinase PINK1. *Nat Cell Biol* **9**, 1243-52 (2007).
89. Villeneuve, L.M., Purnell, P.R., Boska, M.D. & Fox, H.S. Early Expression of Parkinson's Disease-Related Mitochondrial Abnormalities in PINK1 Knockout Rats. *Mol Neurobiol* (2014).
90. Petit, A. et al. Wild-type PINK1 prevents basal and induced neuronal apoptosis, a protective effect abrogated by Parkinson disease-related mutations. *J Biol Chem* **280**, 34025-32 (2005).
91. Kitada, T. et al. Impaired dopamine release and synaptic plasticity in the striatum of PINK1-deficient mice. *Proc Natl Acad Sci U S A* **104**, 11441-6 (2007).
92. Gispert, S. et al. Parkinson phenotype in aged PINK1-deficient mice is accompanied by progressive mitochondrial dysfunction in absence of neurodegeneration. *PLoS One* **4**, e5777 (2009).
93. Matsui, H. et al. PINK1 and Parkin complementarily protect dopaminergic neurons in vertebrates. *Hum Mol Genet* **22**, 2423-34 (2013).
94. Haque, M.E. et al. Inactivation of Pink1 gene in vivo sensitizes dopamine-producing neurons to 1-methyl-4-phenyl-1,2,3,6-tetrahydropyridine (MPTP) and can be rescued by autosomal recessive Parkinson disease genes, Parkin or DJ-1. *J Biol Chem* **287**, 23162-70 (2012).
95. Kim, Y. et al. PINK1 controls mitochondrial localization of Parkin through direct phosphorylation. *Biochem Biophys Res Commun* **377**, 975-80 (2008).
96. Okatsu, K. et al. PINK1 autophosphorylation upon membrane potential dissipation is essential for Parkin recruitment to damaged mitochondria. *Nat Commun* **3**, 1016 (2012).
97. Sun, Y., Vashisht, A.A., Tchieu, J., Wohlschlegel, J.A. & Dreier, L. Voltage-dependent anion channels (VDACs) recruit Parkin to defective mitochondria to promote mitochondrial autophagy. *J Biol Chem* **287**, 40652-60 (2012).
98. Bonifati, V. et al. Mutations in the DJ-1 gene associated with autosomal recessive early-onset parkinsonism. *Science* **299**, 256-9 (2003).
99. Canet-Aviles, R.M. et al. The Parkinson's disease protein DJ-1 is neuroprotective due to cysteine-sulfinic acid-driven mitochondrial localization. *Proc Natl Acad Sci U S A* **101**, 9103-8 (2004).
100. Andres-Mateos, E. et al. DJ-1 gene deletion reveals that DJ-1 is an atypical peroxiredoxin-like peroxidase. *Proc Natl Acad Sci U S A* **104**, 14807-12 (2007).
101. Lee, J.Y. et al. Human DJ-1 and its homologs are novel glyoxalases. *Hum Mol Genet* **21**, 3215-25 (2012).
102. Wang, X. et al. Parkinson's disease-associated DJ-1 mutations impair mitochondrial dynamics and cause mitochondrial dysfunction. *J Neurochem* **121**, 830-9 (2012).
103. Inden, M. et al. PARK7 DJ-1 protects against degeneration of nigral dopaminergic neurons in Parkinson's disease rat model. *Neurobiol Dis* **24**, 144-58 (2006).

104. Goldberg, M.S. et al. Nigrostriatal dopaminergic deficits and hypokinesia caused by inactivation of the familial Parkinsonism-linked gene DJ-1. *Neuron* **45**, 489-96 (2005).
105. Chen, L. et al. Age-dependent motor deficits and dopaminergic dysfunction in DJ-1 null mice. *J Biol Chem* **280**, 21418-26 (2005).
106. Clements, C.M., McNally, R.S., Conti, B.J., Mak, T.W. & Ting, J.P. DJ-1, a cancer- and Parkinson's disease-associated protein, stabilizes the antioxidant transcriptional master regulator Nrf2. *Proc Natl Acad Sci U S A* **103**, 15091-6 (2006).
107. Hao, L.Y., Giasson, B.I. & Bonini, N.M. DJ-1 is critical for mitochondrial function and rescues PINK1 loss of function. *Proc Natl Acad Sci U S A* **107**, 9747-52 (2010).
108. Polymeropoulos, M.H. et al. Mutation in the alpha-synuclein gene identified in families with Parkinson's disease. *Science* **276**, 2045-7 (1997).
109. Choong, C.J. & Say, Y.H. Neuroprotection of alpha-synuclein under acute and chronic rotenone and maneb treatment is abolished by its familial Parkinson's disease mutations A30P, A53T and E46K. *Neurotoxicology* **32**, 857-63 (2011).
110. Musgrove, R.E., King, A.E. & Dickson, T.C. Neuroprotective upregulation of endogenous alpha-synuclein precedes ubiquitination in cultured dopaminergic neurons. *Neurotox Res* **19**, 592-602 (2011).
111. Lemkau, L.R. et al. Site-specific perturbations of alpha-synuclein fibril structure by the Parkinson's disease associated mutations A53T and E46K. *PLoS One* **8**, e49750 (2013).
112. Conway, K.A. et al. Acceleration of oligomerization, not fibrillization, is a shared property of both alpha-synuclein mutations linked to early-onset Parkinson's disease: implications for pathogenesis and therapy. *Proc Natl Acad Sci U S A* **97**, 571-6 (2000).
113. Giasson, B.I. et al. Neuronal alpha-synucleinopathy with severe movement disorder in mice expressing A53T human alpha-synuclein. *Neuron* **34**, 521-33 (2002).
114. Martin, L.J. et al. Parkinson's disease alpha-synuclein transgenic mice develop neuronal mitochondrial degeneration and cell death. *J Neurosci* **26**, 41-50 (2006).
115. Subramaniam, S.R., Vergnes, L., Franich, N.R., Reue, K. & Chesselet, M.F. Region specific mitochondrial impairment in mice with widespread overexpression of alpha-synuclein. *Neurobiol Dis* **70**, 204-13 (2014).
116. Fernagut, P.O. & Chesselet, M.F. Alpha-synuclein and transgenic mouse models. *Neurobiol Dis* **17**, 123-30 (2004).
117. Batelli, S. et al. The Parkinson's Disease-Related Protein DJ-1 Protects Dopaminergic Neurons in vivo and Cultured Cells from Alpha-Synuclein and 6-Hydroxydopamine Toxicity. *Neurodegener Dis* (2014).
118. Zondler, L. et al. DJ-1 interactions with alpha-synuclein attenuate aggregation and cellular toxicity in models of Parkinson's disease. *Cell Death Dis* **5**, e1350 (2014).
119. Gispert, S. et al. Potentiation of neurotoxicity in double-mutant mice with Pink1 ablation and A53T-SNCA overexpression. *Hum Mol Genet* (2014).

120. Todd, A.M. & Staveley, B.E. Pink1 suppresses alpha-synuclein-induced phenotypes in a Drosophila model of Parkinson's disease. *Genome* **51**, 1040-6 (2008).
121. ATSDR. Toxicological profile for manganese (Draft for Public Comment). *U.S. Department of Health and Human Services, Public Service* (2008).
122. Davis, C.D., Zech, L. & Greger, J.L. Manganese metabolism in rats: an improved methodology for assessing gut endogenous losses. *Proceedings of the Society for Experimental Biology and Medicine. Society for Experimental Biology and Medicine* **202**, 103-8 (1993).
123. Finley, J.W., Johnson, P.E. & Johnson, L.K. Sex affects manganese absorption and retention by humans from a diet adequate in manganese. *The American journal of clinical nutrition* **60**, 949-55 (1994).
124. Aschner, J.L. & Aschner, M. Nutritional aspects of manganese homeostasis. *Molecular aspects of medicine* **26**, 353-62 (2005).
125. Davidsson, L., Cederblad, A., Hagebo, E., Lonnerdal, B. & Sandstrom, B. Intrinsic and extrinsic labeling for studies of manganese absorption in humans. *The Journal of nutrition* **118**, 1517-21 (1988).
126. Malecki, E.A., Radzanowski, G.M., Radzanowski, T.J., Gallaher, D.D. & Greger, J.L. Biliary manganese excretion in conscious rats is affected by acute and chronic manganese intake but not by dietary fat. *The Journal of nutrition* **126**, 489-98 (1996).
127. Schroeder, H.A., Balassa, J.J. & Tipton, I.H. Essential trace metals in man: manganese, a study in homeostasis. *J. Chron. Dis.* **19**, 545-571 (1996).
128. Davidson, L.A. & Lonnerdal, B. Fe-saturation and proteolysis of human lactoferrin: effect on brush-border receptor-mediated uptake of Fe and Mn. *Am J Physiol* **257**, G930-4 (1989).
129. Leblondel, G. & Allain, P. Manganese transport by Caco-2 cells. *Biol Trace Elem Res* **67**, 13-28 (1999).
130. Garcia-Aranda, J.A., Wapnir, R.A. & Lifshitz, F. In vivo intestinal absorption of manganese in the rat. *J Nutr* **113**, 2601-7 (1983).
131. Bell, J.G., Keen, C.L. & Lonnerdal, B. Higher retention of manganese in suckling than in adult rats is not due to maturational differences in manganese uptake by rat small intestine. *Journal of toxicology and environmental health* **26**, 387-98 (1989).
132. Garrick, M.D. et al. DMT1: a mammalian transporter for multiple metals. *Biometals* **16**, 41-54 (2003).
133. Davidsson, L., Cederblad, A., Lonnerdal, B. & Sandstrom, B. The effect of individual dietary components on manganese absorption in humans. *The American journal of clinical nutrition* **54**, 1065-70 (1991).
134. Britton, A.A. & Cotzias, G.C. Dependence of manganese turnover on intake. *The American journal of physiology* **211**, 203-6 (1966).
135. Dorman, D.C. et al. Influence of dietary manganese on the pharmacokinetics of inhaled manganese sulfate in male CD rats. *Toxicological sciences : an official journal of the Society of Toxicology* **60**, 242-51 (2001).

136. Keen, C.L., Bell, J.G. & Lonnerdal, B. The effect of age on manganese uptake and retention from milk and infant formulas in rats. *The Journal of nutrition* **116**, 395-402 (1986).
137. Zlotkin, S.H., Atkinson, S. & Lockitch, G. Trace elements in nutrition for premature infants. *Clinics in perinatology* **22**, 223-40 (1995).
138. Aschner, J.L. & Aschner, M. Nutritional aspects of manganese homeostasis. *Mol Aspects Med* **26**, 353-62 (2005).
139. Morris, C.M., Keith, A.B., Edwardson, J.A. & Pullen, R.G. Uptake and distribution of iron and transferrin in the adult rat brain. *J Neurochem* **59**, 300-6 (1992).
140. Dobson, A.W., Erikson, K.M. & Aschner, M. Manganese neurotoxicity. *Ann N Y Acad Sci* **1012**, 115-28 (2004).
141. Touret, N., Furuya, W., Forbes, J., Gros, P. & Grinstein, S. Dynamic traffic through the recycling compartment couples the metal transporter Nramp2 (DMT1) with the transferrin receptor. *J Biol Chem* **278**, 25548-57 (2003).
142. Stredrick, D.L. et al. Manganese-induced cytotoxicity in dopamine-producing cells. *Neurotoxicology* **25**, 543-53 (2004).
143. Fleming, M.D. et al. Nramp2 is mutated in the anemic Belgrade (b) rat: evidence of a role for Nramp2 in endosomal iron transport. *Proc Natl Acad Sci U S A* **95**, 1148-53 (1998).
144. Fleming, M.D. et al. Microcytic anaemia mice have a mutation in Nramp2, a candidate iron transporter gene. *Nat Genet* **16**, 383-6 (1997).
145. Garrick, M.D. et al. DMT1: which metals does it transport? *Biol Res* **39**, 79-85 (2006).
146. Wang, X.S., Ong, W.Y. & Connor, J.R. A light and electron microscopic study of the iron transporter protein DMT-1 in the monkey cerebral neocortex and hippocampus. *J Neurocytol* **30**, 353-60 (2001).
147. Huang, E., Ong, W.Y. & Connor, J.R. Distribution of divalent metal transporter-1 in the monkey basal ganglia. *Neuroscience* **128**, 487-96 (2004).
148. Garcia, S.J., Gellein, K., Syversen, T. & Aschner, M. A manganese-enhanced diet alters brain metals and transporters in the developing rat. *Toxicol Sci* **92**, 516-25 (2006).
149. Erikson, K.M. & Aschner, M. Increased manganese uptake by primary astrocyte cultures with altered iron status is mediated primarily by divalent metal transporter. *Neurotoxicology* **27**, 125-30 (2006).
150. Girijashanker, K. et al. Slc39a14 gene encodes ZIP14, a metal/bicarbonate symporter: similarities to the ZIP8 transporter. *Mol Pharmacol* **73**, 1413-23 (2008).
151. He, L. et al. ZIP8, member of the solute-carrier-39 (SLC39) metal-transporter family: characterization of transporter properties. *Mol Pharmacol* **70**, 171-80 (2006).
152. Lockman, P.R., Roder, K.E. & Allen, D.D. Inhibition of the rat blood-brain barrier choline transporter by manganese chloride. *J Neurochem* **79**, 588-94 (2001).
153. Lucaciu, C.M., Dragu, C., Copaescu, L. & Morariu, V.V. Manganese transport through human erythrocyte membranes. An EPR study. *Biochim Biophys Acta* **1328**, 90-8 (1997).
154. Finley, J.W. Manganese uptake and release by cultured human hepato-carcinoma (Hep-G2) cells. *Biol Trace Elem Res* **64**, 101-18 (1998).

155. Mason, R.P. Membrane interaction of calcium channel antagonists modulated by cholesterol. Implications for drug activity. *Biochem Pharmacol* **45**, 2173-83 (1993).
156. Crossgrove, J.S., Allen, D.D., Bukaveckas, B.L., Rhineheimer, S.S. & Yokel, R.A. Manganese distribution across the blood-brain barrier. I. Evidence for carrier-mediated influx of managanese citrate as well as manganese and manganese transferrin. *Neurotoxicology* **24**, 3-13 (2003).
157. Aschner, M., Guilarte, T.R., Schneider, J.S. & Zheng, W. Manganese: recent advances in understanding its transport and neurotoxicity. *Toxicol Appl Pharmacol* **221**, 131-47 (2007).
158. Gavin, C.E., Gunter, K.K. & Gunter, T.E. Mn2+ sequestration by mitochondria and inhibition of oxidative phosphorylation. *Toxicol Appl Pharmacol* **115**, 1-5 (1992).
159. Gavin, C.E., Gunter, K.K. & Gunter, T.E. Manganese and calcium transport in mitochondria: implications for manganese toxicity. *Neurotoxicology* **20**, 445-53 (1999).
160. Wootton, L.L., Argent, C.C., Wheatley, M. & Michelangeli, F. The expression, activity and localisation of the secretory pathway Ca2+ -ATPase (SPCA1) in different mammalian tissues. *Biochim Biophys Acta* **1664**, 189-97 (2004).
161. Missiaen, L. et al. SPCA1 pumps and Hailey-Hailey disease. *Biochem Biophys Res Commun* **322**, 1204-13 (2004).
162. Sepulveda, M.R., Wuytack, F. & Mata, A.M. High levels of Mn(2)(+) inhibit secretory pathway Ca(2)(+)/Mn(2)(+)-ATPase (SPCA) activity and cause Golgi fragmentation in neurons and glia. *J Neurochem* **123**, 824-36 (2012).
163. Wedler, F.C., Denman, R.B. & Roby, W.G. Glutamine synthetase from ovine brain is a manganese(II) enzyme. *Biochemistry* **21**, 6389-96 (1982).
164. Jitrapakdee, S. et al. Structure, mechanism and regulation of pyruvate carboxylase. *Biochem J* **413**, 369-87 (2008).
165. Scrutton, M.C., Griminger, P. & Wallace, J.C. Pyruvate carboxylase. Bound metal content of the vertebrate liver enzyme as a function of diet and species. *J Biol Chem* **247**, 3305-13 (1972).
166. Kanyo, Z.F., Scolnick, L.R., Ash, D.E. & Christianson, D.W. Structure of a unique binuclear manganese cluster in arginase. *Nature* **383**, 554-7 (1996).
167. Das, A.K., Helps, N.R., Cohen, P.T. & Barford, D. Crystal structure of the protein serine/threonine phosphatase 2C at 2.0 A resolution. *EMBO J* **15**, 6798-809 (1996).
168. Garrick, M.D. et al. Isoform specific regulation of divalent metal (ion) transporter (DMT1) by proteasomal degradation. *Biometals* **25**, 787-93 (2012).
169. Gunshin, H. et al. Cloning and characterization of a mammalian proton-coupled metal-ion transporter. *Nature* **388**, 482-8 (1997).
170. Roth, J.A., Singleton, S., Feng, J., Garrick, M. & Paradkar, P.N. Parkin regulates metal transport via proteasomal degradation of the 1B isoforms of divalent metal transporter 1. *J Neurochem* **113**, 454-64 (2010).
171. Praschberger, R. et al. Impact of D181V and A69T on the function of ferroportin as an iron export pump and hepcidin receptor. *Biochim Biophys Acta* **1842**, 1406-12 (2014).

172. Rochette, L. et al. The iron-regulatory hormone hepcidin: A possible therapeutic target? *Pharmacol Ther* (2014).
173. Yin, Z. et al. Ferroportin is a manganese-responsive protein that decreases manganese cytotoxicity and accumulation. *J Neurochem* **112**, 1190-8 (2010).
174. Madejczyk, M.S. & Ballatori, N. The iron transporter ferroportin can also function as a manganese exporter. *Biochim Biophys Acta* **1818**, 651-7 (2012).
175. Mitchell, C.J., Shawki, A., Ganz, T., Nemeth, E. & Mackenzie, B. Functional properties of human ferroportin, a cellular iron exporter reactive also with cobalt and zinc. *Am J Physiol Cell Physiol* **306**, C450-9 (2014).
176. Tuschl, K. et al. Syndrome of hepatic cirrhosis, dystonia, polycythemia, and hypermanganesemia caused by mutations in SLC30A10, a manganese transporter in man. *Am J Hum Genet* **90**, 457-66 (2012).
177. Leyva-Illades, D. et al. SLC30A10 is a cell surface-localized manganese efflux transporter, and parkinsonism-causing mutations block its intracellular trafficking and efflux activity. *J Neurosci* **34**, 14079-95 (2014).
178. Stamelou, M. et al. Dystonia with brain manganese accumulation resulting from SLC30A10 mutations: a new treatable disorder. *Mov Disord* **27**, 1317-22 (2012).
179. Di Toro Mammarella, L. et al. Two-year follow-up after chelating therapy in a patient with adult-onset parkinsonism and hypermanganesaemia due to SLC30A10 mutations. *J Neurol* **261**, 227-8 (2014).
180. Roth, J.A. Homeostatic and toxic mechanisms regulating manganese uptake, retention, and elimination. *Biol Res* **39**, 45-57 (2006).
181. Racette, B.A. et al. Increased risk of parkinsonism associated with welding exposure. *Neurotoxicology* **33**, 1356-61 (2012).
182. Criswell, S.R. et al. Basal ganglia intensity indices and diffusion weighted imaging in manganese-exposed welders. *Occup Environ Med* **69**, 437-43 (2012).
183. Zeron, H.M., Rodriguez, M.R., Montes, S. & Castaneda, C.R. Blood manganese levels in patients with hepatic encephalopathy. *J Trace Elem Med Biol* **25**, 225-9 (2011).
184. Fitzgerald, K. et al. Hypermanganesemia in patients receiving total parenteral nutrition. *JPEN J Parenter Enteral Nutr* **23**, 333-6 (1999).
185. Smith, E.A., Newland, P., Bestwick, K.G. & Ahmed, N. Increased whole blood manganese concentrations observed in children with iron deficiency anaemia. *J Trace Elem Med Biol* (2012).
186. Fitsanakis, V.A. et al. Changes in dietary iron exacerbate regional brain manganese accumulation as determined by magnetic resonance imaging. *Toxicol Sci* **120**, 146-53 (2011).
187. Lucchini, R.G., Martin, C.J. & Doney, B.C. From manganism to manganese-induced parkinsonism: a conceptual model based on the evolution of exposure. *Neuromolecular Med* **11**, 311-21 (2009).
188. Calne, D.B., Chu, N.S., Huang, C.C., Lu, C.S. & Olanow, W. Manganism and idiopathic parkinsonism: similarities and differences. *Neurology* **44**, 1583-6 (1994).
189. Bowler, R.M. et al. Prospective study on neurotoxic effects in manganese-exposed bridge construction welders. *Neurotoxicology* **32**, 596-605 (2011).

190. Erikson, K.M., Syversen, T., Steinnes, E. & Aschner, M. Globus pallidus: a target brain region for divalent metal accumulation associated with dietary iron deficiency. *The Journal of nutritional biochemistry* **15**, 335-341 (2004).
191. Anderson, J.G., Cooney, P.T. & Erikson, K.M. Brain Manganese Accumulation is Inversely Related to γ-Amino Butyric Acid Uptake in Male and Female Rats. *Toxicological Sciences* **95**, 188-195 (2007).
192. Kim, Y. Neuroimaging in manganism. *Neurotoxicology* **27**, 369-72 (2006).
193. Chang, Y. et al. Decreased brain volumes in manganese-exposed welders. *Neurotoxicology* **37**, 182-9 (2013).
194. Guilarte, T.R. Manganese and Parkinson's disease: a critical review and new findings. *Environ Health Perspect* **118**, 1071-80 (2010).
195. Wang, F. et al. Protective role of sodium para-amino salicylic acid against manganese-induced hippocampal neurons damage. *Environ Toxicol Pharmacol* **37**, 1071-8 (2014).
196. Tuschl, K., Mills, P.B. & Clayton, P.T. Manganese and the brain. *Int Rev Neurobiol* **110**, 277-312 (2013).
197. Racette, B.A. et al. Prevalence of parkinsonism and relationship to exposure in a large sample of Alabama welders. *Neurology* **64**, 230-5 (2005).
198. Kenborg, L., Lassen, C.F., Hansen, J. & Olsen, J.H. Parkinson's disease and other neurodegenerative disorders among welders: a Danish cohort study. *Mov Disord* **27**, 1283-9 (2012).
199. Goldman, S.M. et al. Occupation and parkinsonism in three movement disorders clinics. *Neurology* **65**, 1430-5 (2005).
200. Solis-Vivanco, R. et al. Cognitive impairment in an adult Mexican population non-occupationally exposed to manganese. *Environ Toxicol Pharmacol* **28**, 172-8 (2009).
201. Standridge, J.S., Bhattacharya, A., Succop, P., Cox, C. & Haynes, E. Effect of chronic low level manganese exposure on postural balance: a pilot study of residents in southern Ohio. *J Occup Environ Med* **50**, 1421-9 (2008).
202. Guarneros, M., Ortiz-Romo, N., Alcaraz-Zubeldia, M., Drucker-Colin, R. & Hudson, R. Nonoccupational environmental exposure to manganese is linked to deficits in peripheral and central olfactory function. *Chem Senses* **38**, 783-91 (2013).
203. Loranger, S. & Zayed, J. Environmental and occupational exposure to manganese: a multimedia assessment. *Int Arch Occup Environ Health* **67**, 101-10 (1995).
204. Palacios, N. et al. A Prospective Analysis of Airborne Metal Exposures and Risk of Parkinson Disease in the Nurses Health Study Cohort. *Environ Health Perspect* (2014).
205. Gunter, T.E. et al. An analysis of the effects of Mn2+ on oxidative phosphorylation in liver, brain, and heart mitochondria using state 3 oxidation rate assays. *Toxicol Appl Pharmacol* **249**, 65-75 (2010).
206. Stephenson, A.P. et al. Manganese-induced oxidative DNA damage in neuronal SH-SY5Y cells: attenuation of thymine base lesions by glutathione and N-acetylcysteine. *Toxicol Lett* **218**, 299-307 (2013).

207. Chun, H.S., Lee, H. & Son, J.H. Manganese induces endoplasmic reticulum (ER) stress and activates multiple caspases in nigral dopaminergic neuronal cells, SN4741. *Neurosci Lett* **316**, 5-8 (2001).
208. Oubrahim, H., Chock, P.B. & Stadtman, E.R. Manganese(II) induces apoptotic cell death in NIH3T3 cells via a caspase-12-dependent pathway. *J Biol Chem* **277**, 20135-8 (2002).
209. Park, E.J. & Park, K. Induction of oxidative stress and inflammatory cytokines by manganese chloride in cultured T98G cells, human brain glioblastoma cell line. *Toxicol In Vitro* **24**, 472-9 (2010).
210. Alaimo, A. et al. Manganese induces mitochondrial dynamics impairment and apoptotic cell death: a study in human Gli36 cells. *Neurosci Lett* **554**, 76-81 (2013).
211. Karki, P., Lee, E. & Aschner, M. Manganese neurotoxicity: a focus on glutamate transporters. *Ann Occup Environ Med* **25**, 4 (2013).
212. Planchard, M.S., Exley, S.E., Morgan, S.E. & Rangachari, V. Dopamine-induced alpha-synuclein oligomers show self- and cross-propagation properties. *Protein Sci* (2014).
213. Verina, T., Schneider, J.S. & Guilarte, T.R. Manganese exposure induces alpha-synuclein aggregation in the frontal cortex of non-human primates. *Toxicol Lett* **217**, 177-83 (2013).
214. Sistrunk, S.C., Ross, M.K. & Filipov, N.M. Direct effects of manganese compounds on dopamine and its metabolite Dopac: an in vitro study. *Environ Toxicol Pharmacol* **23**, 286-96 (2007).
215. Roth, J.A., Li, Z., Sridhar, S. & Khoshbouei, H. The effect of manganese on dopamine toxicity and dopamine transporter (DAT) in control and DAT transfected HEK cells. *Neurotoxicology* **35**, 121-8 (2013).
216. Erikson, K.M., John, C.E., Jones, S.R. & Aschner, M. Manganese accumulation in striatum of mice exposed to toxic doses is dependent upon a functional dopamine transporter. *Environ Toxicol Pharmacol* **20**, 390-4 (2005).
217. Salazar, J. et al. Divalent metal transporter 1 (DMT1) contributes to neurodegeneration in animal models of Parkinson's disease. *Proc Natl Acad Sci U S A* **105**, 18578-83 (2008).
218. He, Q. et al. DMT1 polymorphism and risk of Parkinson's disease. *Neurosci Lett* **501**, 128-31 (2011).
219. Aboud, A.A. et al. Genetic risk for Parkinson's disease correlates with alterations in neuronal manganese sensitivity between two human subjects. *Neurotoxicology* **33**, 1443-9 (2012).
220. Roth, J.A., Ganapathy, B. & Ghio, A.J. Manganese-induced toxicity in normal and human B lymphocyte cell lines containing a homozygous mutation in parkin. *Toxicol In Vitro* **26**, 1143-9 (2012).
221. Higashi, Y. et al. Parkin attenuates manganese-induced dopaminergic cell death. *J Neurochem* **89**, 1490-7 (2004).
222. Sriram, K. et al. Mitochondrial dysfunction and loss of Parkinson's disease-linked proteins contribute to neurotoxicity of manganese-containing welding fumes. *FASEB J* **24**, 4989-5002 (2010).

223. Chakraborty, S., Bornhorst, J., Nguyen, T.T. & Aschner, M. Oxidative stress mechanisms underlying Parkinson's disease-associated neurodegeneration in C. elegans. *Int J Mol Sci* **14**, 23103-28 (2013).
224. Chakraborty, S. & Aschner, M. Altered manganese homeostasis: implications for BLI-3-dependent dopaminergic neurodegeneration and SKN-1 protection in C. elegans. *J Trace Elem Med Biol* **26**, 183-7 (2012).
225. Sulston, J., Dew, M. & Brenner, S. Dopaminergic neurons in the nematode Caenorhabditis elegans. *J Comp Neurol* **163**, 215-26 (1975).
226. Jayanthi, L.D. et al. The Caenorhabditis elegans gene T23G5.5 encodes an antidepressant- and cocaine-sensitive dopamine transporter. *Mol Pharmacol* **54**, 601-9 (1998).
227. Duerr, J.S. et al. The cat-1 gene of Caenorhabditis elegans encodes a vesicular monoamine transporter required for specific monoamine-dependent behaviors. *J Neurosci* **19**, 72-84 (1999).
228. Sawin, E.R., Ranganathan, R. & Horvitz, H.R. C. elegans locomotory rate is modulated by the environment through a dopaminergic pathway and by experience through a serotonergic pathway. *Neuron* **26**, 619-31 (2000).
229. Chase, D.L. & Koelle, M.R. Biogenic amine neurotransmitters in C. elegans. *WormBook*, 1-15 (2007).
230. Nass, R., Hall, D.H., Miller, D.M., 3rd & Blakely, R.D. Neurotoxin-induced degeneration of dopamine neurons in Caenorhabditis elegans. *Proc Natl Acad Sci U S A* **99**, 3264-9 (2002).
231. Consortium, C.e.S. Genome sequence of the nematode C. elegans: a platform for investigating biology. *Science* **282**, 2012-8 (1998).
232. Martinez-Finley, E.J., Avila, D.S., Chakraborty, S. & Aschner, M. Insights from Caenorhabditis elegans on the role of metals in neurodegenerative diseases. *Metallomics* **3**, 271-9 (2011).
233. Ahringer, J. in Wormbook, ed. The C. elegans Research Community (2006).
234. Isik, M. & Berezikov, E. Biolistic transformation of Caenorhabditis elegans. *Methods Mol Biol* **940**, 77-86 (2013).
235. Antoshechkin, I. & Sternberg, P.W. The versatile worm: genetic and genomic resources for Caenorhabditis elegans research. *Nat Rev Genet* **8**, 518-32 (2007).
236. Springer, W., Hoppe, T., Schmidt, E. & Baumeister, R. A Caenorhabditis elegans Parkin mutant with altered solubility couples alpha-synuclein aggregation to proteotoxic stress. *Hum Mol Genet* **14**, 3407-23 (2005).
237. Martinez-Finley, E.J., Chakraborty, S., Slaughter, J.C. & Aschner, M. Early-Life Exposure to Methylmercury in Wildtype and pdr-1/parkin Knockout C. elegans. *Neurochem Res* **38**, 1543-52 (2013).
238. Ved, R. et al. Similar patterns of mitochondrial vulnerability and rescue induced by genetic modification of alpha-synuclein, parkin, and DJ-1 in Caenorhabditis elegans. *J Biol Chem* **280**, 42655-68 (2005).
239. Samann, J. et al. Caenorhabditits elegans LRK-1 and PINK-1 act antagonistically in stress response and neurite outgrowth. *J Biol Chem* **284**, 16482-91 (2009).
240. Lee, J.Y., Kim, C., Kim, J. & Park, C. DJR-1.2 of Caenorhabditis elegans is induced by DAF-16 in the dauer state. *Gene* (2013).

241. Au, C. et al. SMF-1, SMF-2 and SMF-3 DMT1 orthologues regulate and are regulated differentially by manganese levels in C. elegans. *PLoS One* **4**, e7792 (2009).
242. De Domenico, I. et al. The role of ubiquitination in hepcidin-independent and hepcidin-dependent degradation of ferroportin. *Cell Metab* **14**, 635-46 (2011).
243. Van Baelen, K., Vanoevelen, J., Missiaen, L., Raeymaekers, L. & Wuytack, F. The Golgi PMR1 P-type ATPase of Caenorhabditis elegans. Identification of the gene and demonstration of calcium and manganese transport. *J Biol Chem* **276**, 10683-91 (2001).
244. Cho, J.H., Ko, K.M., Singaravelu, G. & Ahnn, J. Caenorhabditis elegans PMR1, a P-type calcium ATPase, is important for calcium/manganese homeostasis and oxidative stress response. *FEBS Lett* **579**, 778-82 (2005).
245. Buttner, S. et al. The Ca2+/Mn2+ ion-pump PMR1 links elevation of cytosolic Ca(2+) levels to alpha-synuclein toxicity in Parkinson's disease models. *Cell Death Differ* **20**, 465-77 (2013).
246. Bornhorst, J. et al. The effects of pdr1, djr1.1 and pink1 loss in manganese-induced toxicity and the role of alpha-synuclein in C. elegans. *Metallomics* **6**, 476-90 (2014).
247. Sang, T.K. et al. A Drosophila model of mutant human parkin-induced toxicity demonstrates selective loss of dopaminergic neurons and dependence on cellular dopamine. *J Neurosci* **27**, 981-92 (2007).
248. Unoki, M. & Nakamura, Y. Growth-suppressive effects of BPOZ and EGR2, two genes involved in the PTEN signaling pathway. *Oncogene* **20**, 4457-65 (2001).
249. Jendrach, M. et al. The mitochondrial kinase PINK1, stress response and Parkinson's disease. *J Bioenerg Biomembr* **41**, 481-6 (2009).
250. Gandhi, S. et al. Dopamine induced neurodegeneration in a PINK1 model of Parkinson's disease. *PLoS One* **7**, e37564 (2012).
251. Alerte, T.N. et al. Alpha-synuclein aggregation alters tyrosine hydroxylase phosphorylation and immunoreactivity: lessons from viral transduction of knockout mice. *Neurosci Lett* **435**, 24-9 (2008).
252. Aschner, M., Erikson, K.M., Herrero Hernandez, E. & Tjalkens, R. Manganese and its role in Parkinson's disease: from transport to neuropathology. *Neuromolecular Med* **11**, 252-66 (2009).
253. Burton, N.C. & Guilarte, T.R. Manganese neurotoxicity: lessons learned from longitudinal studies in nonhuman primates. *Environ Health Perspect* **117**, 325-32 (2009).
254. Uversky, V.N., Li, J. & Fink, A.L. Metal-triggered structural transformations, aggregation, and fibrillation of human alpha-synuclein. A possible molecular NK between Parkinson's disease and heavy metal exposure. *J Biol Chem* **276**, 44284-96 (2001).
255. Brenner, S. The genetics of Caenorhabditis elegans. *Genetics* **77**, 71-94 (1974).
256. Boumans, P.W.J.M. *Inductively Coupled Plasma Emission Spectroscopy, Part 2: Applications And Fundamentals. John Wiley & Sons, New York.* (1987).
257. Rahman, I., Kode, A. & Biswas, S.K. Assay for quantitative determination of glutathione and glutathione disulfide levels using enzymatic recycling method. *Nat Protoc* **1**, 3159-65 (2006).

258. Caito, S.W., Valentine, W.M. & Aschner, M. Dopaminergic neurotoxicity of S-ethyl N,N-dipropylthiocarbamate (EPTC), molinate, and S-methyl-N,N-diethylthiocarbamate (MeDETC) in Caenorhabditis elegans. *J Neurochem*, 10.1111/jnc.12349 (2013).
259. Livak, K.J. & Schmittgen, T.D. Analysis of relative gene expression data using real-time quantitative PCR and the 2(-Delta Delta C(T)) Method. *Methods* **25**, 402-8 (2001).
260. Benedetto, A., Au, C., Avila, D.S., Milatovic, D. & Aschner, M. Extracellular dopamine potentiates mn-induced oxidative stress, lifespan reduction, and dopaminergic neurodegeneration in a BLI-3-dependent manner in Caenorhabditis elegans. *PLoS Genet* **6** (2010).
261. Avila, D.S., Somlyai, G., Somlyai, I. & Aschner, M. Anti-aging effects of deuterium depletion on Mn-induced toxicity in a C. elegans model. *Toxicol Lett* **211**, 319-24 (2012).
262. WormBase.org. http://www.wormbase.org/species/c_elegans/gene/WBGene00015184 - 0-9d6-3.
263. Milatovic, D., Zaja-Milatovic, S., Gupta, R.C., Yu, Y. & Aschner, M. Oxidative damage and neurodegeneration in manganese-induced neurotoxicity. *Toxicol Appl Pharmacol* **240**, 219-25 (2009).
264. Wilhelmus, M.M., Nijland, P.G., Drukarch, B., de Vries, H.E. & van Horssen, J. Involvement and interplay of Parkin, PINK1, and DJ1 in neurodegenerative and neuroinflammatory disorders. *Free Radic Biol Med* **53**, 983-92 (2012).
265. Oliveira, R.P. et al. Condition-adapted stress and longevity gene regulation by Caenorhabditis elegans SKN-1/Nrf. *Aging Cell* **8**, 524-41 (2009).
266. Swant, J. et al. alpha-Synuclein stimulates a dopamine transporter-dependent chloride current and modulates the activity of the transporter. *J Biol Chem* **286**, 43933-43 (2011).
267. Becker, J.S., Zoriy, M.V., Pickhardt, C., Palomero-Gallagher, N. & Zilles, K. Imaging of copper, zinc, and other elements in thin section of human brain samples (hippocampus) by laser ablation inductively coupled plasma mass spectrometry. *Anal Chem* **77**, 3208-16 (2005).
268. Kipreos, E.T. Ubiquitin-mediated pathways in C. elegans. *WormBook*, 1-24 (2005).
269. Saini, N. et al. Extended lifespan of Drosophila parkin mutants through sequestration of redox-active metals and enhancement of anti-oxidative pathways. *Neurobiol Dis* **40**, 82-92 (2010).
270. Saini, N., Georgiev, O. & Schaffner, W. The parkin mutant phenotype in the fly is largely rescued by metal-responsive transcription factor (MTF-1). *Mol Cell Biol* **31**, 2151-61 (2011).
271. Bjorkblom, B. et al. Parkinson Disease Protein DJ-1 Binds Metals and Protects against Metal-induced Cytotoxicity. *J Biol Chem* **288**, 22809-20 (2013).
272. Duplan, E. et al. ER-stress-associated functional link between Parkin and DJ-1 via a transcriptional cascade involving the tumor suppressor p53 and the spliced X-box binding protein XBP-1. *J Cell Sci* **126**, 2124-33 (2013).

273. Casarejos, M.J. et al. Parkin deficiency increases the resistance of midbrain neurons and glia to mild proteasome inhibition: the role of autophagy and glutathione homeostasis. *J Neurochem* **110**, 1523-37 (2009).
274. Erikson, K.M., Syversen, T., Aschner, J.L. & Aschner, M. Interactions between excessive manganese exposures and dietary iron-deficiency in neurodegeneration. *Environ Toxicol Pharmacol* **19**, 415-21 (2005).
275. Snyder, R.D. & Friedman, M.B. Enhancement of cytotoxicity and clastogenicity of l-DOPA and dopamine by manganese and copper. *Mutat Res* **405**, 1-8 (1998).
276. Park, J. et al. Mitochondrial dysfunction in Drosophila PINK1 mutants is complemented by parkin. *Nature* **441**, 1157-61 (2006).
277. Miyama, A. et al. Oxidation of DJ-1 induced by 6-hydroxydopamine decreasing intracellular glutathione. *PLoS One* **6**, e27883 (2011).
278. Moi, P., Chan, K., Asunis, I., Cao, A. & Kan, Y.W. Isolation of NF-E2-related factor 2 (Nrf2), a NF-E2-like basic leucine zipper transcriptional activator that binds to the tandem NF-E2/AP1 repeat of the beta-globin locus control region. *Proc Natl Acad Sci U S A* **91**, 9926-30 (1994).
279. McMahon, M., Itoh, K., Yamamoto, M. & Hayes, J.D. Keap1-dependent proteasomal degradation of transcription factor Nrf2 contributes to the negative regulation of antioxidant response element-driven gene expression. *J Biol Chem* **278**, 21592-600 (2003).
280. An, J.H. & Blackwell, T.K. SKN-1 links C. elegans mesendodermal specification to a conserved oxidative stress response. *Genes Dev* **17**, 1882-93 (2003).
281. Imaizumi, Y. et al. Mitochondrial dysfunction associated with increased oxidative stress and alpha-synuclein accumulation in PARK2 iPSC-derived neurons and postmortem brain tissue. *Mol Brain* **5**, 35 (2012).
282. Xu, J. et al. Dopamine-dependent neurotoxicity of alpha-synuclein: a mechanism for selective neurodegeneration in Parkinson disease. *Nat Med* **8**, 600-6 (2002).
283. Sidhu, A., Wersinger, C., Moussa, C.E. & Vernier, P. The role of alpha-synuclein in both neuroprotection and neurodegeneration. *Ann N Y Acad Sci* **1035**, 250-70 (2004).
284. George, J.M. The synucleins. *Genome Biol* **3**, REVIEWS3002 (2002).
285. Clayton, D.F. & George, J.M. The synucleins: a family of proteins involved in synaptic function, plasticity, neurodegeneration and disease. *Trends Neurosci* **21**, 249-54 (1998).
286. Brown, D.R. Interactions between metals and alpha-synuclein--function or artefact? *FEBS J* **274**, 3766-74 (2007).
287. Binolfi, A. et al. Interaction of alpha-synuclein with divalent metal ions reveals key differences: a link between structure, binding specificity and fibrillation enhancement. *J Am Chem Soc* **128**, 9893-901 (2006).
288. Santner, A. & Uversky, V.N. Metalloproteomics and metal toxicology of alpha-synuclein. *Metallomics* **2**, 378-92 (2010).
289. Bisaglia, M., Tessari, I., Mammi, S. & Bubacco, L. Interaction between alpha-synuclein and metal ions, still looking for a role in the pathogenesis of Parkinson's disease. *Neuromolecular Med* **11**, 239-51 (2009).
290. Ahmad, A., Burns, C.S., Fink, A.L. & Uversky, V.N. Peculiarities of copper binding to alpha-synuclein. *J Biomol Struct Dyn* **29**, 825-42 (2012).

291. Davies, P., Moualla, D. & Brown, D.R. Alpha-synuclein is a cellular ferrireductase. *PLoS One* **6**, e15814 (2011).
292. Melachroinou, K. et al. Deregulation of calcium homeostasis mediates secreted alpha-synuclein-induced neurotoxicity. *Neurobiol Aging* (2013).
293. Emmanouilidou, E., Stefanis, L. & Vekrellis, K. Cell-produced alpha-synuclein oligomers are targeted to, and impair, the 26S proteasome. *Neurobiol Aging* **31**, 953-68 (2010).
294. Pan-Montojo, F. et al. Environmental toxins trigger PD-like progression via increased alpha-synuclein release from enteric neurons in mice. *Sci Rep* **2**, 898 (2012).
295. Lee, M., Hyun, D., Halliwell, B. & Jenner, P. Effect of the overexpression of wild-type or mutant alpha-synuclein on cell susceptibility to insult. *J Neurochem* **76**, 998-1009 (2001).
296. Fitsanakis, V.A. et al. Catalysis of catechol oxidation by metal-dithiocarbamate complexes in pesticides. *Free Radic Biol Med* **33**, 1714-23 (2002).
297. Liu, Y.Y. et al. [Overexpression of alpha-synuclein in SH-SY5Y cells partially protected against oxidative stress induced by rotenone]. *Sheng Li Xue Bao* **58**, 421-8 (2006).
298. Bonifati, V. et al. The parkin gene and its phenotype. Italian PD Genetics Study Group, French PD Genetics Study Group and the European Consortium on Genetic Susceptibility in Parkinson's Disease. *Neurol Sci* **22**, 51-2 (2001).
299. Takahashi, H. et al. Familial juvenile parkinsonism: clinical and pathologic study in a family. *Neurology* **44**, 437-41 (1994).
300. Shimada, S. et al. Cloning and expression of a cocaine-sensitive dopamine transporter complementary DNA. *Science* **254**, 576-8 (1991).
301. Cass, W.A., Zahniser, N.R., Flach, K.A. & Gerhardt, G.A. Clearance of exogenous dopamine in rat dorsal striatum and nucleus accumbens: role of metabolism and effects of locally applied uptake inhibitors. *J Neurochem* **61**, 2269-78 (1993).
302. Kilty, J.E., Lorang, D. & Amara, S.G. Cloning and expression of a cocaine-sensitive rat dopamine transporter. *Science* **254**, 578-9 (1991).
303. Huotari, M. et al. Effect of dopamine uptake inhibition on brain catecholamine levels and locomotion in catechol-O-methyltransferase-disrupted mice. *J Pharmacol Exp Ther* **303**, 1309-16 (2002).
304. McDonald, P.W. et al. Vigorous motor activity in Caenorhabditis elegans requires efficient clearance of dopamine mediated by synaptic localization of the dopamine transporter DAT-1. *J Neurosci* **27**, 14216-27 (2007).
305. Lundblad, M., Decressac, M., Mattsson, B. & Bjorklund, A. Impaired neurotransmission caused by overexpression of alpha-synuclein in nigral dopamine neurons. *Proc Natl Acad Sci U S A* **109**, 3213-9 (2012).
306. Nemani, V.M. et al. Increased expression of alpha-synuclein reduces neurotransmitter release by inhibiting synaptic vesicle reclustering after endocytosis. *Neuron* **65**, 66-79 (2010).
307. Todd, A.M. & Staveley, B.E. Expression of Pink1 with alpha-synuclein in the dopaminergic neurons of Drosophila leads to increases in both lifespan and healthspan. *Genet Mol Res* **11**, 1497-502 (2012).

308. Febbraro, F., Giorgi, M., Caldarola, S., Loreni, F. & Romero-Ramos, M. alpha-Synuclein expression is modulated at the translational level by iron. *Neuroreport* **23**, 576-80 (2012).
309. Chakraborty, S. et al. Loss of pdr-1/parkin influences Mn homeostasis through altered ferroportin expression in C. elegans. *Metallomics* (2015).
310. Blesa, J., Phani, S., Jackson-Lewis, V. & Przedborski, S. Classic and new animal models of Parkinson's disease. *J Biomed Biotechnol* **2012**, 845618 (2012).
311. Bhuie, A.K., Ogunseitan, O.A., White, R.R., Sain, M. & Roy, D.N. Modeling the environmental fate of manganese from methylcyclopentadienyl manganese tricarbonyl in urban landscapes. *Sci Total Environ* **339**, 167-78 (2005).
312. Finkelstein, M.M. & Jerrett, M. A study of the relationships between Parkinson's disease and markers of traffic-derived and environmental manganese air pollution in two Canadian cities. *Environ Res* **104**, 420-32 (2007).
313. Klos, K.J. et al. Neurologic spectrum of chronic liver failure and basal ganglia T1 hyperintensity on magnetic resonance imaging: probable manganese neurotoxicity. *Arch Neurol* **62**, 1385-90 (2005).
314. Smith, E.A., Newland, P., Bestwick, K.G. & Ahmed, N. Increased whole blood manganese concentrations observed in children with iron deficiency anaemia. *J Trace Elem Med Biol* **27**, 65-9 (2013).
315. Anderson, C.P. & Leibold, E.A. Mechanisms of iron metabolism in Caenorhabditis elegans. *Front Pharmacol* **5**, 113 (2014).
316. Leyva-Illades, D. et al. SLC30A10 Is a Cell Surface-Localized Manganese Efflux Transporter, and Parkinsonism-Causing Mutations Block Its Intracellular Trafficking and Efflux Activity. *The Journal of Neuroscience* **34**, 14079-14095 (2014).
317. Hunter, S.E., Jung, D., Di Giulio, R.T. & Meyer, J.N. The QPCR assay for analysis of mitochondrial DNA damage, repair, and relative copy number. *Methods* **51**, 444-51 (2010).
318. Lee, H.C., Yin, P.H., Lu, C.Y., Chi, C.W. & Wei, Y.H. Increase of mitochondria and mitochondrial DNA in response to oxidative stress in human cells. *Biochem J* **348 Pt 2**, 425-32 (2000).
319. Papaevgeniou, N. & Chondrogianni, N. The ubiquitin proteasome system in Caenorhabditis elegans and its regulation. *Redox Biol* **2**, 333-47 (2014).
320. Sriram, K. et al. Dopaminergic neurotoxicity following pulmonary exposure to manganese-containing welding fumes. *Arch Toxicol* **84**, 521-40 (2010).
321. Prohaska, J.R. & Broderius, M. Copper deficiency has minimal impact on ferroportin expression or function. *Biometals* **25**, 633-42 (2012).
322. Prohaska, J.R. Impact of copper deficiency in humans. *Ann N Y Acad Sci* **1314**, 1-5 (2014).
323. Ayton, S. et al. Iron accumulation confers neurotoxicity to a vulnerable population of nigral neurons: implications for Parkinson's disease. *Mol Neurodegener* **9**, 27 (2014).
324. Mounsey, R.B. & Teismann, P. Chelators in the treatment of iron accumulation in Parkinson's disease. *Int J Cell Biol* **2012**, 983245 (2012).

325. Ben-Shachar, D., Eshel, G., Riederer, P. & Youdim, M.B. Role of iron and iron chelation in dopaminergic-induced neurodegeneration: implication for Parkinson's disease. *Ann Neurol* **32 Suppl**, S105-10 (1992).
326. Angeli, S. et al. Manganese disturbs metal and protein homeostasis in Caenorhabditis elegans. *Metallomics* **6**, 1816-23 (2014).
327. de Vries, R.L. & Przedborski, S. Mitophagy and Parkinson's disease: be eaten to stay healthy. *Mol Cell Neurosci* **55**, 37-43 (2013).
328. Podlesniy, P. et al. Low cerebrospinal fluid concentration of mitochondrial DNA in preclinical Alzheimer disease. *Ann Neurol* **74**, 655-68 (2013).
329. Gu, F. et al. Alterations in mitochondrial DNA copy number and the activities of electron transport chain complexes and pyruvate dehydrogenase in the frontal cortex from subjects with autism. *Transl Psychiatry* **3**, e299 (2013).
330. Aracena, P., Aguirre, P., Munoz, P. & Nunez, M.T. Iron and glutathione at the crossroad of redox metabolism in neurons. *Biol Res* **39**, 157-65 (2006).
331. Graumann, R. et al. Oxidation of dopamine to aminochrome as a mechanism for neurodegeneration of dopaminergic systems in Parkinson's disease. Possible neuroprotective role of DT-diaphorase. *Pol J Pharmacol* **54**, 573-9 (2002).
332. Garner, C.D. & Nachtman, J.P. Manganese catalyzed auto-oxidation of dopamine to 6-hydroxydopamine in vitro. *Chem Biol Interact* **69**, 345-51 (1989).
333. Bridelli, M.G., Tampellini, D. & Zecca, L. The structure of neuromelanin and its iron binding site studied by infrared spectroscopy. *FEBS Lett* **457**, 18-22 (1999).
334. Kordower, J.H., Chu, Y., Hauser, R.A., Freeman, T.B. & Olanow, C.W. Lewy body-like pathology in long-term embryonic nigral transplants in Parkinson's disease. *Nat Med* **14**, 504-6 (2008).
335. Brundin, P., Barker, R.A. & Parmar, M. Neural grafting in Parkinson's disease Problems and possibilities. *Prog Brain Res* **184**, 265-94 (2010).
336. Lee, H.J. et al. Dopamine promotes formation and secretion of non-fibrillar alpha-synuclein oligomers. *Exp Mol Med* **43**, 216-22 (2011).
337. Lee, H.J. et al. Autophagic failure promotes the exocytosis and intercellular transfer of alpha-synuclein. *Exp Mol Med* **45**, e22 (2013).
338. Lonskaya, I., Desforges, N.M., Hebron, M.L. & Moussa, C.E. Ubiquitination increases parkin activity to promote autophagic alpha-synuclein clearance. *PLoS One* **8**, e83914 (2013).
339. Pifl, C. et al. alpha-Synuclein selectively increases manganese-induced viability loss in SK-N-MC neuroblastoma cells expressing the human dopamine transporter. *Neurosci Lett* **354**, 34-7 (2004).
340. Rasia, R.M. et al. Structural characterization of copper(II) binding to alpha-synuclein: Insights into the bioinorganic chemistry of Parkinson's disease. *Proc Natl Acad Sci U S A* **102**, 4294-9 (2005).
341. Chase, D.L., Pepper, J.S. & Koelle, M.R. Mechanism of extrasynaptic dopamine signaling in Caenorhabditis elegans. *Nat Neurosci* **7**, 1096-103 (2004).
342. Jorgensen, E.M. Dopamine: should I stay or should I go now? *Nat Neurosci* **7**, 1019-21 (2004).
343. Zhang, Y., Shao, Z., Zhai, Z., Shen, C. & Powell-Coffman, J.A. The HIF-1 hypoxia-inducible factor modulates lifespan in C. elegans. *PLoS One* **4**, e6348 (2009).

344. Romney, S.J., Newman, B.S., Thacker, C. & Leibold, E.A. HIF-1 regulates iron homeostasis in Caenorhabditis elegans by activation and inhibition of genes involved in iron uptake and storage. *PLoS Genet* **7**, e1002394 (2011).
345. Lei, P. et al. Tau deficiency induces parkinsonism with dementia by impairing APP-mediated iron export. *Nat Med* **18**, 291-5 (2012).
346. Wong, B.X. et al. beta-Amyloid precursor protein does not possess ferroxidase activity but does stabilize the cell surface ferrous iron exporter ferroportin. *PLoS One* **9**, e114174 (2014).
347. Ewald, C.Y., Raps, D.A. & Li, C. APL-1, the Alzheimer's Amyloid precursor protein in Caenorhabditis elegans, modulates multiple metabolic pathways throughout development. *Genetics* **191**, 493-507 (2012).
348. Gan, L., Johnson, D.A. & Johnson, J.A. Keap1-Nrf2 activation in the presence and absence of DJ-1. *Eur J Neurosci* **31**, 967-77 (2010).
349. Kwakye, G.F., Li, D. & Bowman, A.B. Novel high-throughput assay to assess cellular manganese levels in a striatal cell line model of Huntington's disease confirms a deficit in manganese accumulation. *Neurotoxicology* **32**, 630-9 (2011).
350. Linder, M.C. Mobilization of stored iron in mammals: a review. *Nutrients* **5**, 4022-50 (2013).
351. Hafer, K. & Schiestl, R.H. Biological aspects of dichlorofluorescein measurement of cellular reactive oxygen species. *Radiat Res* **170**, 408 (2008).